International Workshop on

Thin films and New Ideas for Pushing the Limits of RF Superconductivity

INFN - Legnaro National Laboratory - Padua University, October 9-12, 2006

Enzo Palmieri:

what did we learn from this workshop?

Some Figures …

- 47 talks over 3 ½ days
- 68 participants
- International workshop → 3 regions represented

INFN / CNR / Univ. - DESY / Max Plank Inst. / Nurnberg Univ.

- CNRS / CEA – CERN - Andrzej Soltan Inst. - Tel Aviv Univ.

JLab – Los Alamos - Argonne - Fermi Lab - Cornell / California / Florida Univ.
- SLAC

KEK – China Institute of Atomic Energy

Beijing 2004 - International Conference on High Energy Physics

***International Technology Recommendation Panel** of the*
International Committee for Future Accelerators (ICFA)

Front line from left to right:
Akira Masaike, George Kalmus, Volker Soergel, Barry Barish, Giorgio Bellettini, Hirotaka Sugawara,Paul Grannis
Back line from left to right:
Gyung-Su Lee, Jean-Eude Augustin, David Plane, Jonathan Bagger, Norbert Holtkamp, Katsunobu Oide

European cost approach for mass scale production

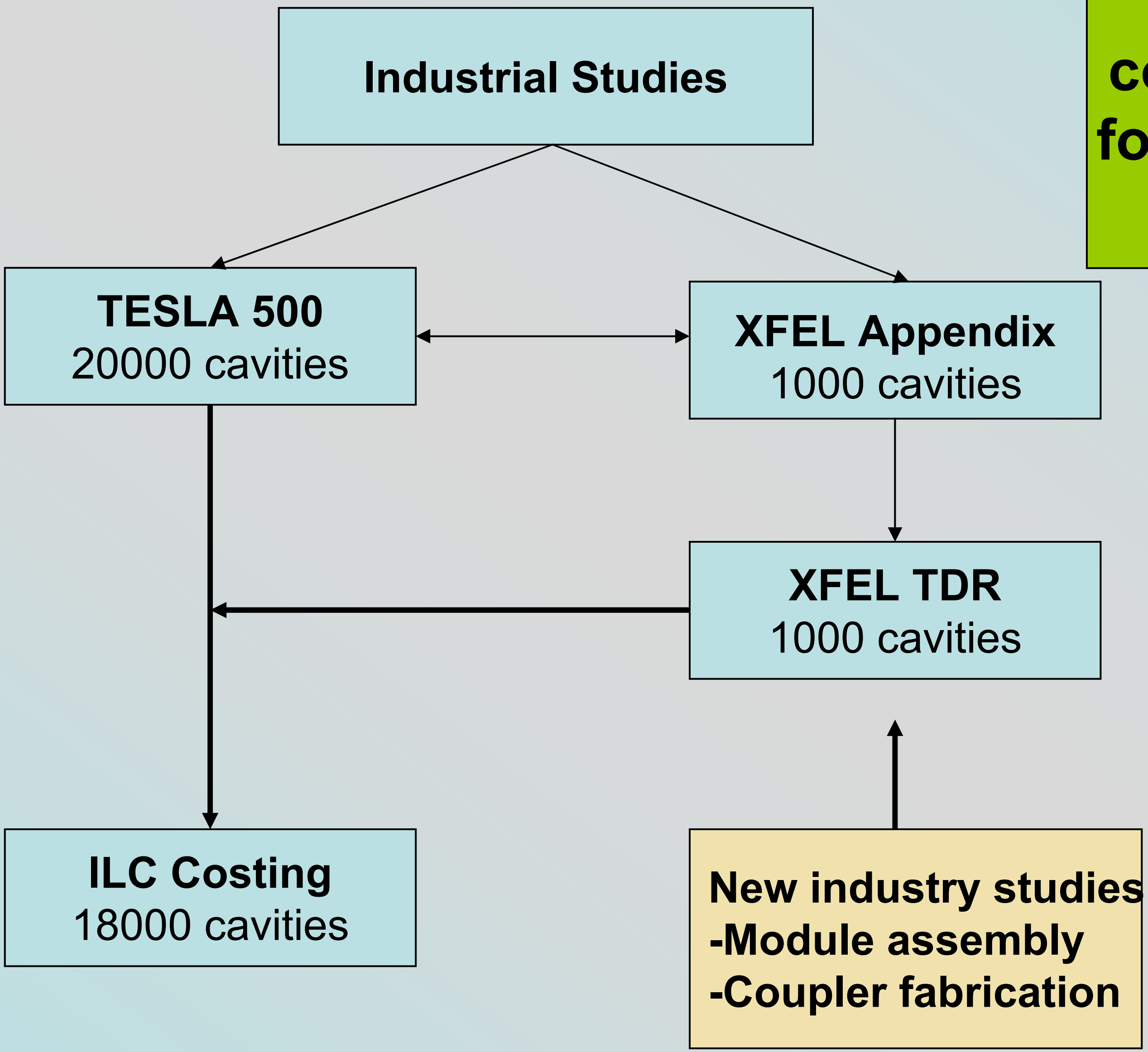

D. Proch, DESY

Comments to cost evaluation

- **Nb Material** (high purity, RRR 300)
  - No shortage of raw Nb material (40.000 tons annual production, ILC needs around 500 tons
  - But limited number of high purity melting facilities
    - Today there are 4 qualified companies, but only one is capable of producing full yield
  - Marginal savings in mass production (from industrial study)
    - Size of melting furnace is limited
    - But some saving can be realized by
      - Disc rather than rectangular sheet (scrap can be recovered)
      - Other material produced ready for fabrication, e.g. flange material
    - But: Latest developments in large/single crystal cavities promise cost reductions
- **The result is robust costing**

500KW electron beam cold hearth furnace

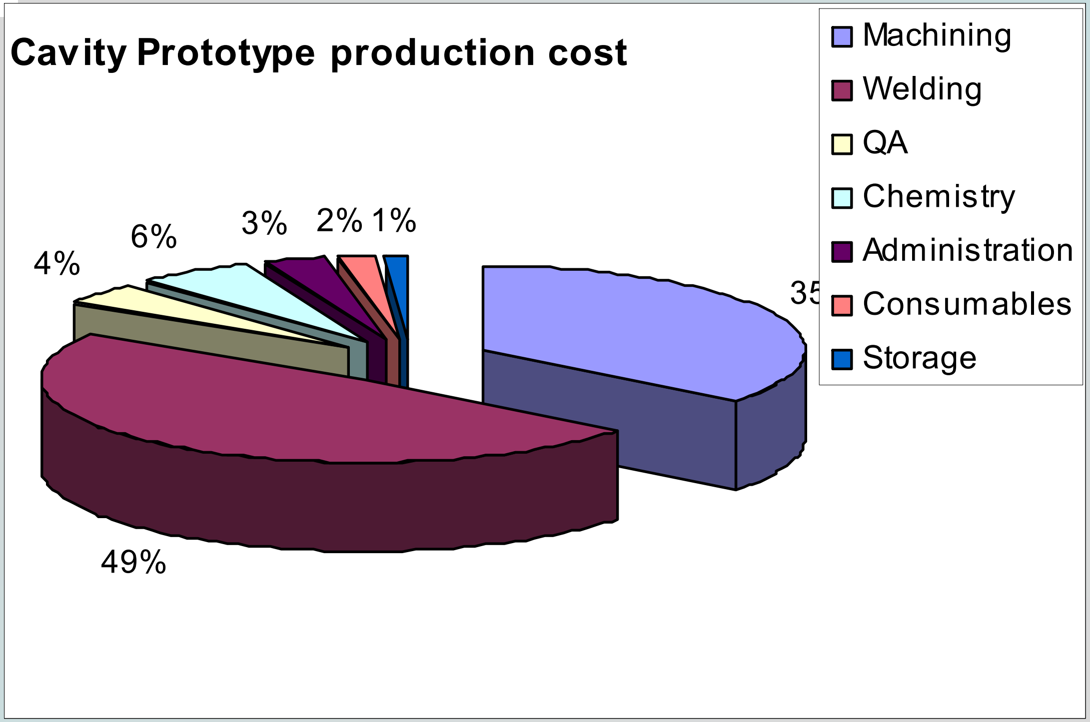
Cavity Prototype production cost
Machining
Welding
QA
Chemistry
Administration
Consumables
Storage
4%
6%
3%
2%
1%
35
49%

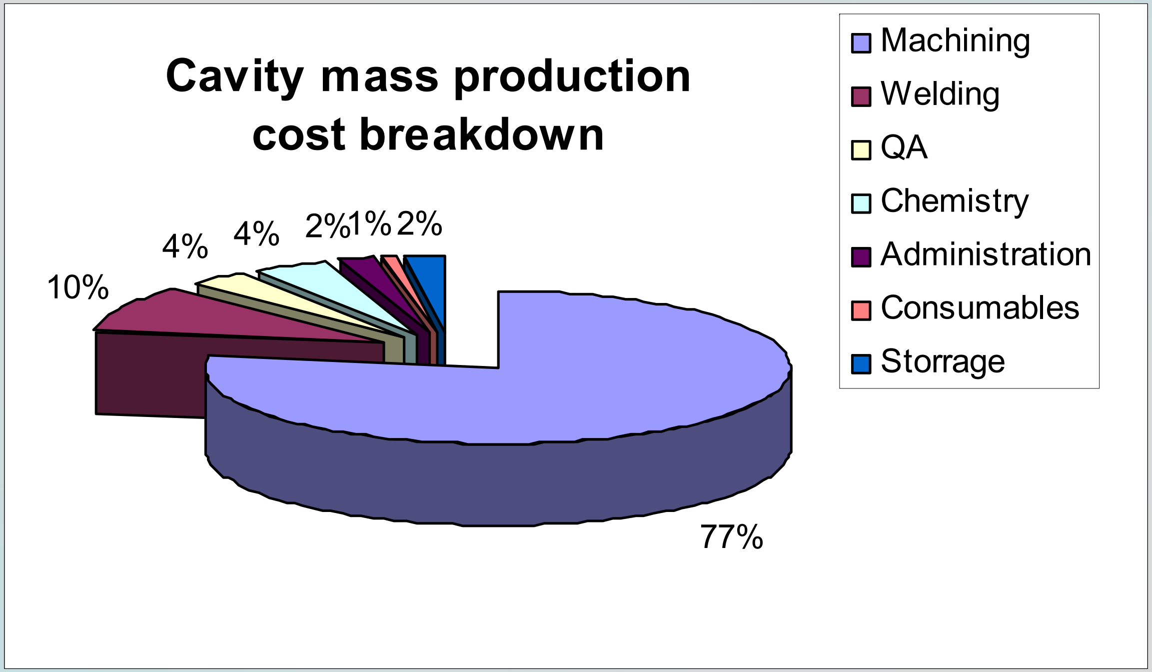
Cavity mass production cost breakdown
Machining
Welding
QA
Chemistry
Administration
Consumables
Storrage
10%
4%
4%
2%
1%
2%
77%

D. Proch, DESY

D. Bloess

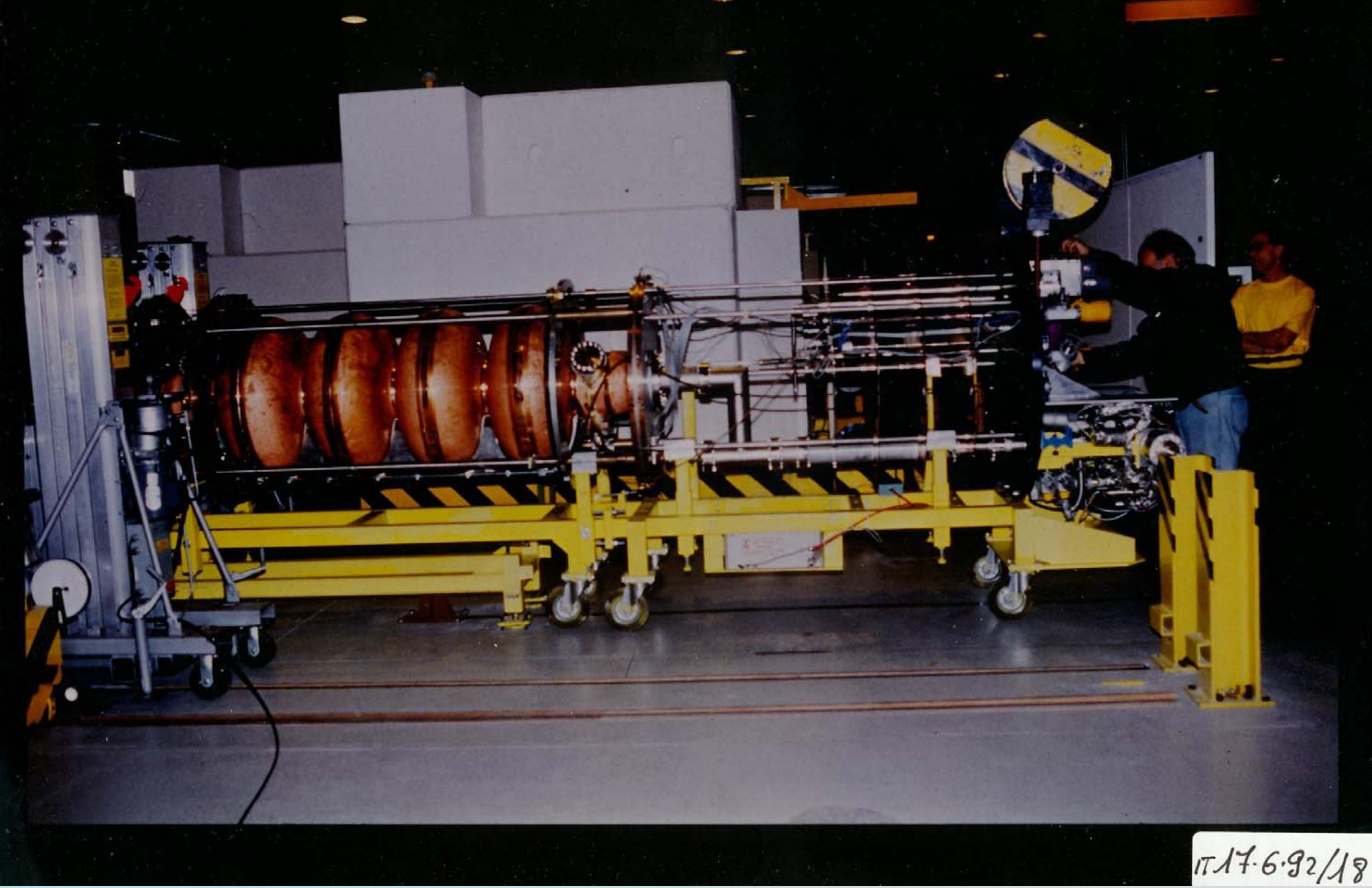

0 739 - 7 · 88

Nb/Cu-cavities are of course cheaper, however, more difficult to produce:

- EB-welding is delicate because of the high thermal conductivity more power than for bulk Nb is needed:

  problems with thermal deformation,

  holes in the weld,

  porosities due to very fast cooldown of vortices in the liquid copper, and due to impurities on the surface

D. Bloess

- Great care has to be taken to produce a smooth and clean surface without holes and inclusions:

- → Electrochemical polishing(EP) 60 μm
- → Inspection and carefull grinding
- → EP 60 μm
- → Inspection and if necessary another correction
- → EB-welding
- → Inspection and grinding of welding beads
- → Chemical polishing (CP) 20-25 μm
- → Rinsing with high purity water in clean room
- → Drying with reagent grade ethanol in clean room

D. Bloess

Why films

S. Calatroni - CERN

- Advantages (primary objectives)
  - Thermal stability
  - Cost
  - Innovative materials
- Advantages (learned from experience)
  - Optimisation of R_{BCS} at 4.2 K (sputtered niobium films)
  - Reduced sensitivity to earth magnetic field
- Disadvantages (known from the beginning)
  - Fabrication and surface preparation (at least) as difficult as for bulk
- Disadvantages (learned from experience)
  - Deposition of innovative materials is very difficult
  - Steep R_{res} increase with RF field (sputtered niobium films)

Defects in Cu substrate

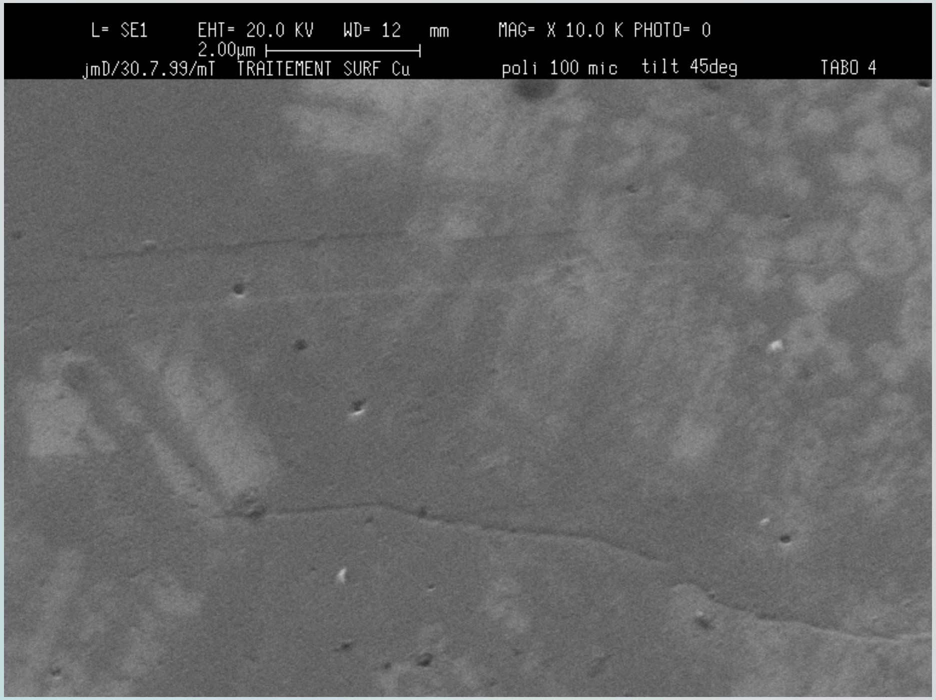

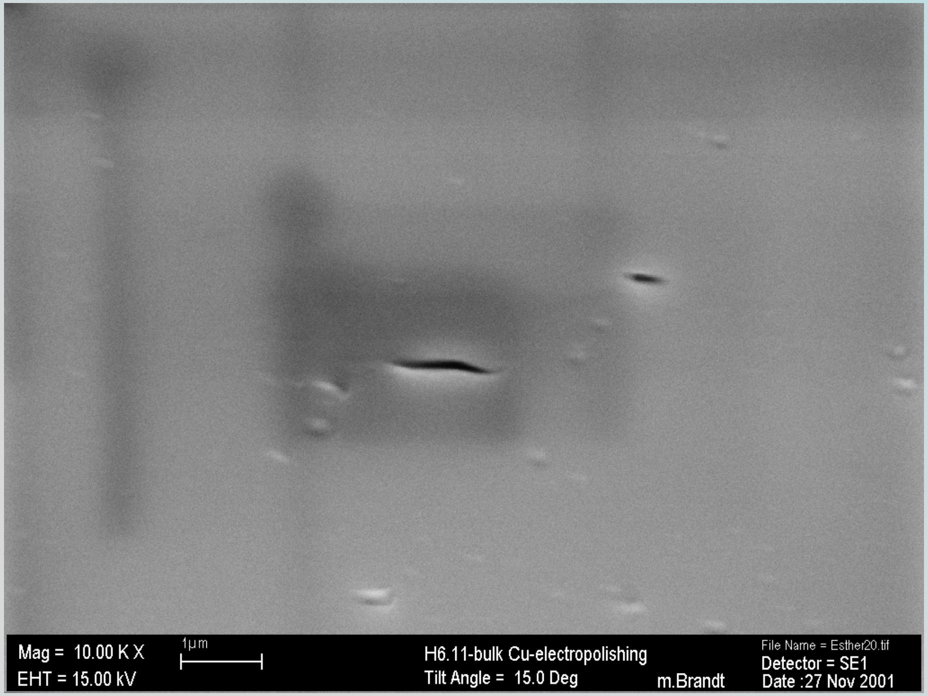

Electropolished copper surface

- average roughness: 0.02 μm
- A few defects still appearing

Cross section of a copper cavity

- Defects are present inside !
- Not an artifact of the preparation

Thanks to: G. Arnau-Izquierdo

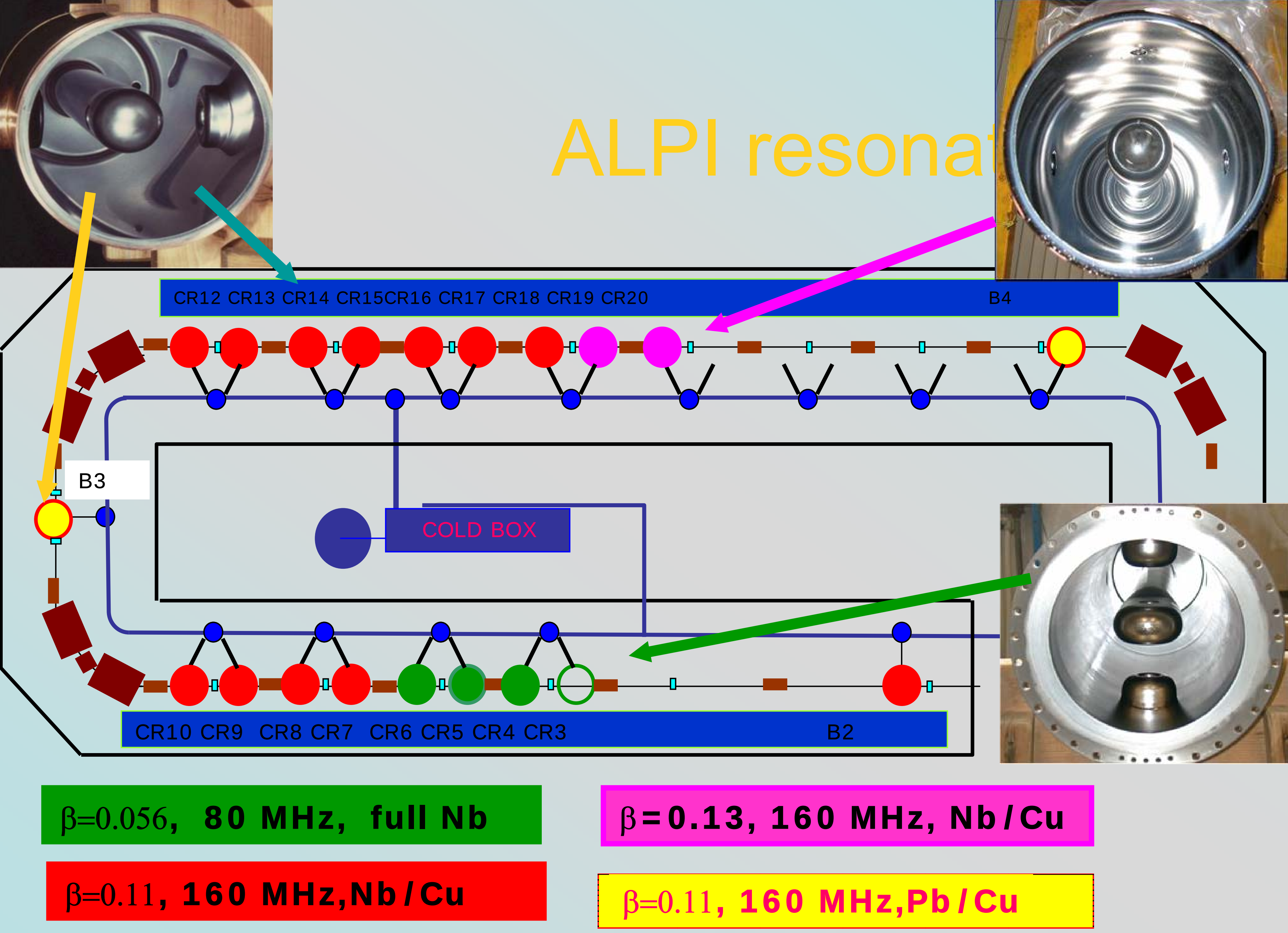
ALPI resonat
CR12 CR13 CR14 CR15CR16 CR17 CR18 CR19 CR20
B4
B3
COLD BOX
CR10 CR9 CR8 CR7 CR6 CR5 CR4 CR3
B2
β=0.056, 80 MHz, full Nb
β=0.13, 160 MHz, Nb/Cu
β=0.11, 160 MHz,Nb/Cu
β=0.11, 160 MHz,Pb/Cu

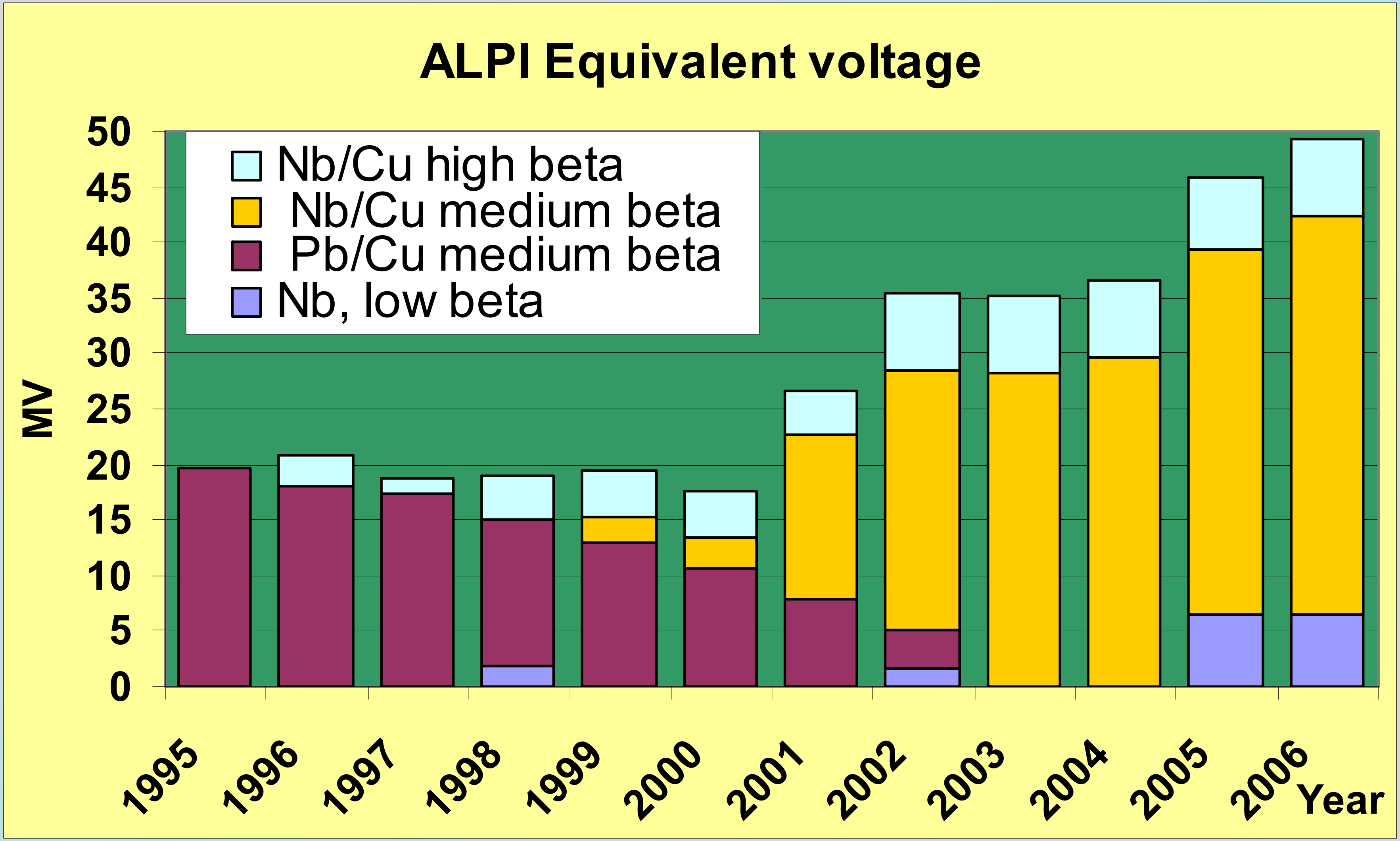

A. Porcellato, INFN-LNL

QWR Sputtering development strategy

- 1987: Funding a research project on QWR Nb sputtering
- 1988-1999: DC biased sputtering choice and system set-up
- 1990: Obtaining good SC performance on samples
- 1991: Sputtering on a simplified prototype
- 1994: Design of a ALPI high β resonator suitable for sputtering production and compatible with existing cryostats
- 1995/1998 Production and installation of 4 high β cavities in ALPI

- 7W reached in laboratory
- 1998: Installation of four high β QWRs, operating at 6 MV/m @ 7W in ALPI
- 1998: First medium β ALPI QWR reaches 4 MV/m @ 7W
- 1999: The upgrading of medium β resonators begin
- 2003 : All the old 44 accelerating cavities have their Pb superconducting layer replaced by Nb

A. Porcellato, INFN-LNL

The Thornton graph has in realilty one more dimension:
the energy of bombarding particles.

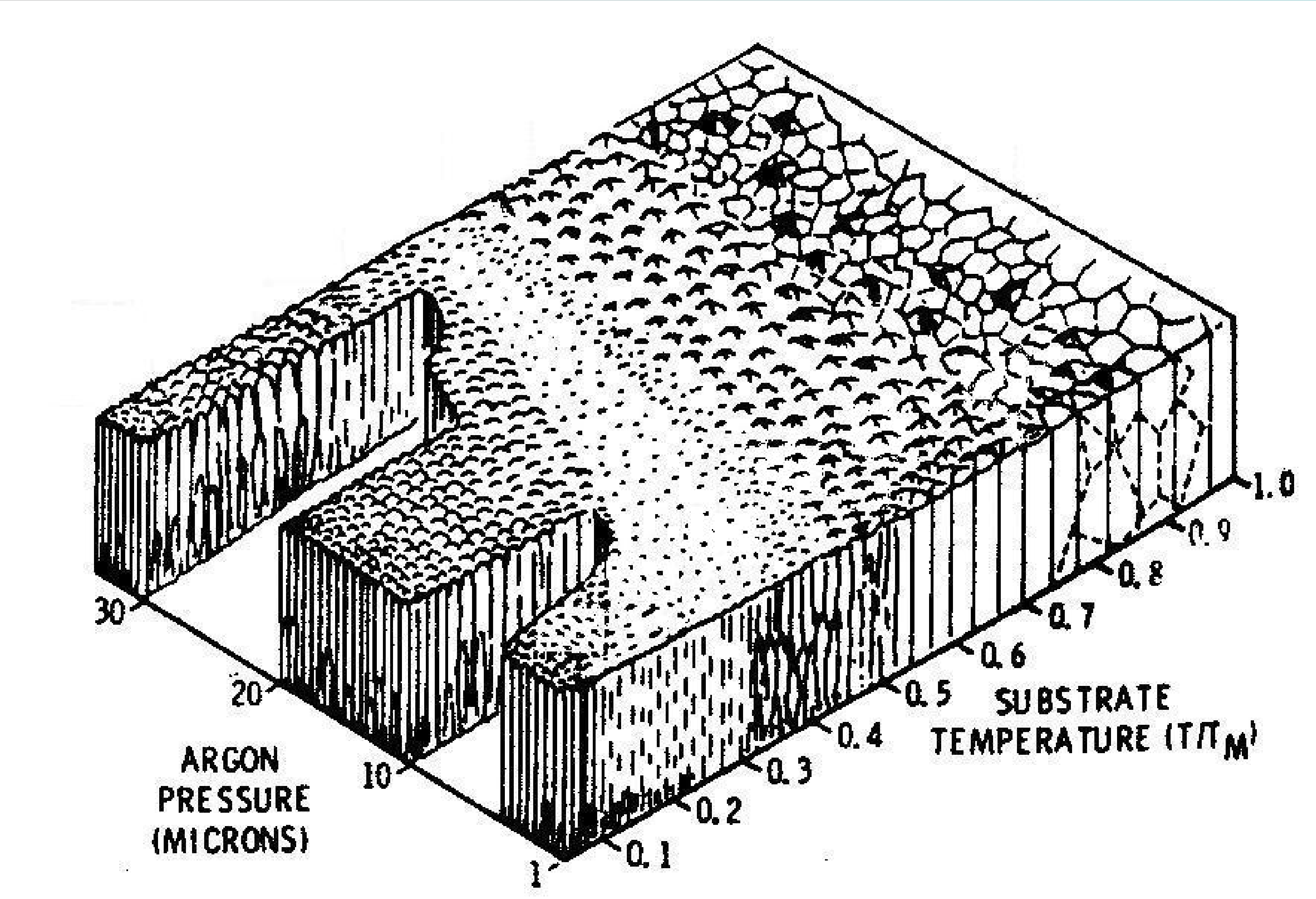

Larry Phillips, Jlab

Illustration of the energetic vacuum deposition by ECR plasma

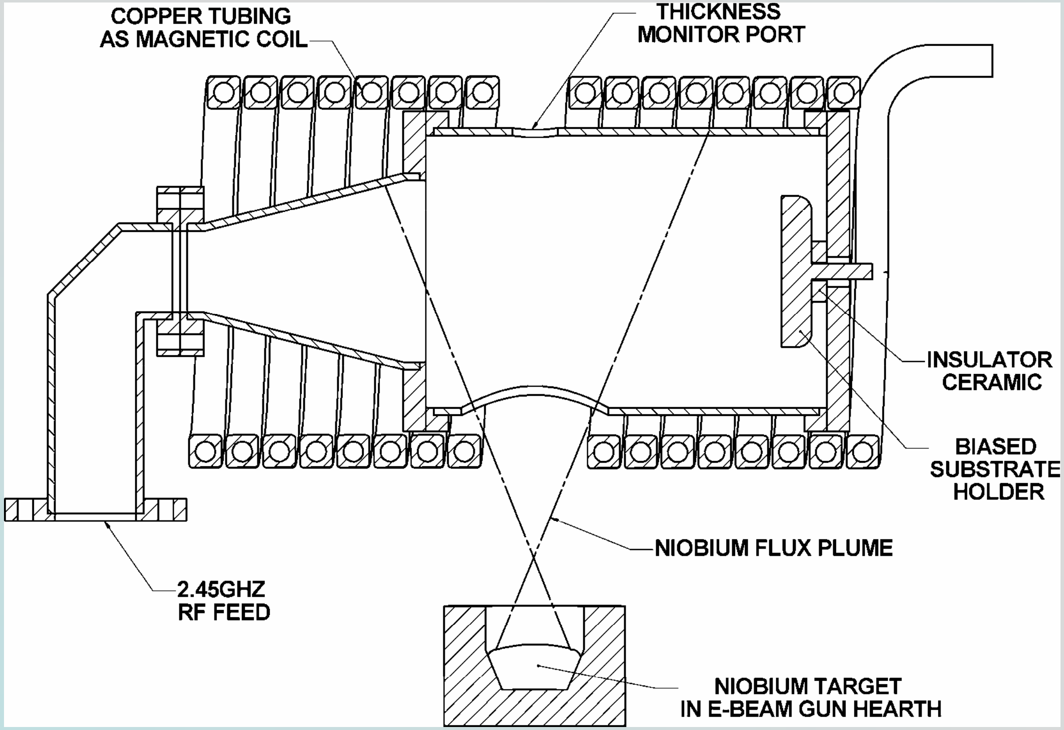

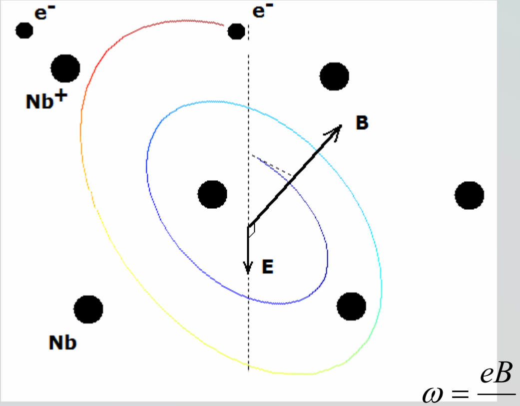

$$\omega = \frac{eB}{m}$$

Wu, G., et al., J. Vac. Sci. Technol. A Vol. 21, No. 4, (2003)

ECR cavity deposition system

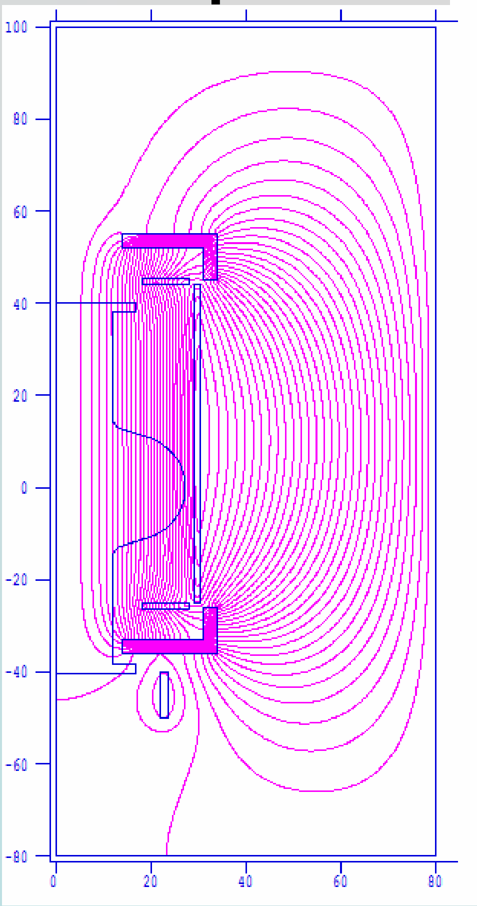

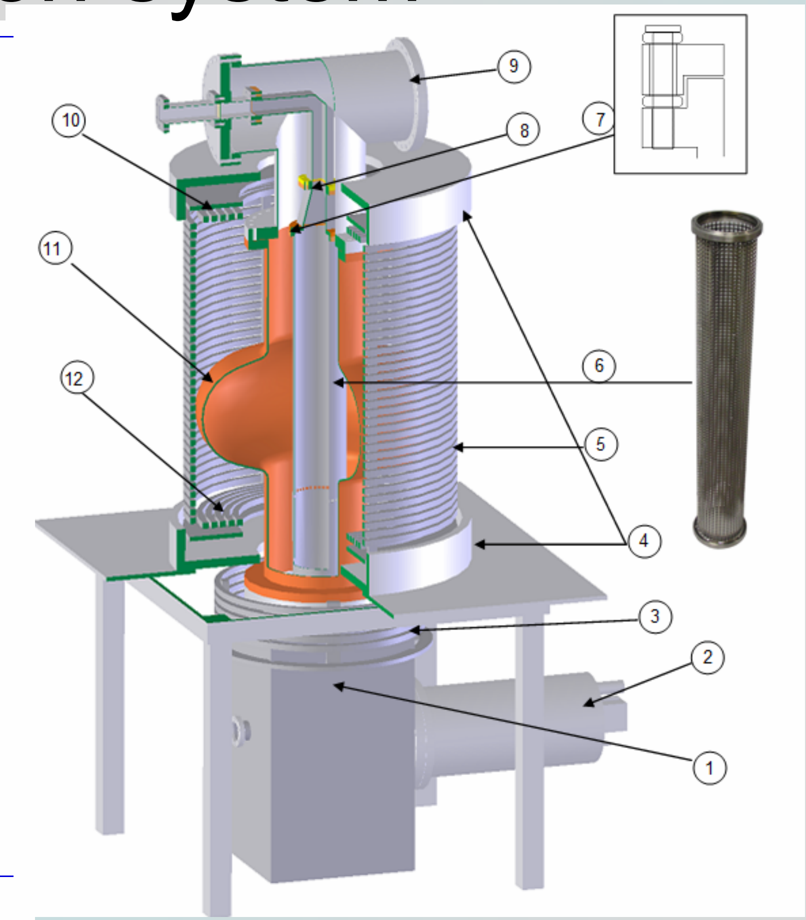

(1) 14kW rod-fed E-gun
(2) 9000 l/s cryopump system
(3) bucking coil for E-gun
(4) top and bottom iron yokes (outer iron shield is removed for illustration)
(5) center coils
(6) Nb grid tube
(7) bias insulator
(8) WR284 waveguide E-bend and horn to the grid tube
(9) "T" vacuum chamber
(10) top pancake coil
(11) Cu cavity
(12) bottom pancake coil.

Potential use for surface cleaning and Nb_3Sn, NbN coatings

Genfa Wu

Inside

E-gun chamber

Genfa Wu

A multilayer sample of Nb-NbO_x-Nb

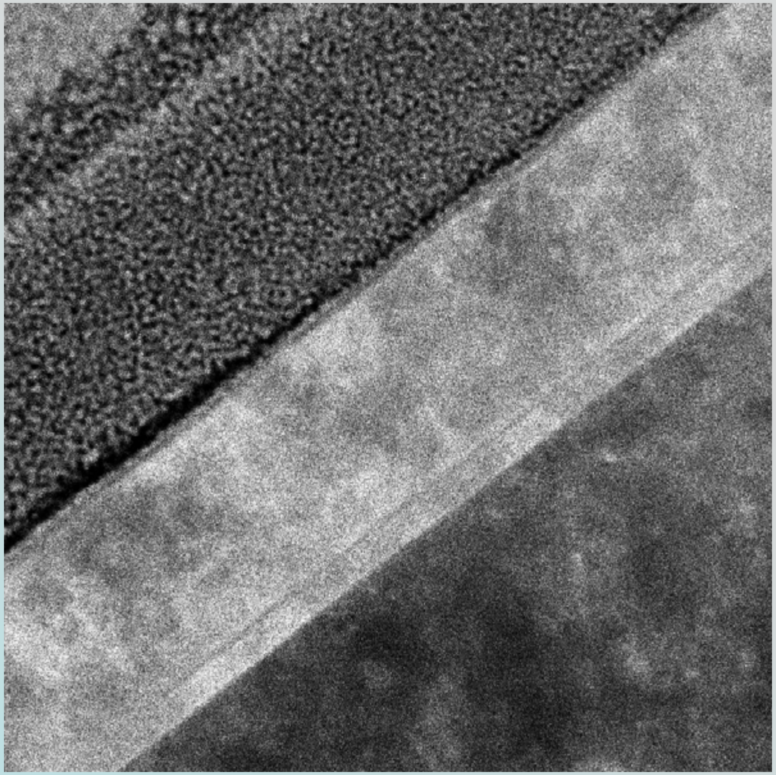

- Copper substrate was prepared by electropolishing.
- First layer of Nb was deposited at 500 V bias voltage.
- Exposed to air to form Nb oxides.
- Second layer (thicker) of Nb was deposited at 60 V bias voltage.
- TEM sample prepared (FIB) and analyzed at SANDIA

TEM by T. Renk, P. Provencio, SNL

Genfa Wu

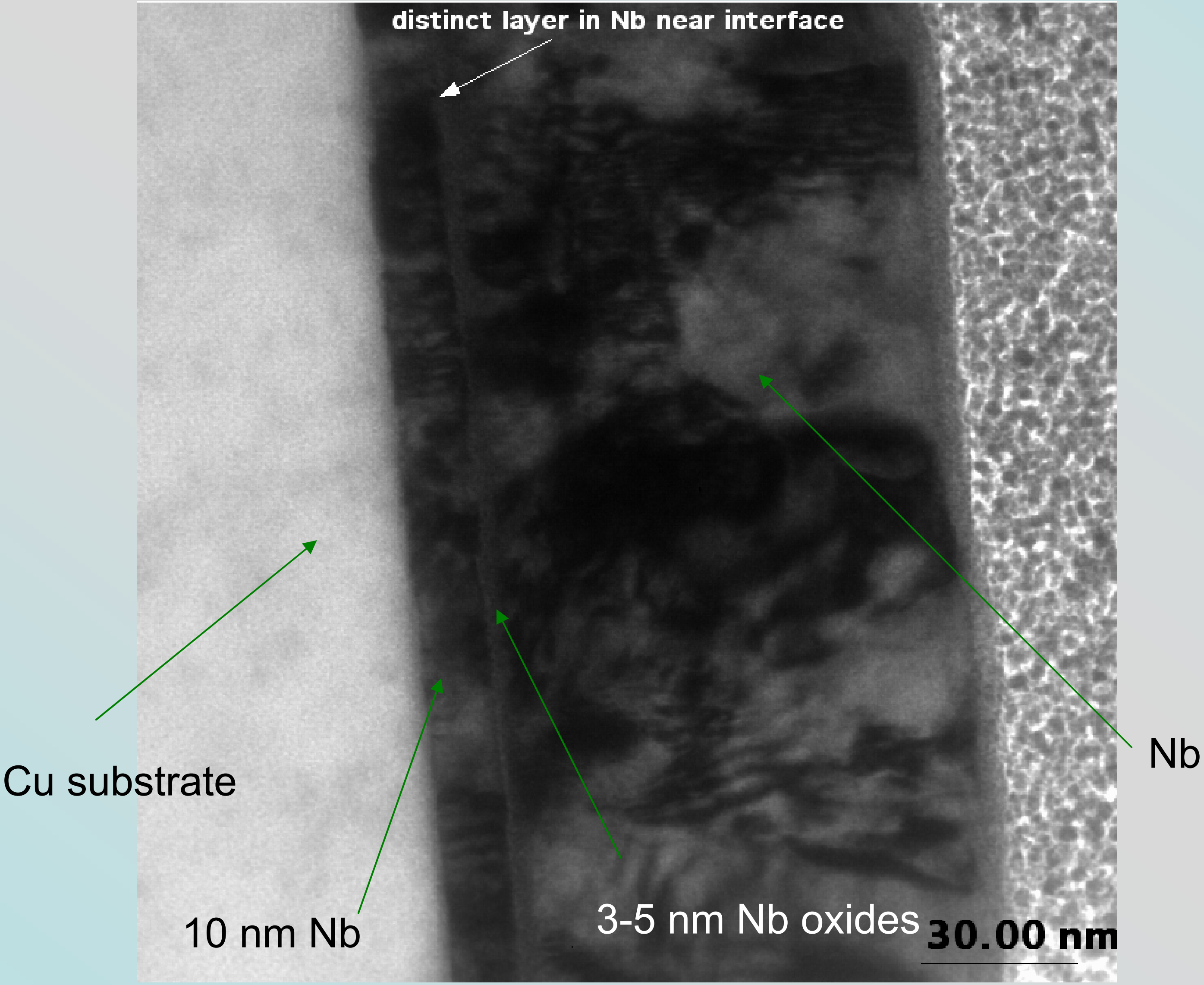
distinct layer in Nb near interface
Cu substrate
10 nm Nb
3-5 nm Nb oxides
Nb
30.00 nm

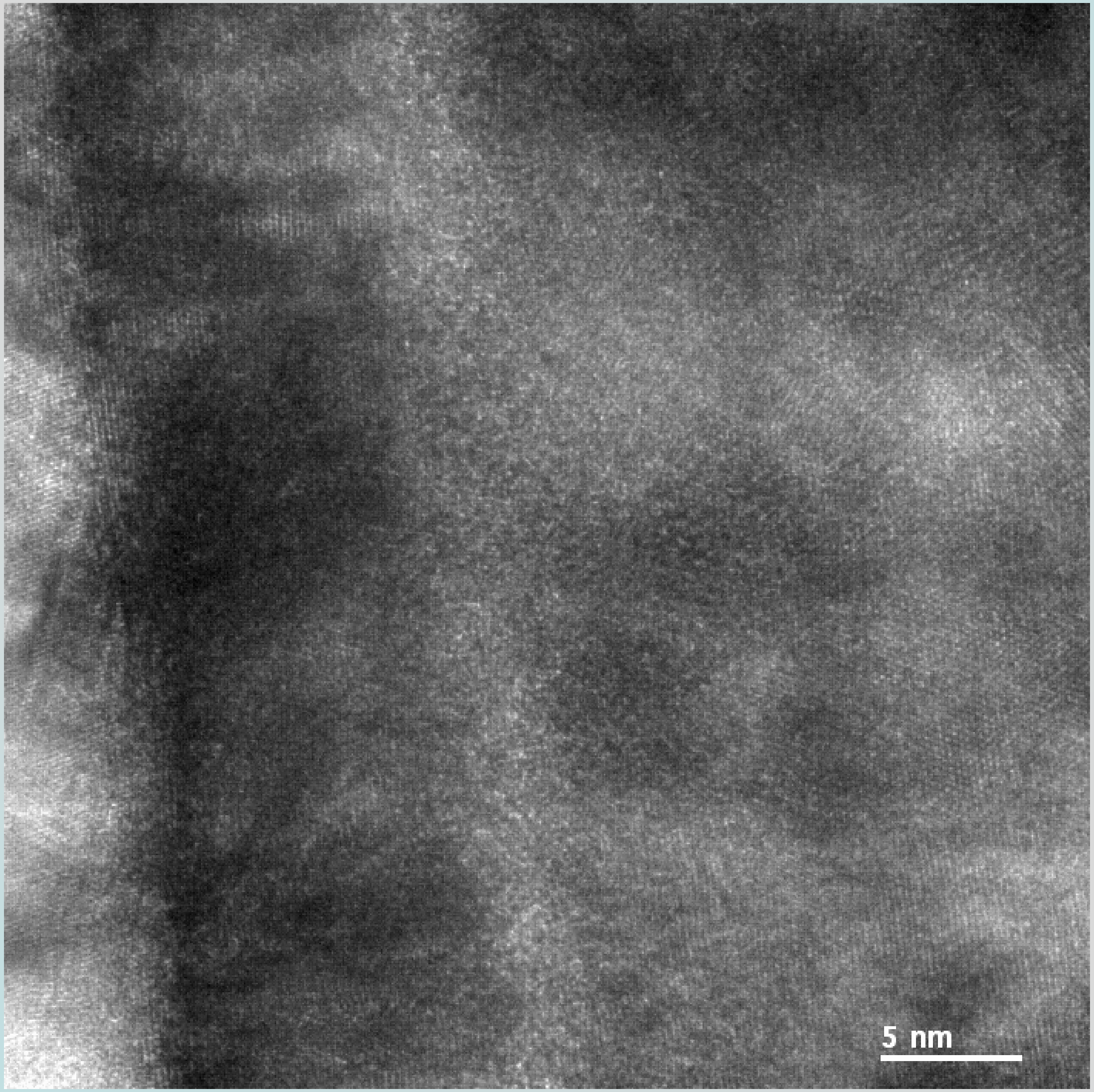

Zoomed view of the interface

Biased Magnetron Sputtering:the construction

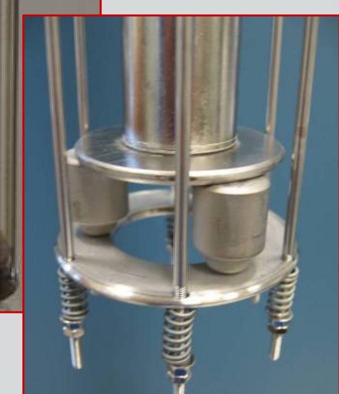

G. Lanza

Biased Magnetron Sputtering:parameters

	CERN type	BIAS INFN-LNL
Cathode Current (A)	3	7
Cathode Power (kW)	1.38	1.86
Bias Voltage (V)	0	100
Pressure (mbar)	$2x10^{-3}$	$3x10^{-3}$
Time (min)	15	20

Biased Magnetron Sputtering: RRR results

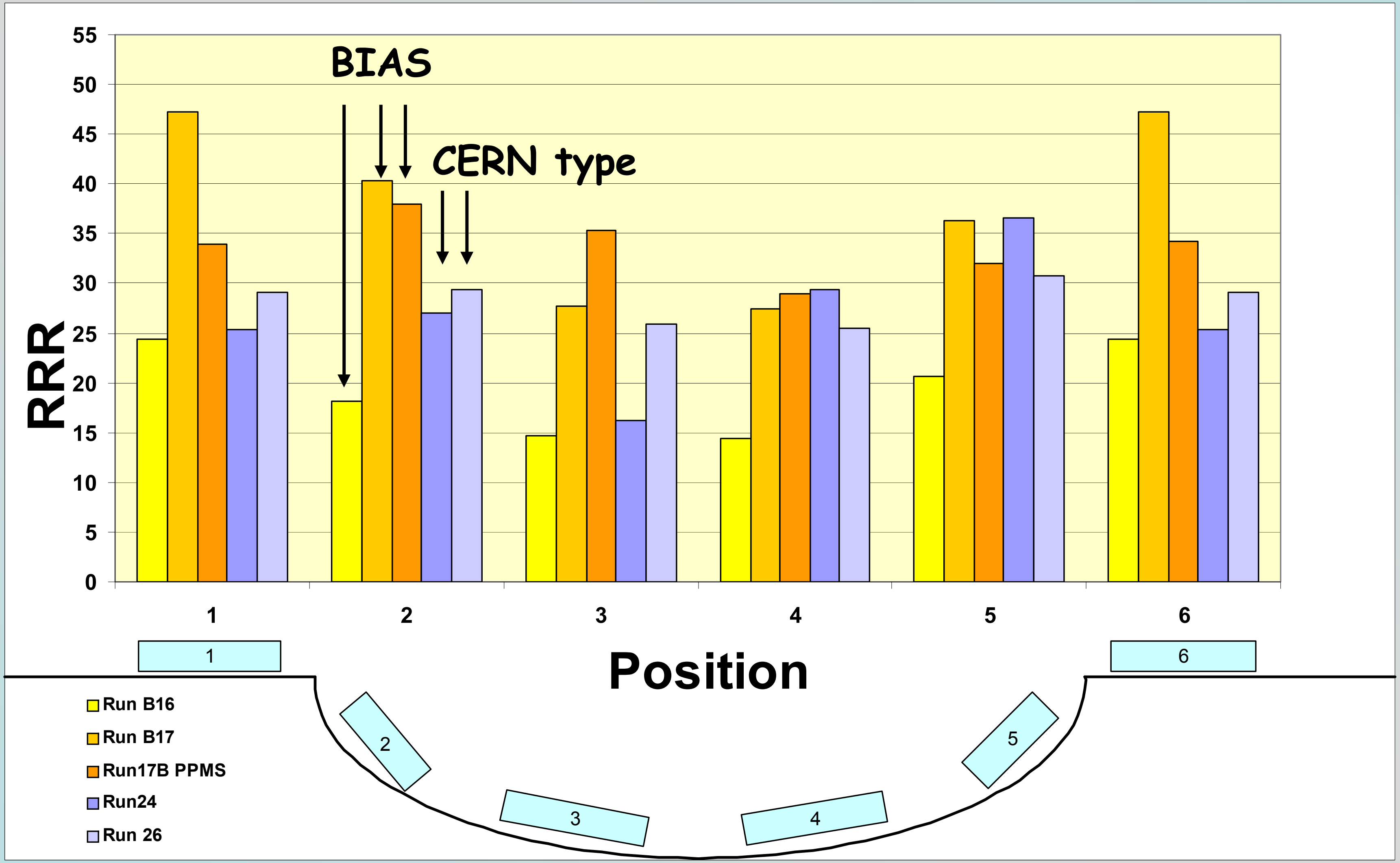

The grid still doesn't affect much the equator part

Elastic modulus and ISE

Biased MS E = 88,95 GPa

unbiased MS E = 54,33 GPa

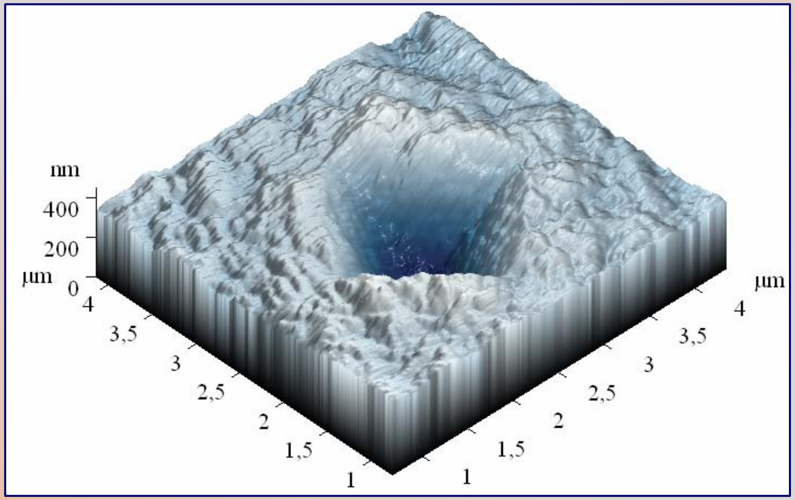

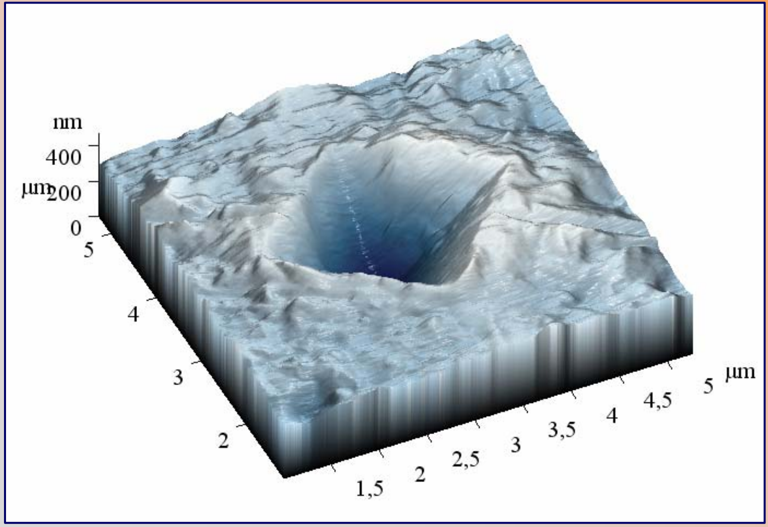

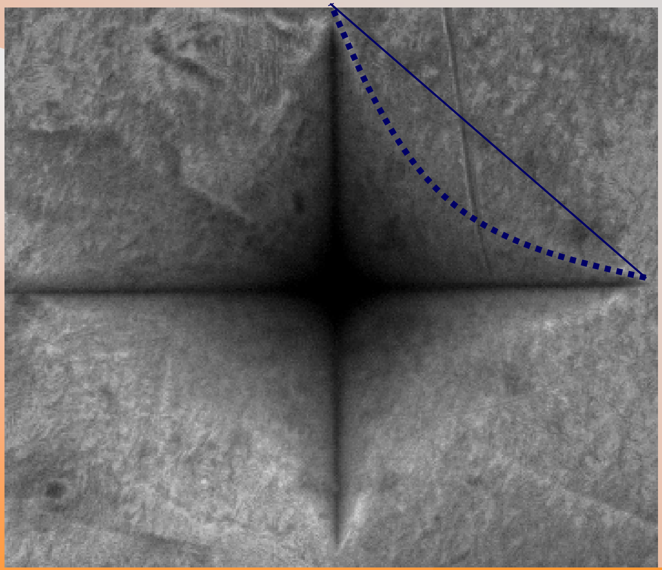

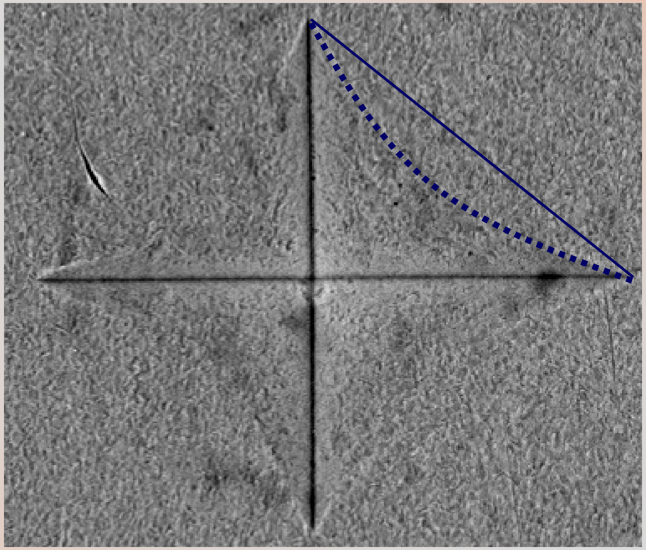

Bemporad et al.: High resolution morphological and mechanical characterization of niobium films obtained by MS and Bias-MS PVD

Vickers indentation at different loads

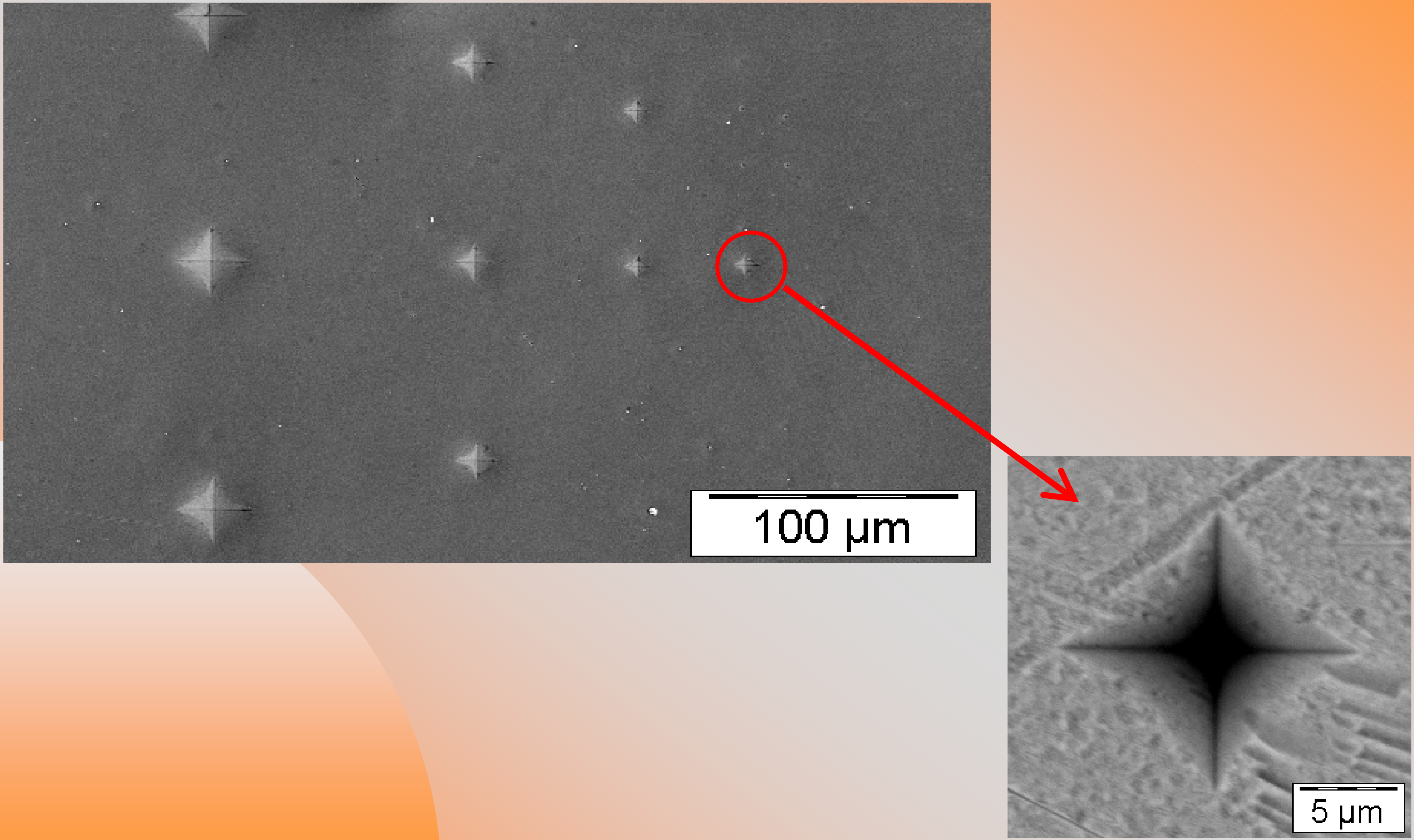

Bemporad et al.: High resolution morphological and mechanical characterization of niobium films obtained by MS and Bias-MS PVD

Hardness comparison

biased MS (#YY-767)

unbiased MS (#12-766)

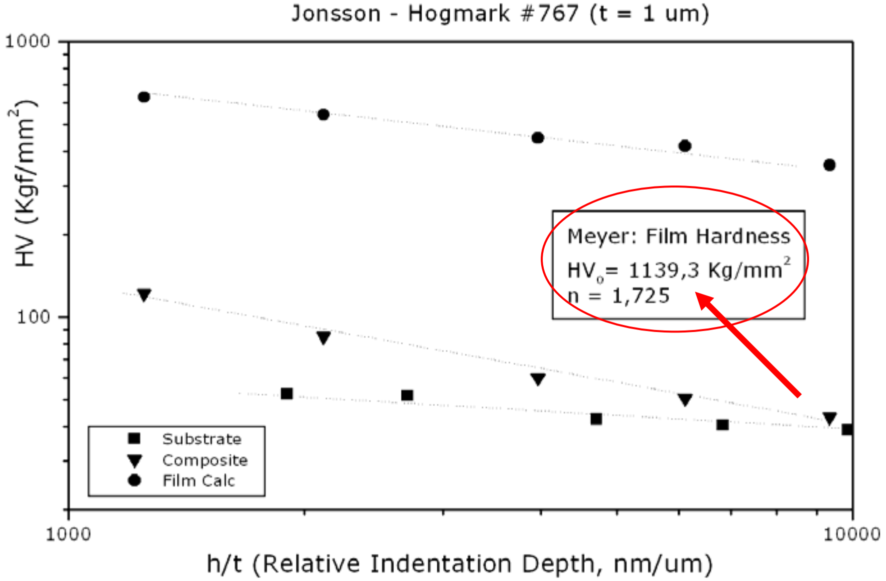

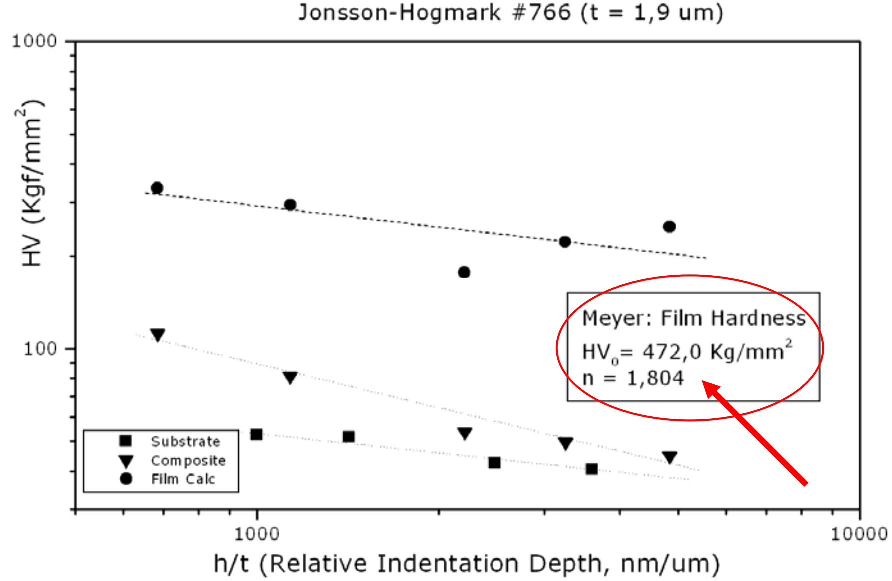

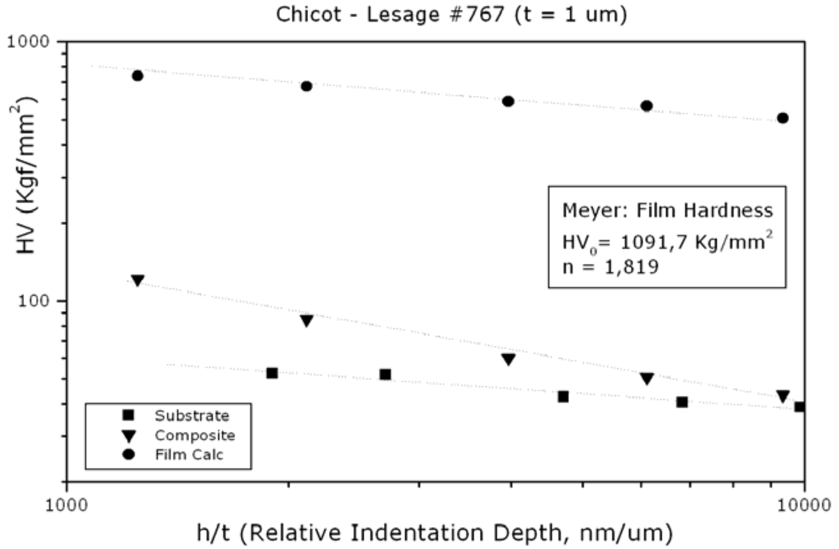

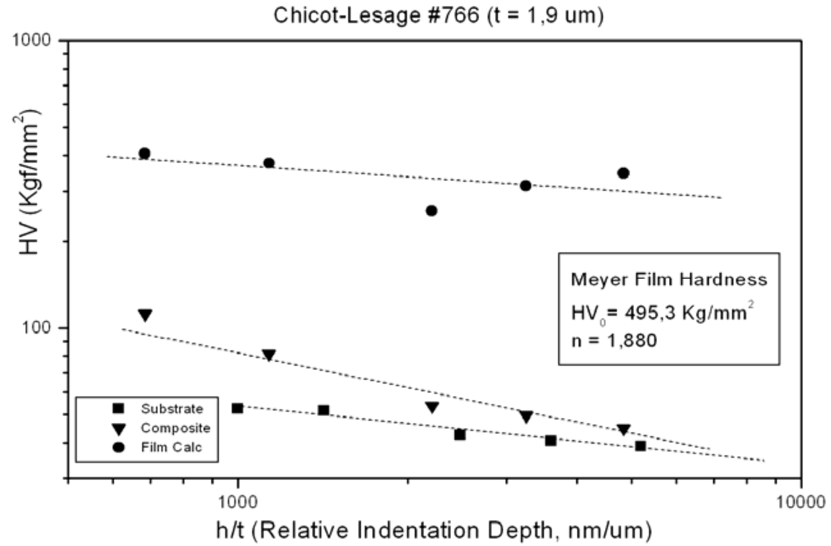

Hardness comparison

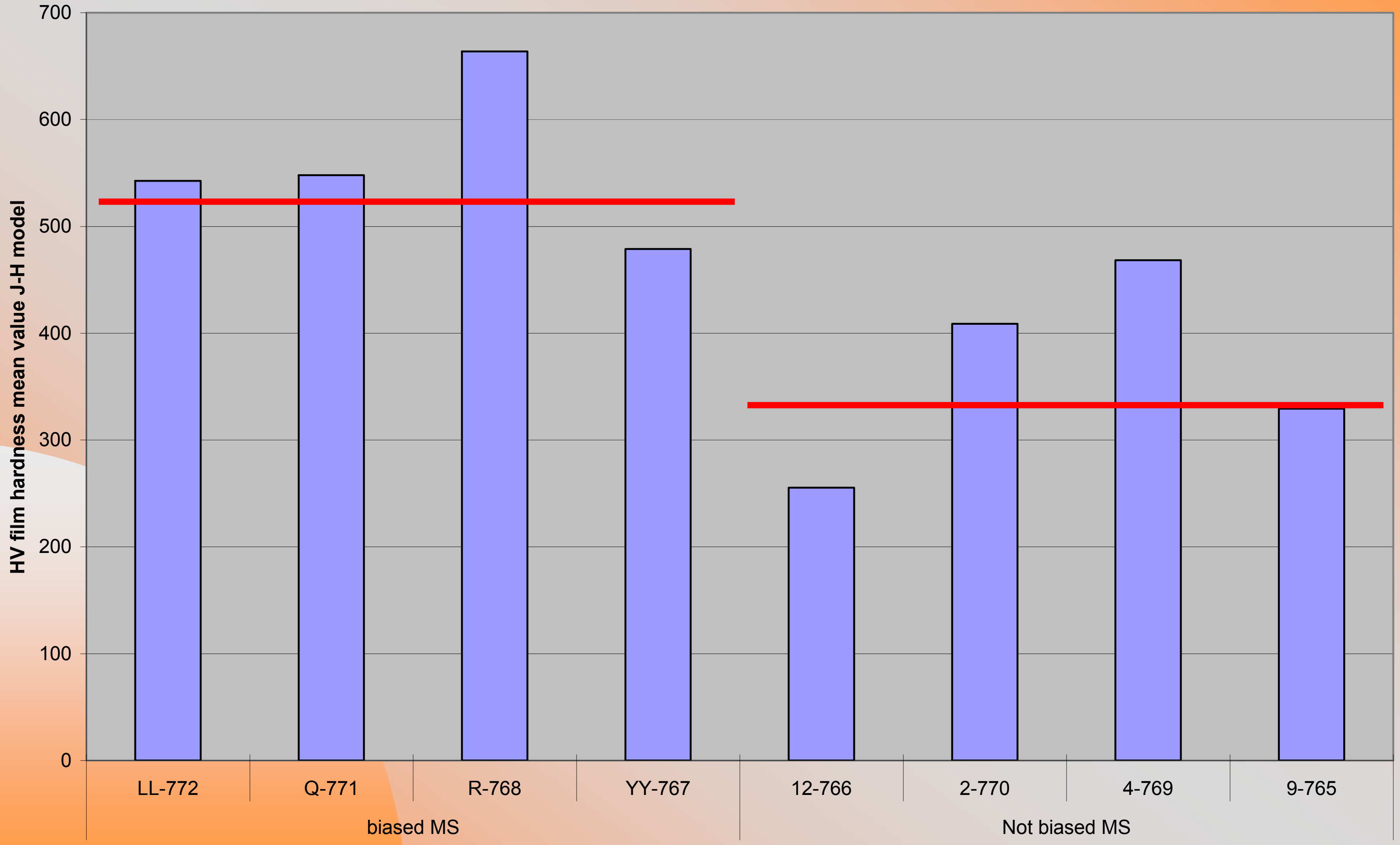

Bemporad et al.: High resolution morphological and mechanical characterization of niobium films obtained by MS and Bias-MS PVD

Surface defects: FIB

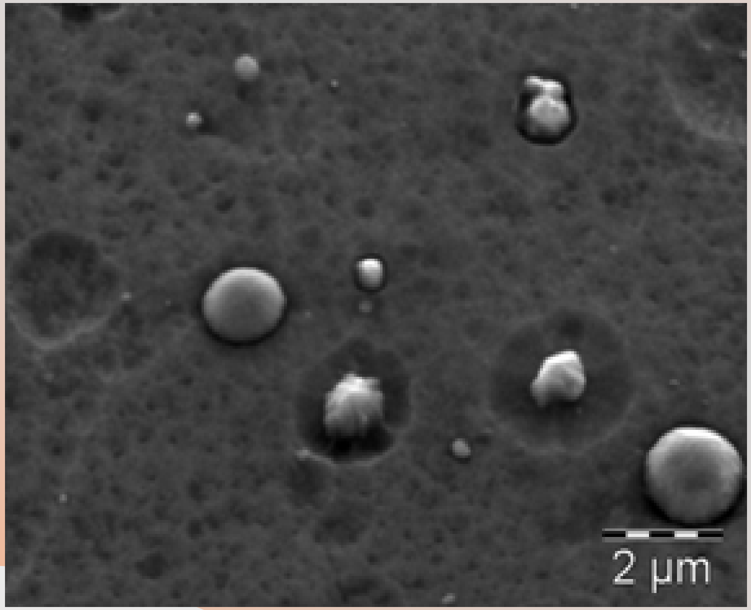

(25 kV, 8.000 x, SEM SE detector)

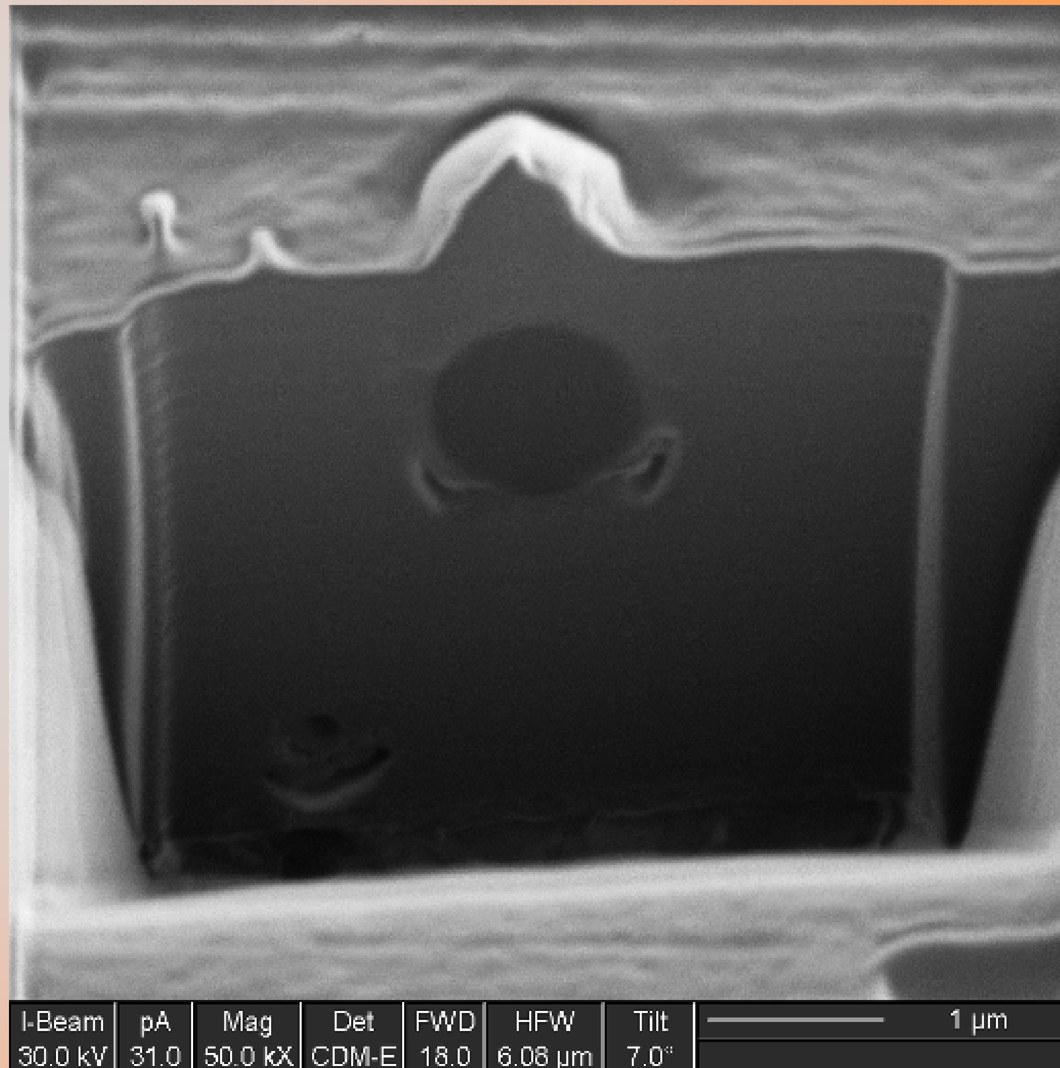

Bemporad et al.: High resolution morphological and mechanical characterization of niobium films obtained by MS and Bias-MS PVD

MORPHOLOGY OF NIOBIUM FILMS SPUTTERED AT DIFFERENT TARGET – SUBSTRATE ANGLE

D. Tonini, C. Greggio, G. Keppel, F. Laviano, M. Musiani, G. Torzo, V. Palmieri

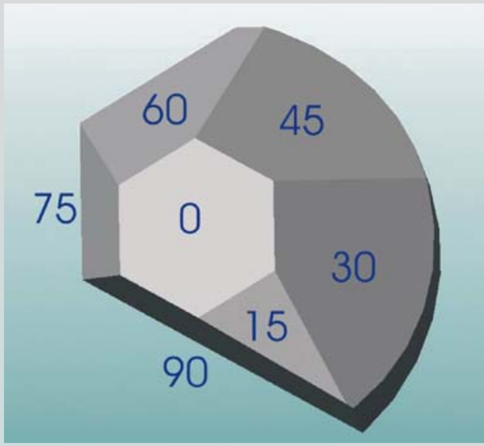

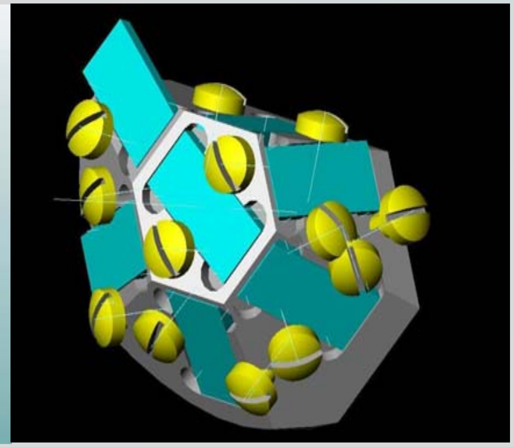

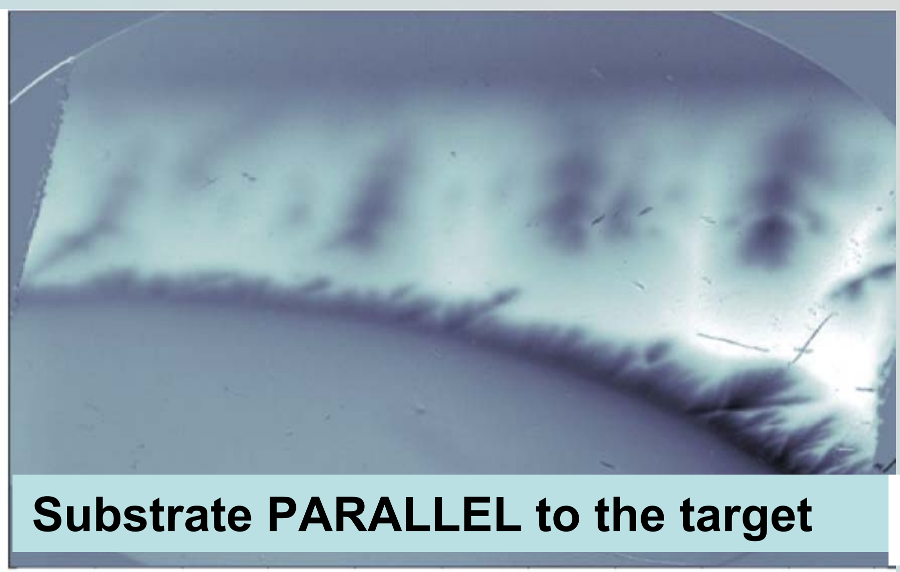
Substrate PARALLEL to the target

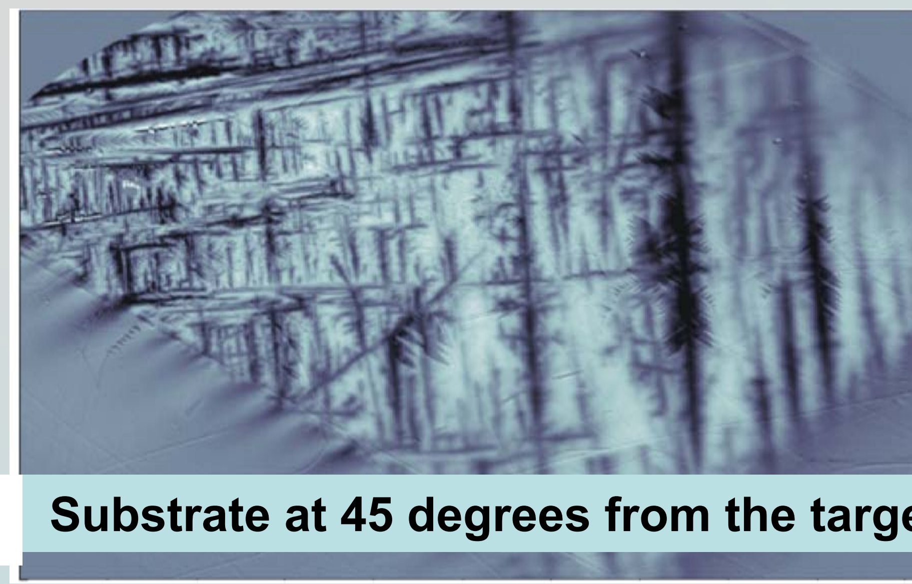
Substrate at 45 degrees from the target

Simulation of film growth

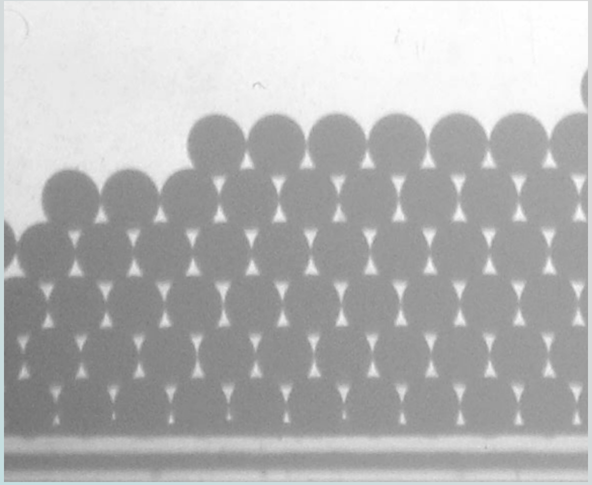

0 degrees

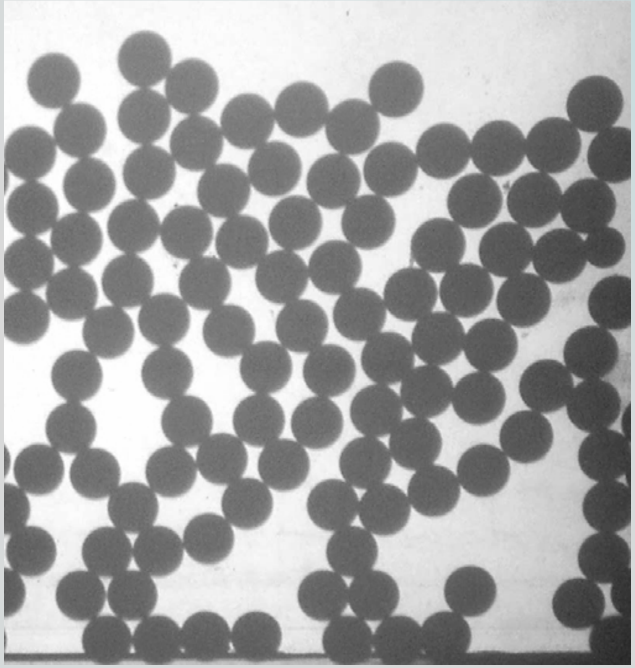

45 degrees

MgB_2 film ID # MO 6006 from Brian Moeckly. Alumina substrate. ZFC T=5.3K. Dendridic flux instability

#15 H=13.2 mT

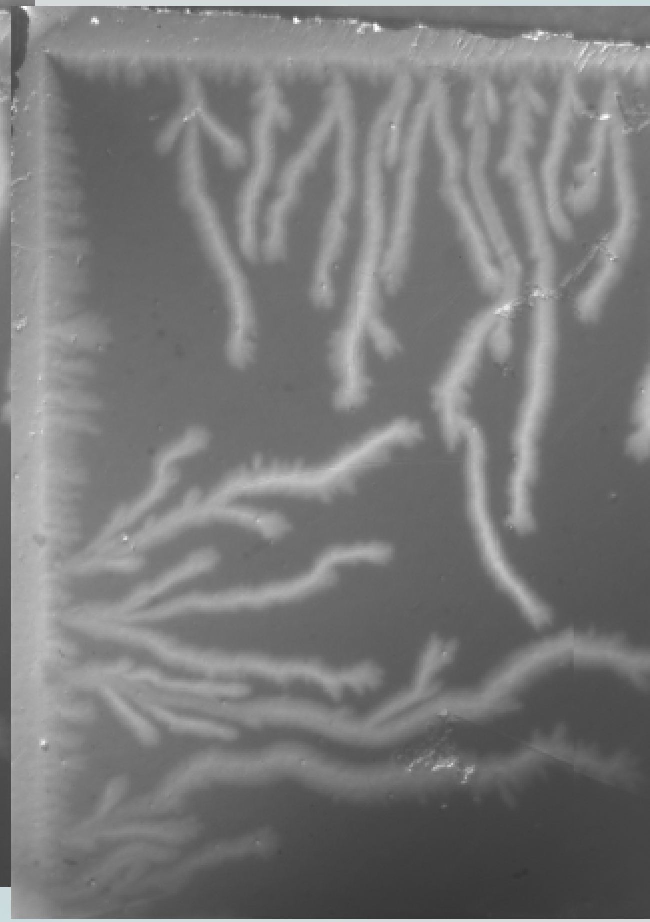

#19 H=20 mT

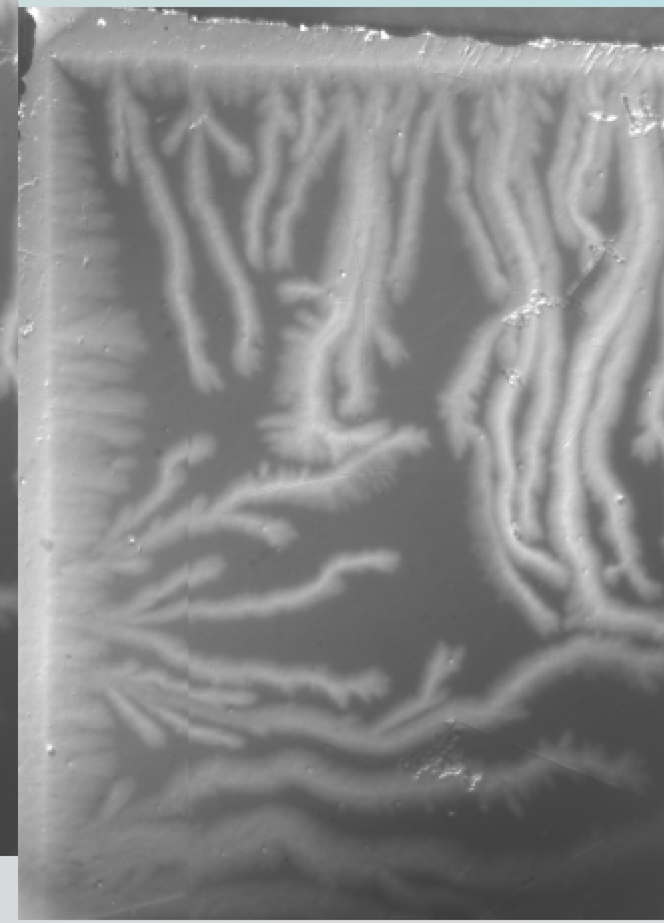

#23 H=32 mT

A. Polyanskii

MgB_2 film ID # MO 6006 from Brian Moeckly. Alumina substrate. ZFC T=5.3K Dendridic flux instability

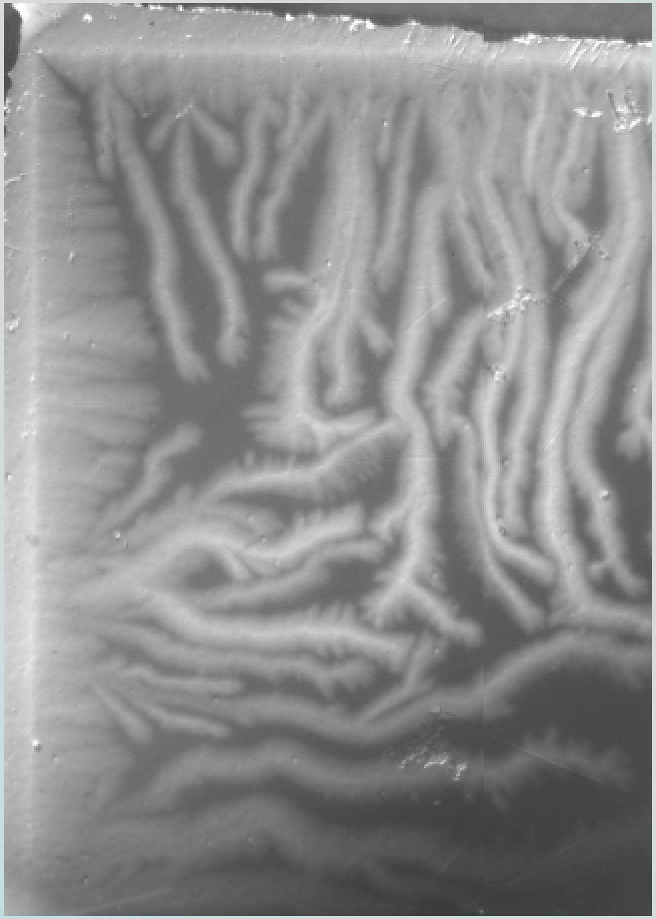

#25 H=40 mT

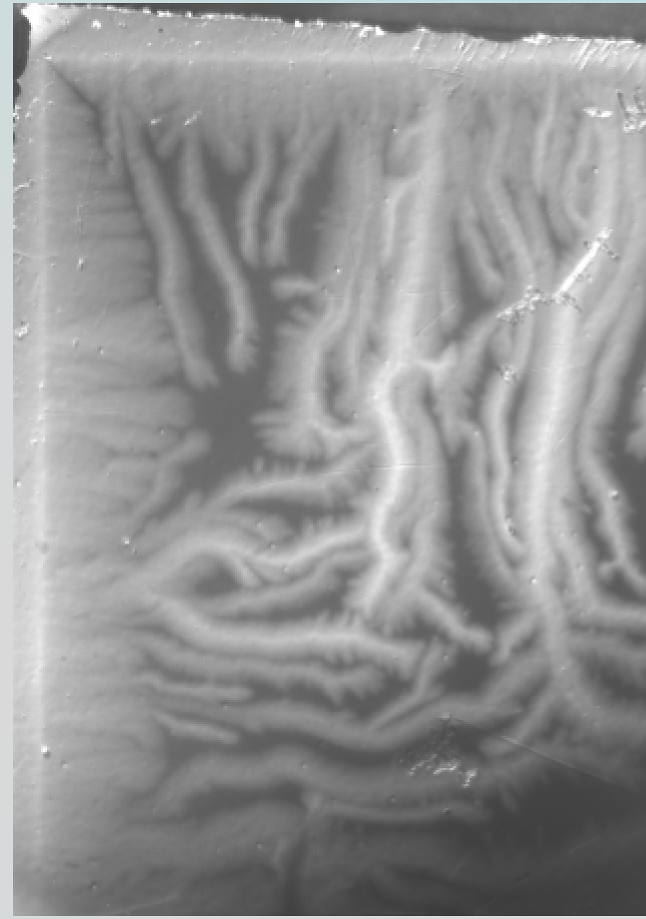

#27 H=48 mT

A. Polyanskii

MgB2 thin film on STOCBS 33-1-5 ZFC T=16K increasing H from 0 to 120mT Bean flux penetration

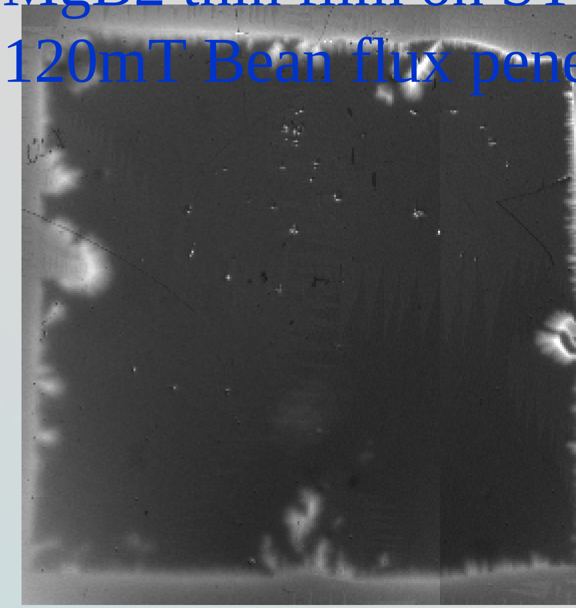

#1 H=8mT

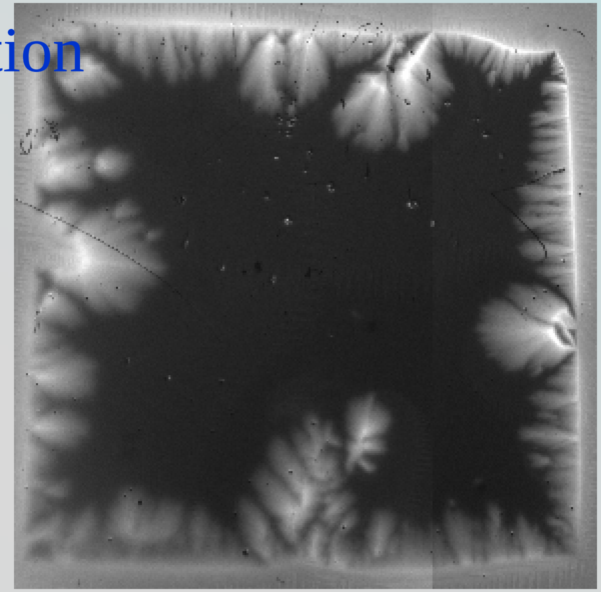

#5 H=20mT

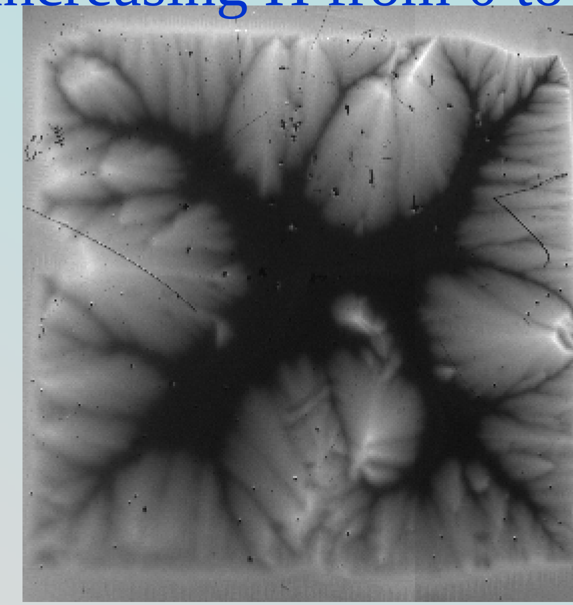

#9 H=40mT

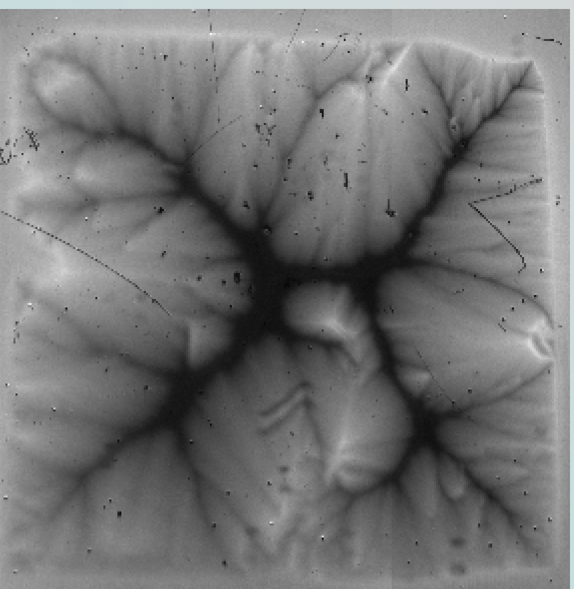

#11 H=60mT

#13 H=80mT

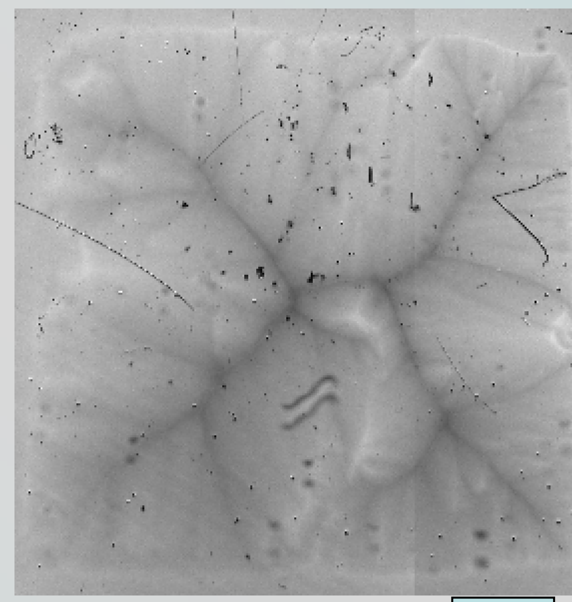

#17 H=120mT

1 mm

OPTICAL IMAGES OF REGULAR AND WELD SAMPLES

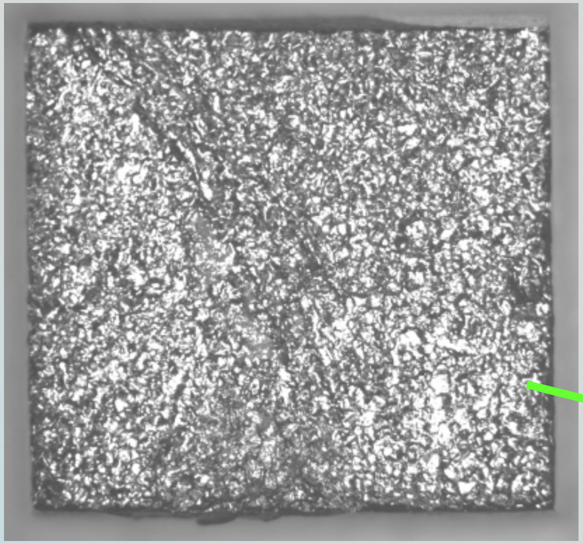

REGULAR AREA: small grain size

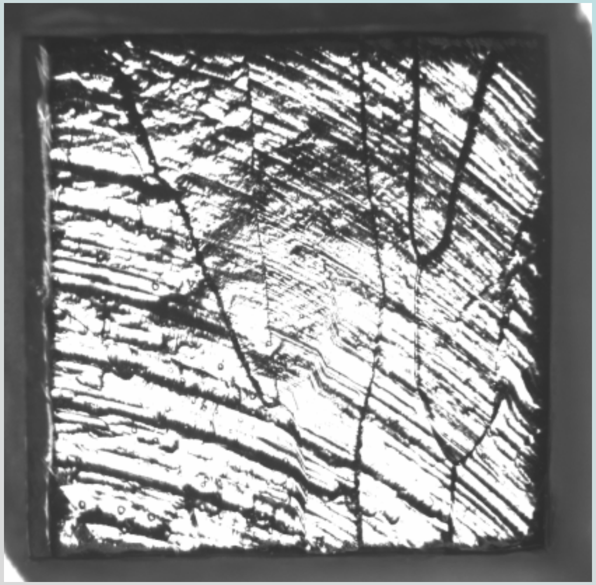

WELDED AREA: large grain size

Machine marks (like grooves), large grains and height steps at GBs are well visible

MOI of Weld samples with big grains taken through a typical cavity optimization process: 5 steps

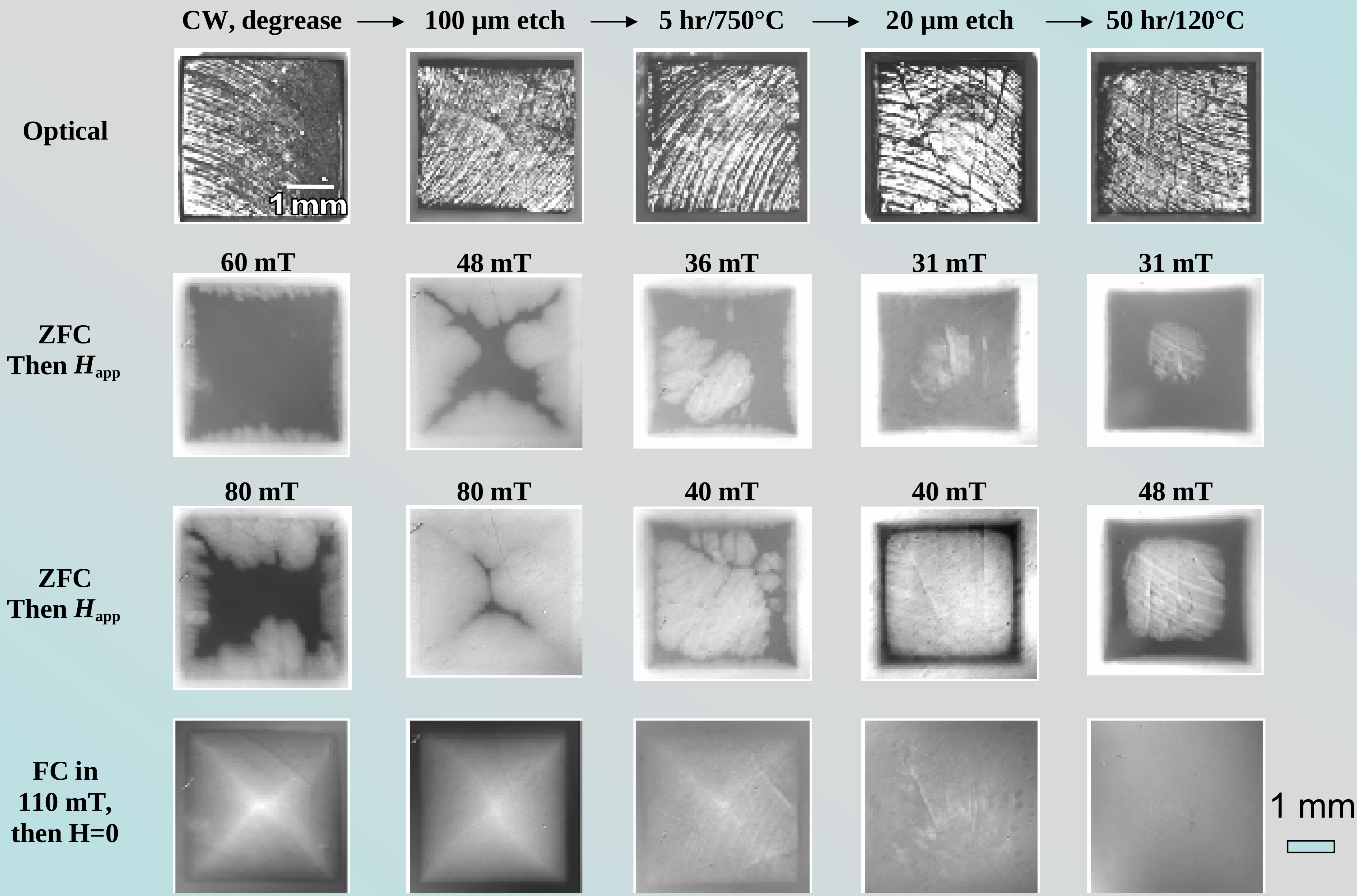

Erlangen LSM setup

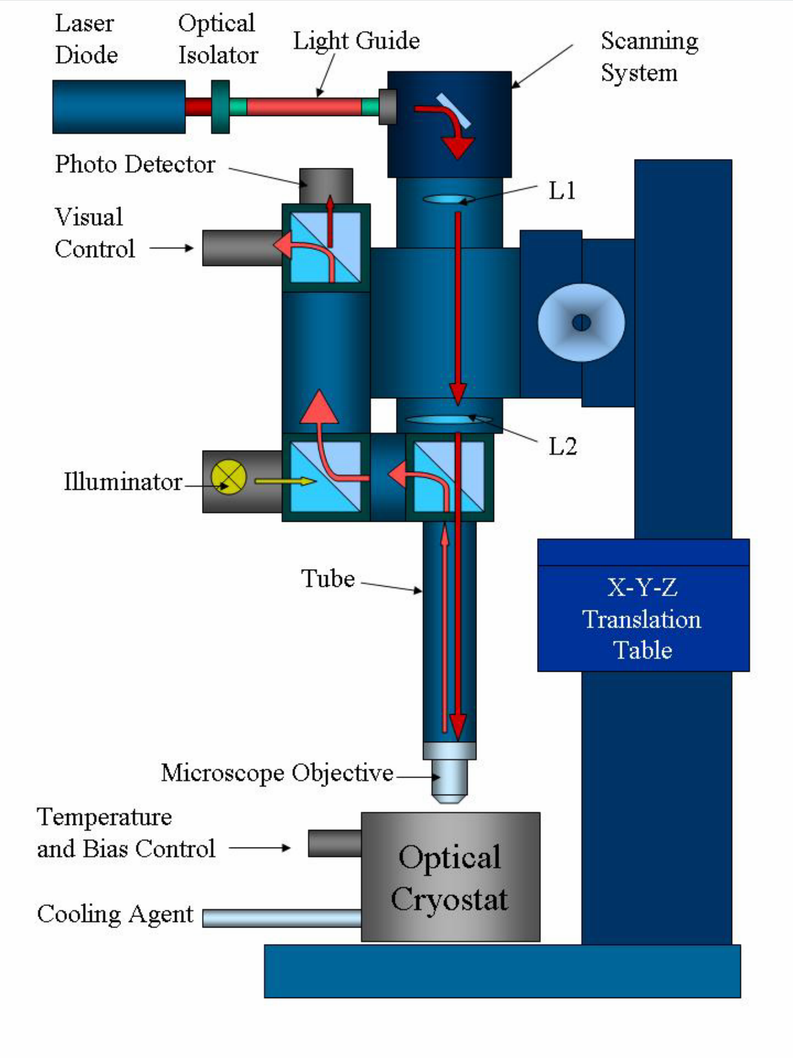

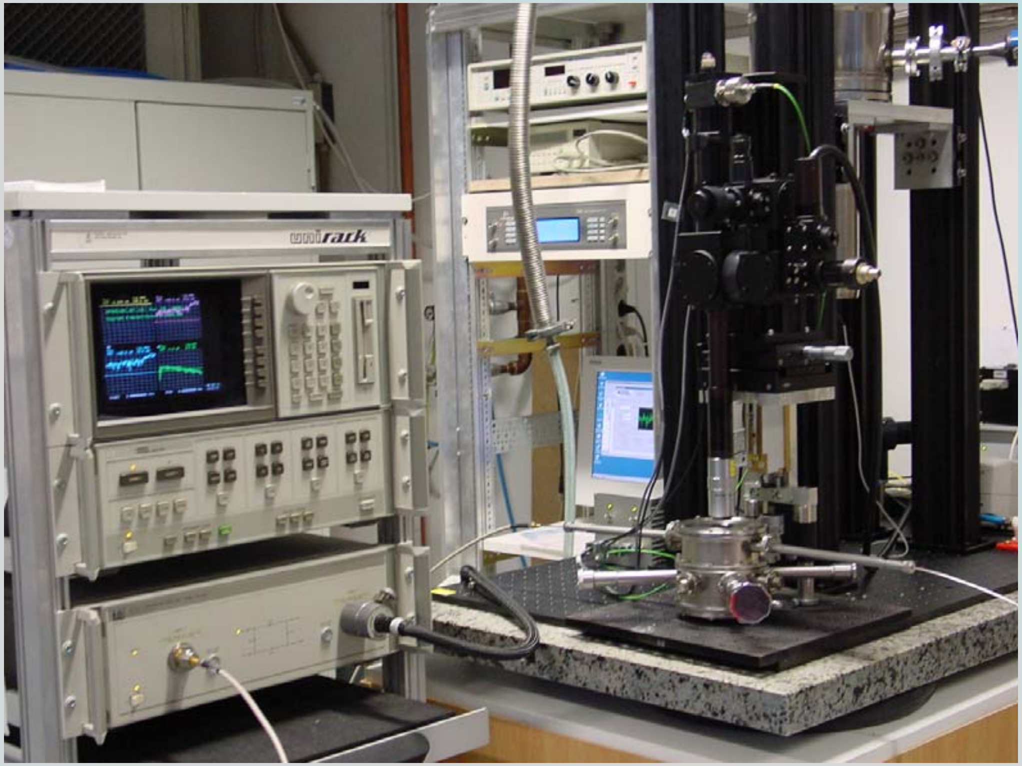

A.P. Zhuravel, S. M. Anlage and A.V. Ustinov,

Imaging of Microwave Currents and Microscopic Sources of Nonlinearities in Superconducting Resonators

Motivation / Goals

To **image rf currents** in operating superconducting microwave circuits and devices

To identify **sources of microwave nonlinearities** in superconductors

To investigate how rf currents are redistributed by **μm- and nm-scale defects**

To **develop new methods** to investigate microwave nonlinearities in superconductors

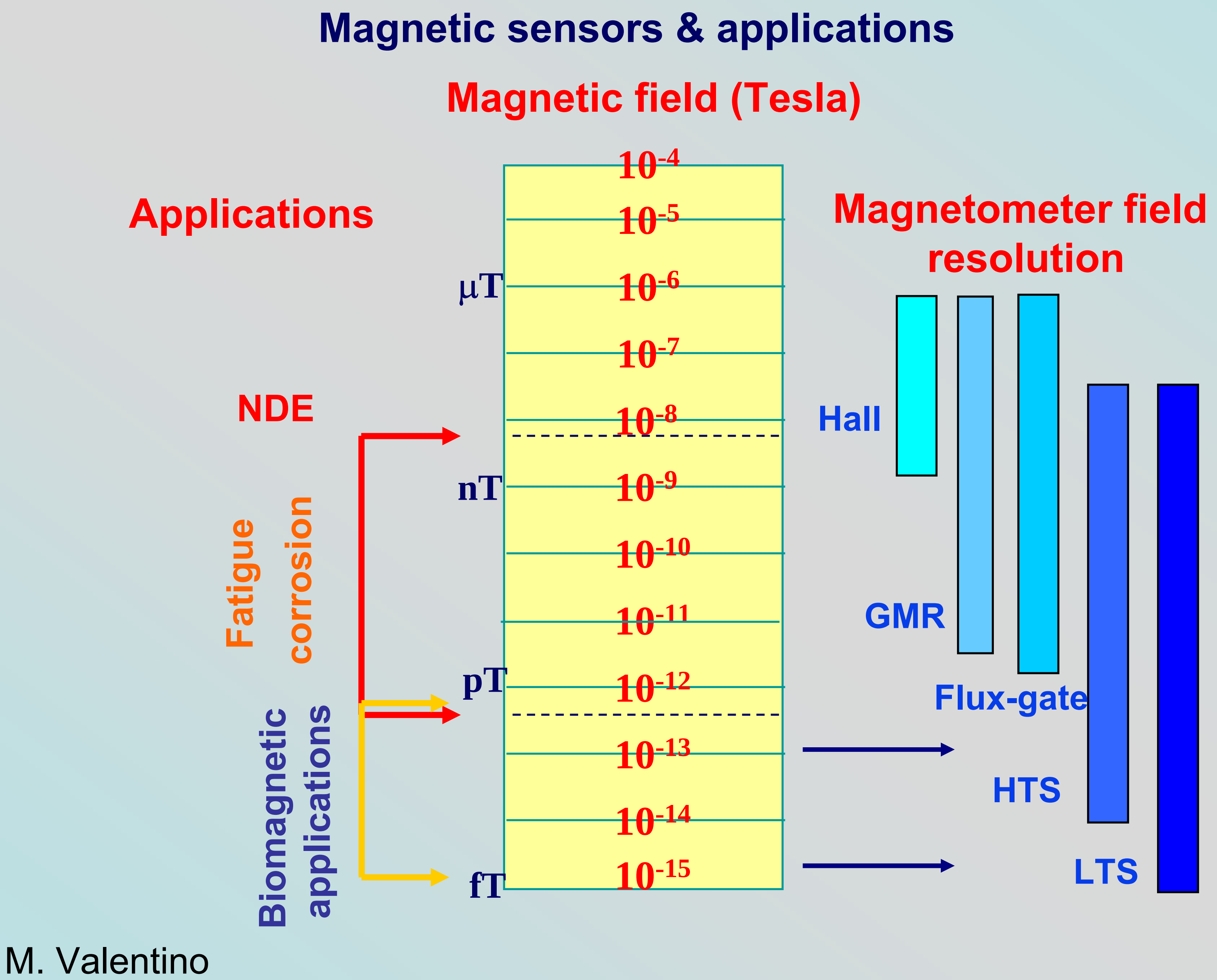
Magnetic sensors & applications
Magnetic field (Tesla)
Applications
Magnetometer field resolution
10-4
10-5
10-6
10-7
10-8
10-9
10-10
10-11
10-12
10-13
10-14
10-15
μT
nT
pT
fT
NDE
Fatigue
corrosion
Biomagnetic
applications
Hall
GMR
Flux-gate
HTS
LTS
M. Valentino

Buffered Chemical polishing of Niobium

BCP 1:1:1 to BCP 1:1:2 increasing the H_3PO_4 percentage the magnetic signal Intensity increase

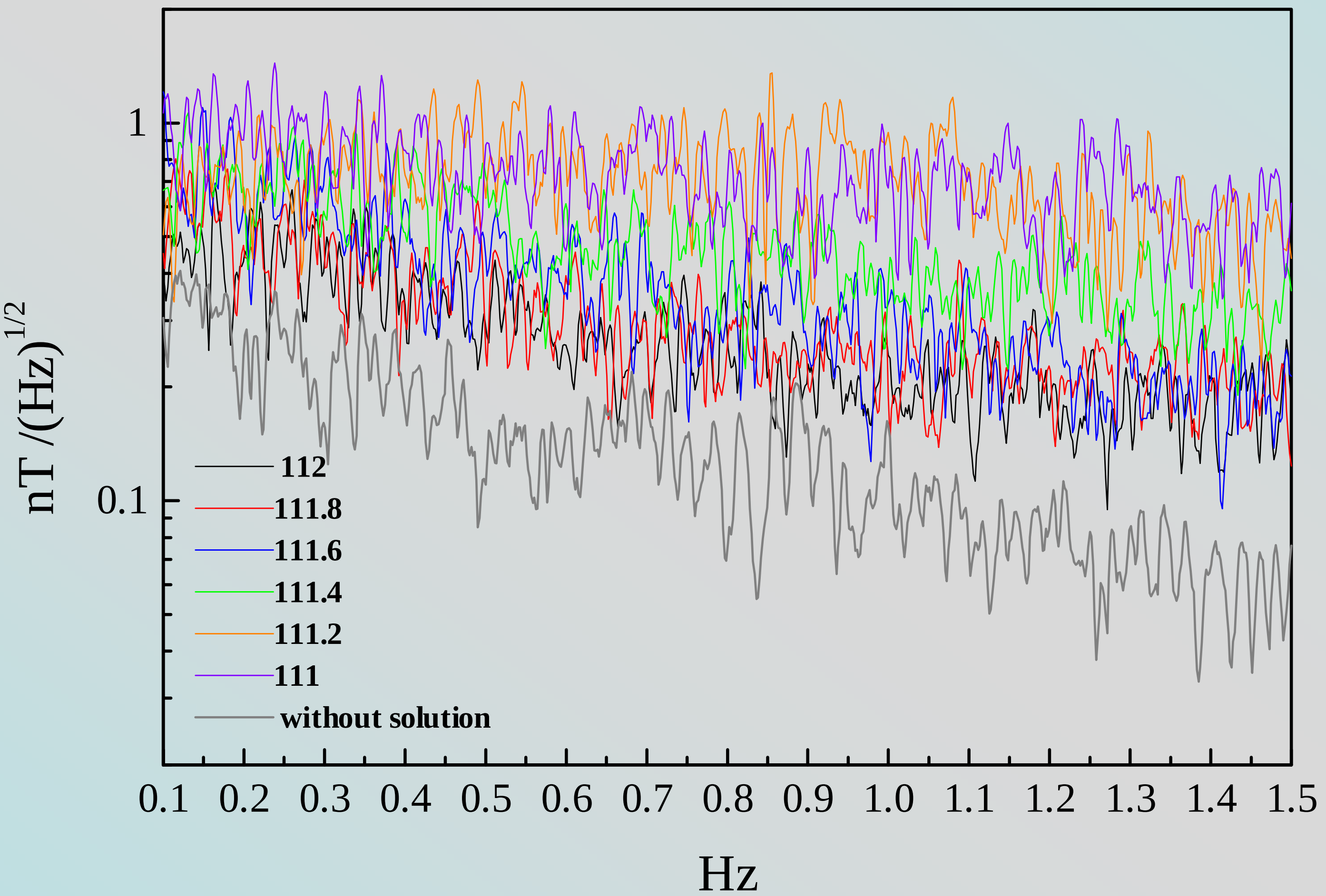

M. Valentino

The IMD technique

Input signal made up of two signals of equal magnitude but different frequencies:

$$V_{in} = V_1 \cos(2\pi f_1 t + a_1) + V_2 \cos(2\pi f_2 t + a_2)$$

$|V_1 - V_2| < 0.1$ dBm, $f_1 - f_2 = 20$kHz << 3 dB bandwidth

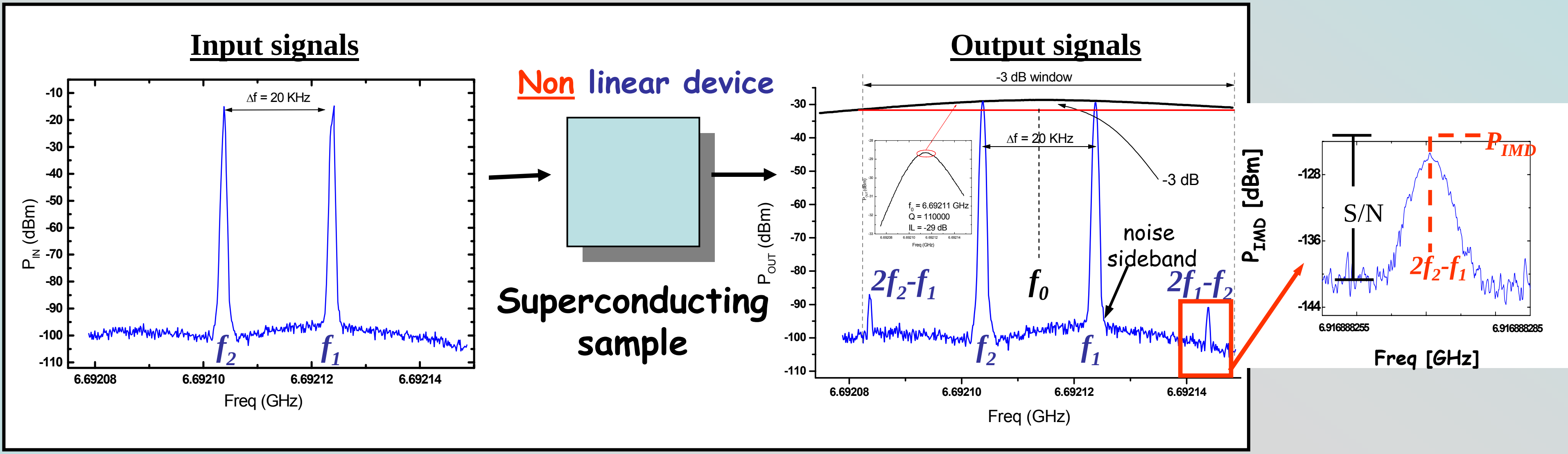

High purity CW mw sources and high sensitivity spectrum analyser set noise threshold ~ -140 dBm

Dynamic range can be larger than 100 dB

Higher order products are usually reduced in amplitude

A. Andreone

Experimental set-up

A. Andreone

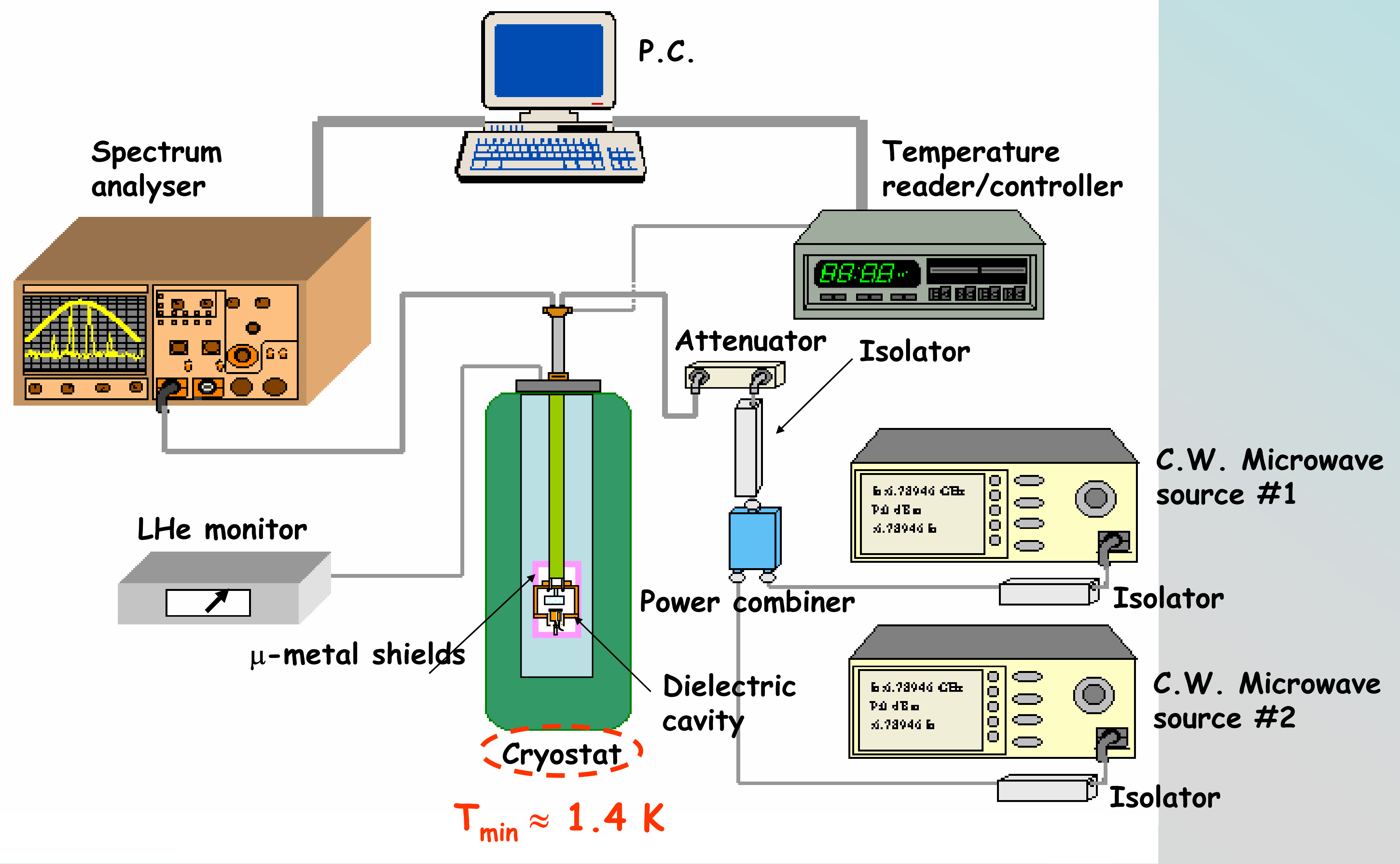

CaC_6: a graphite intercalated superconductor

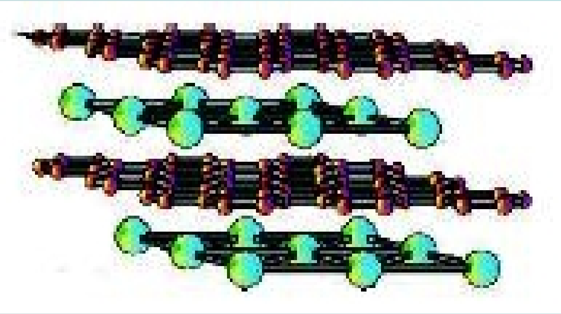

$T_C = 11.2$ K

Both superfluid density and microwave losses give evidence of conventional, weak-coupled, superconductivity ($2\Delta/K_BT_C \sim 3.6$)

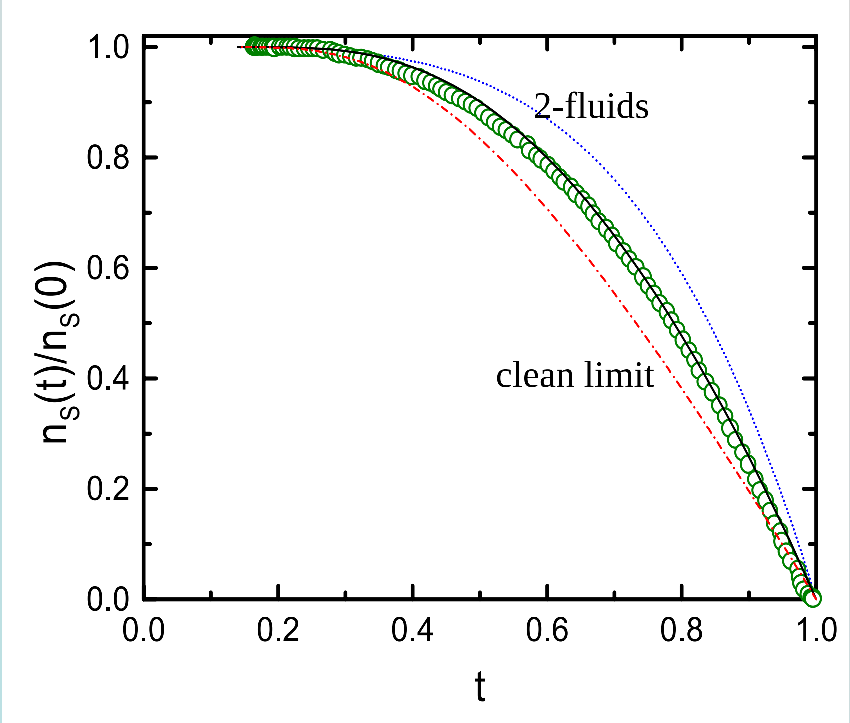

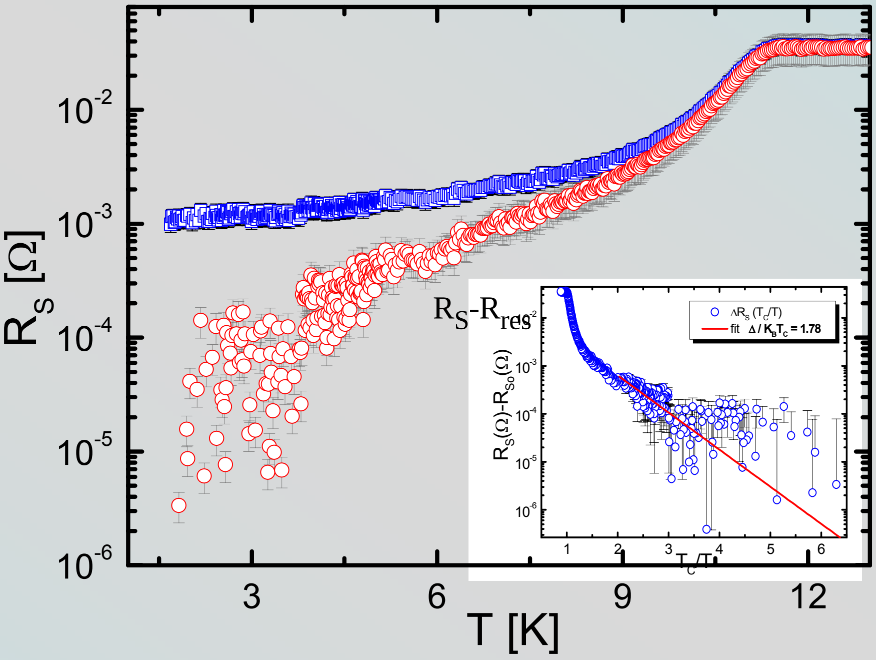

G. Lamura *al*, Phys. Rev. Lett. **96**, 107008 (2006); G. Cifariello *et al.*, M²S 2006

Thermometric system (2)

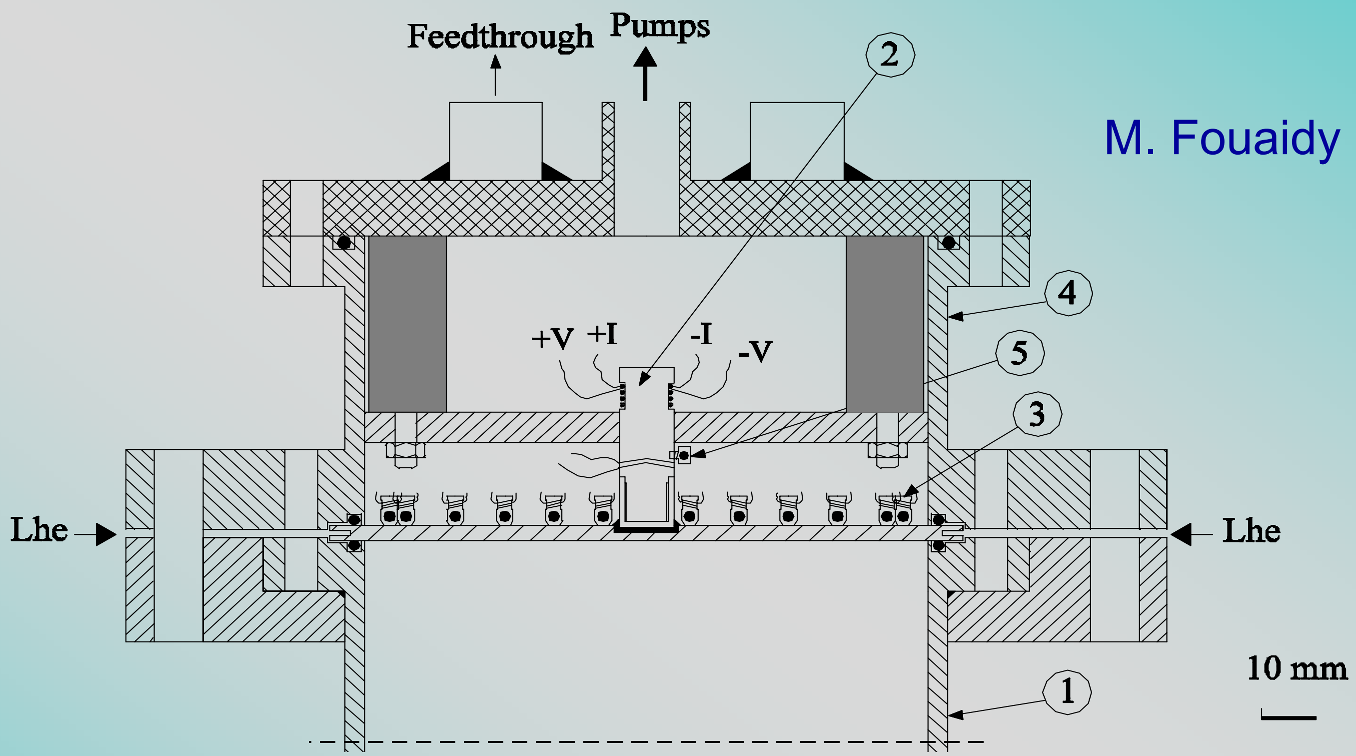

M. Fouaidy

① Niobium cavity TE011 mode f=4GHz TE012 mode f=5.6GHz

② Calibration heater

③ thermometers

④ Vacuum

⑤ Heater thermometer

Thermometric system (3)

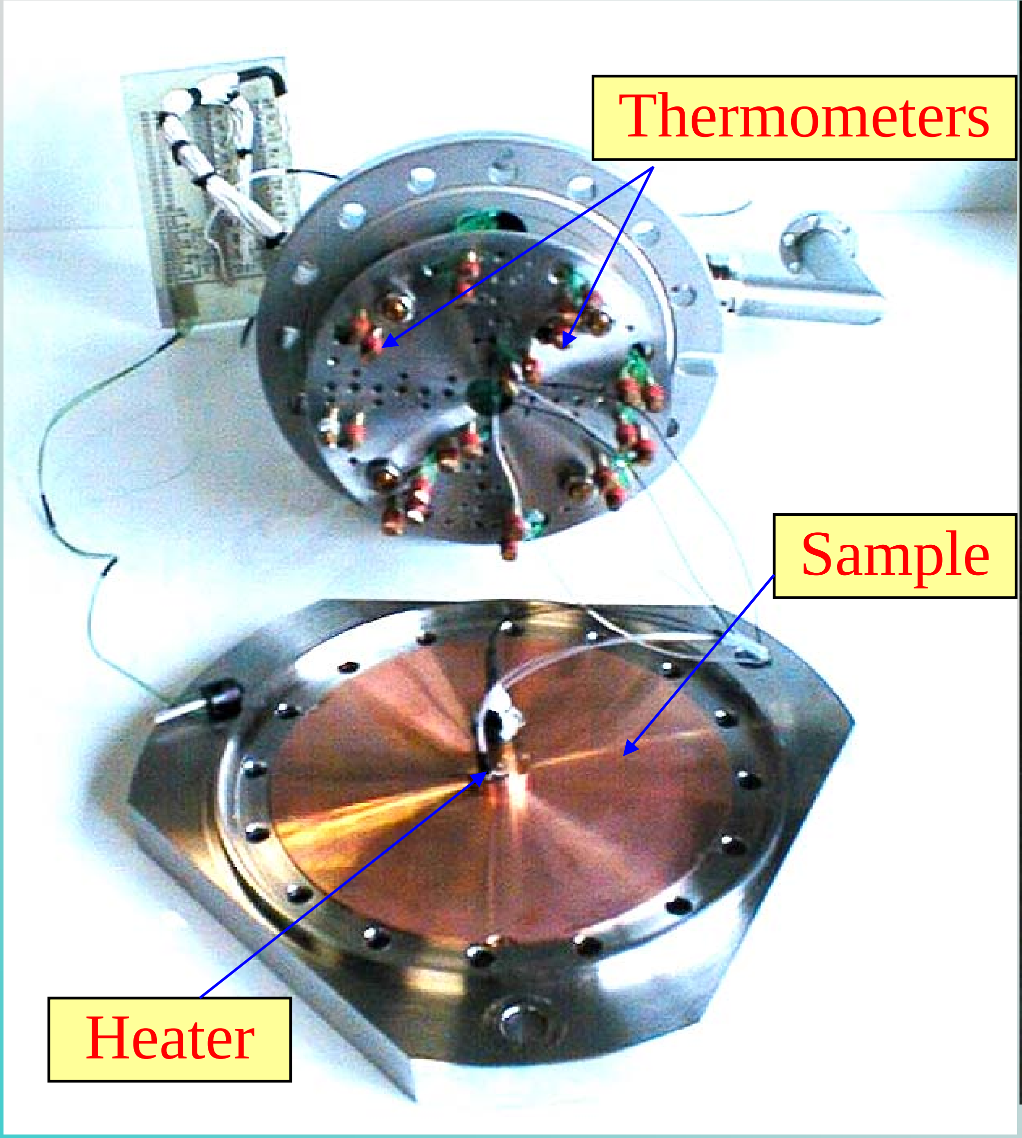

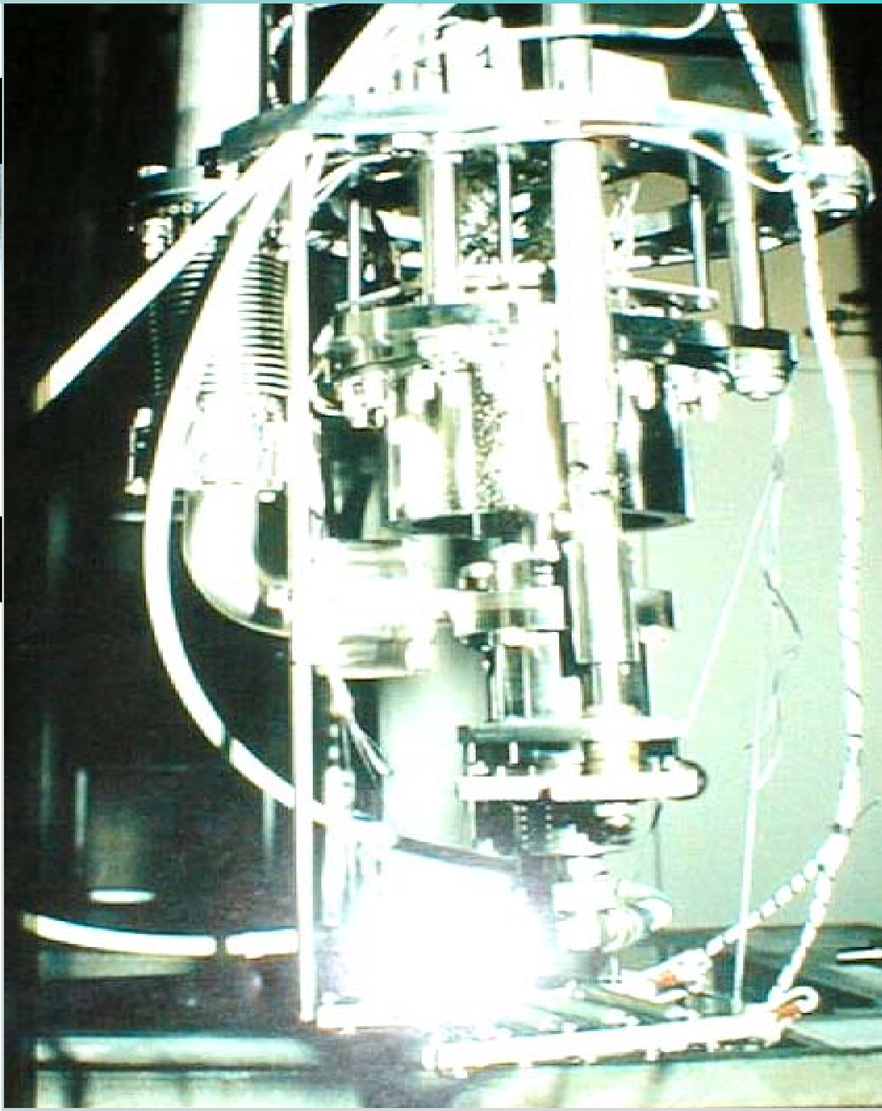

High Field Superconductor With Technological Potential

Material	Structure Classification	Tc (K)	H_{c2} (T) Obs. 4.2K	Jc ($A.cm^{-2}$) 4.2 K (T)
Nb-Ti	A-2	10.2	12	5×10^5 (5 T)
Nb-Zr	A-2	10.8	11	
V_3Ga	A-15	15.5	23.6	2×10^6 (10T)
V_3Si	A-15	17.0	23	
Nb_3Sn	A-15	18.3	26	3×10^5 (10T)
Nb_3Al	A-15	18.9	29.5	10^5 (22T)
$Nb_3(Al,B,Be)$	A-15	20.0		3×10^4 (8T)
Nb_3Ga	A-15	20.3	33	
$Nb_3(Al,Ge)$	A-15	20.5	41	1×10^4 (12T)
Nb_3Ge	A-15	23.2	37	
NbCN	B-1	17.8	12	1×10^3 (7T)
$V_2(Hf,Zr)$Lave	C-15	10.1	23	3×10^5 (6T)
$PbMo_6S_8$	C-15	14.0	65	

- **Crossection of Diffusion Nb_3Sn Tapes**

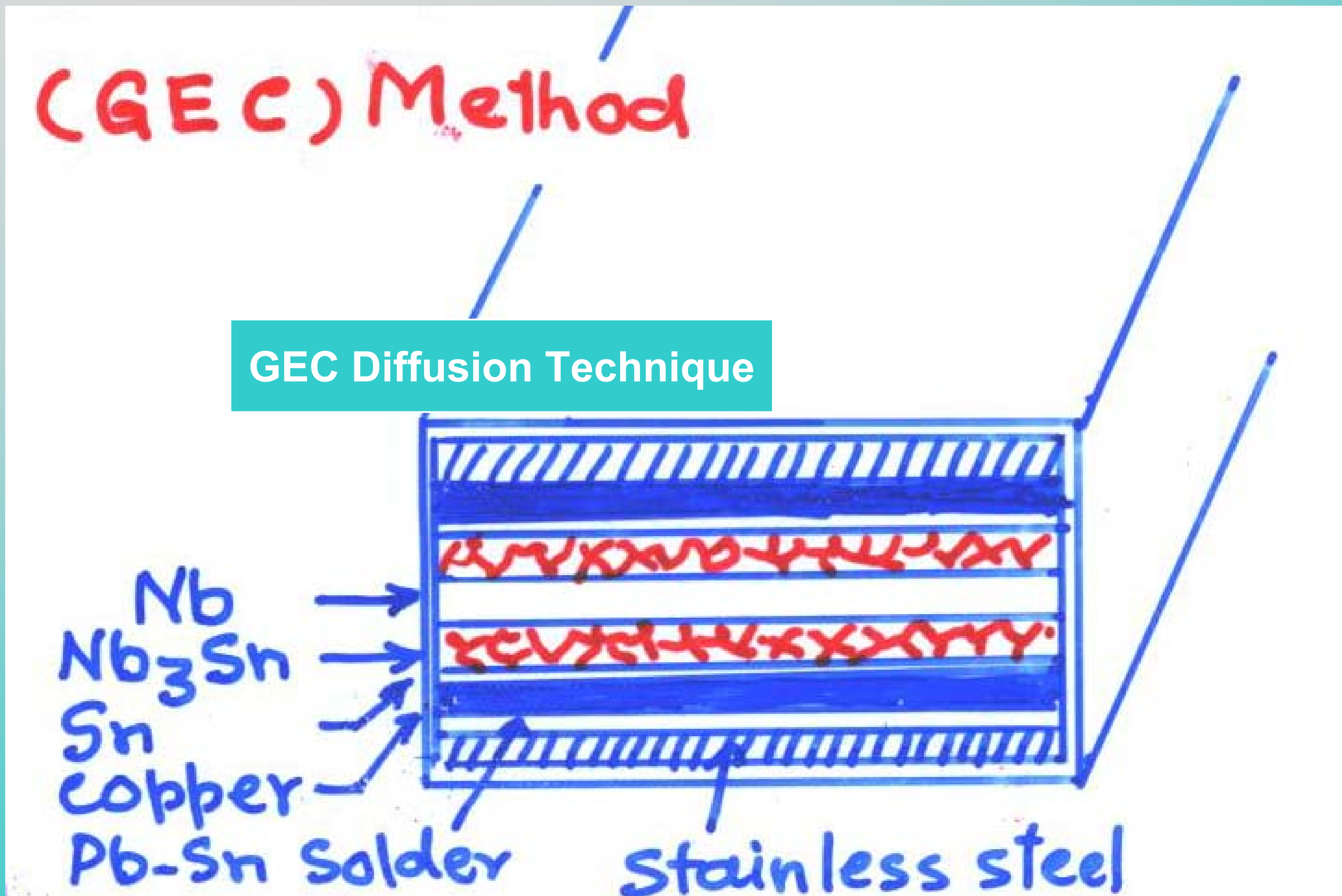

What happens with changing Sn content?

Pure Nb

- *bcc* Nb spacing 0.286 nm
- T_c = 9.2 K

Nb_3Sn → A15 unit cell

- *bcc* Sn, orthogonal Nb chains
- Nb spacing 0.265 nm
- High peaks in d-band DOS
- Increased T_c = 18 K

Off-stoichiometry

- Sn vacancies unstable
- Excess Nb on Sn sites
  - Additional d-band
  - Less electrons for chains
  - Rounded off DOS peaks
  - Reduced T_c

A15 lattice and DOS

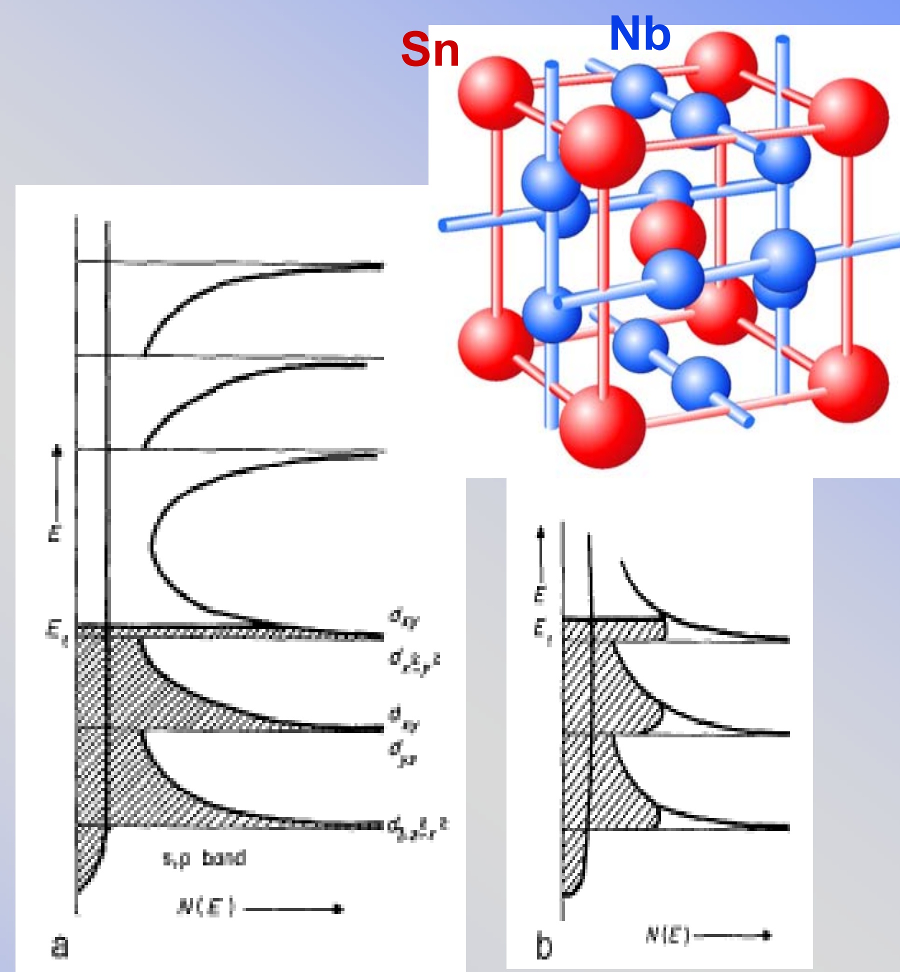

- Dew-Hughes, Cryogenics 1975

Sn content: Lattice parameter

a increases with Sn content (as does T_c (below))

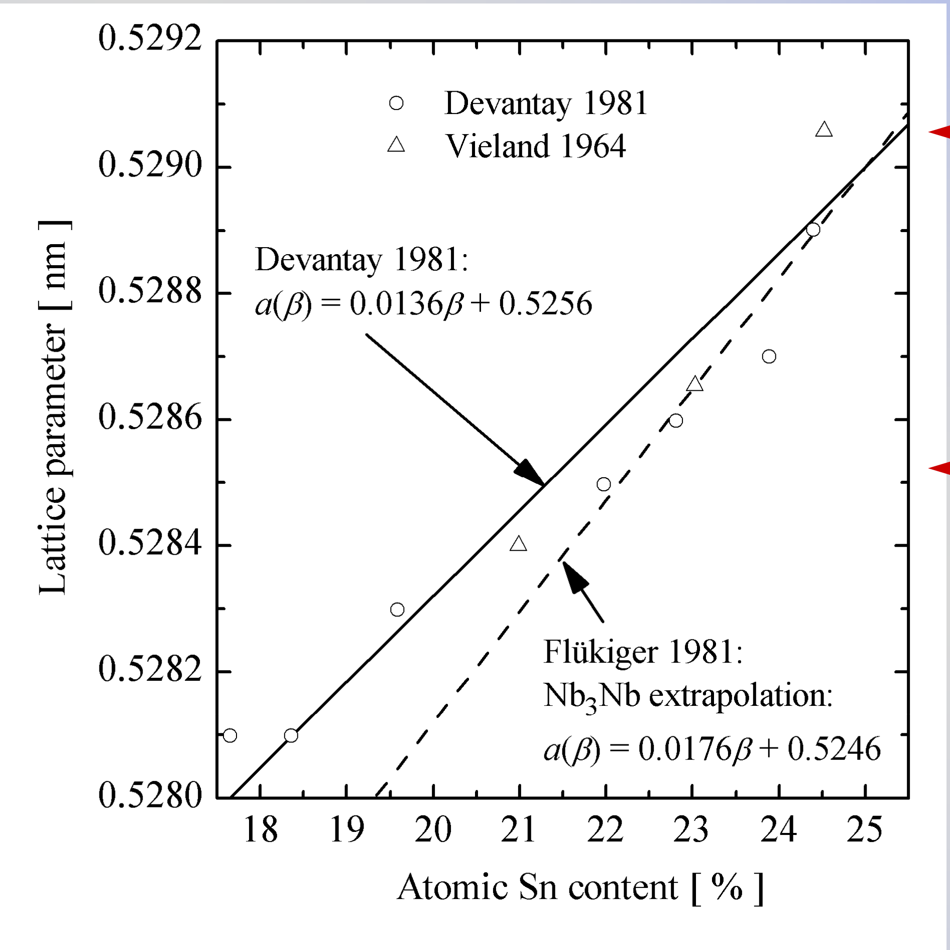

Maximum T_c

Reduced T_c (from Sn deficiency though Nb spacing is smaller)

- Devantay, JMS 1981; Vieland, RCA Rev. 1964; Flükiger, 1981

Sn content: Resistivity

Nb_3Sn is cleanest at stoichiometry

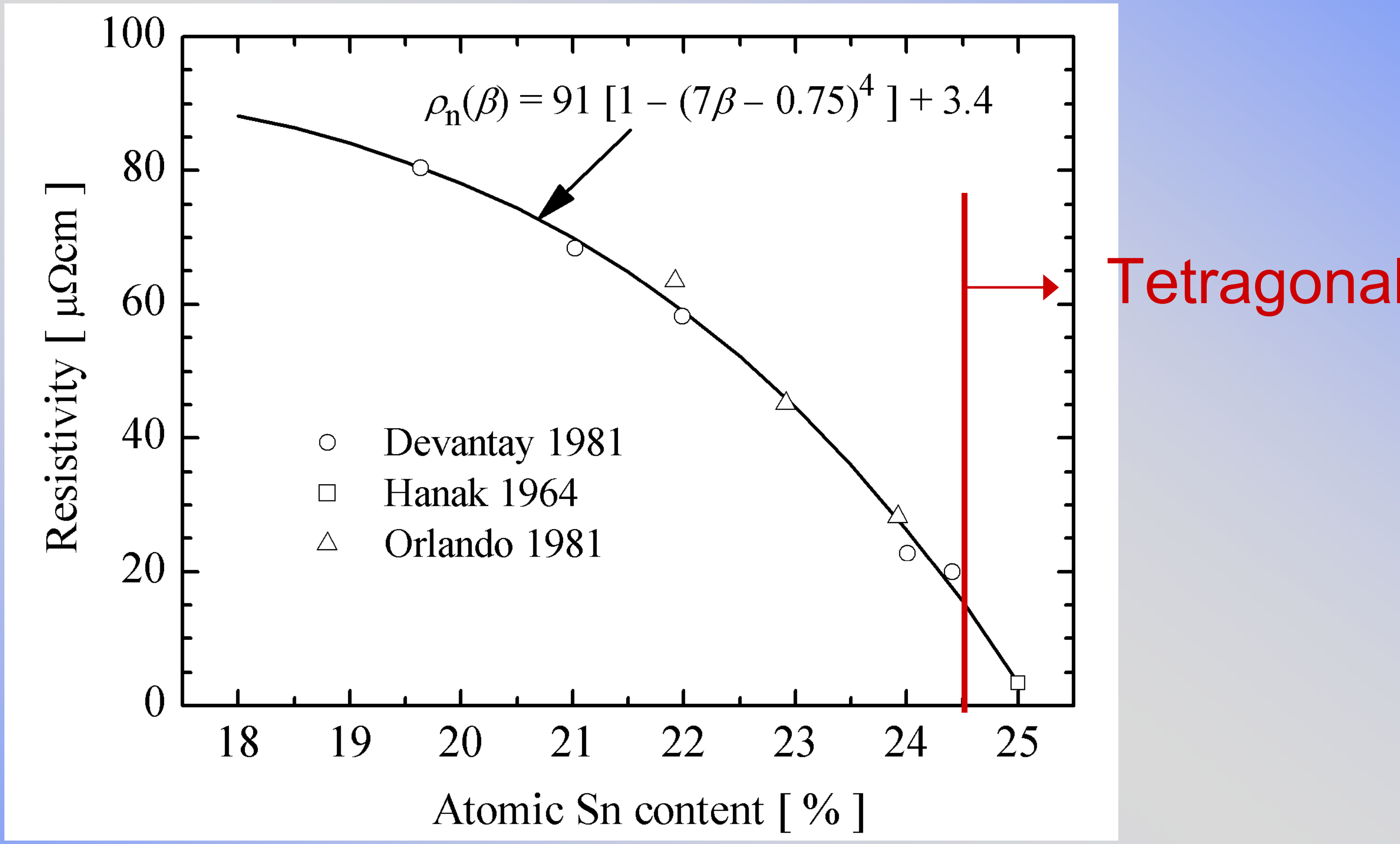

- Devantay, JMS 1981; Hanak, RCA Rev. 1964; Orlando, TM 1981

Resistivity and Long Range Order

Bragg-Williams Order Parameter varied through irradiation

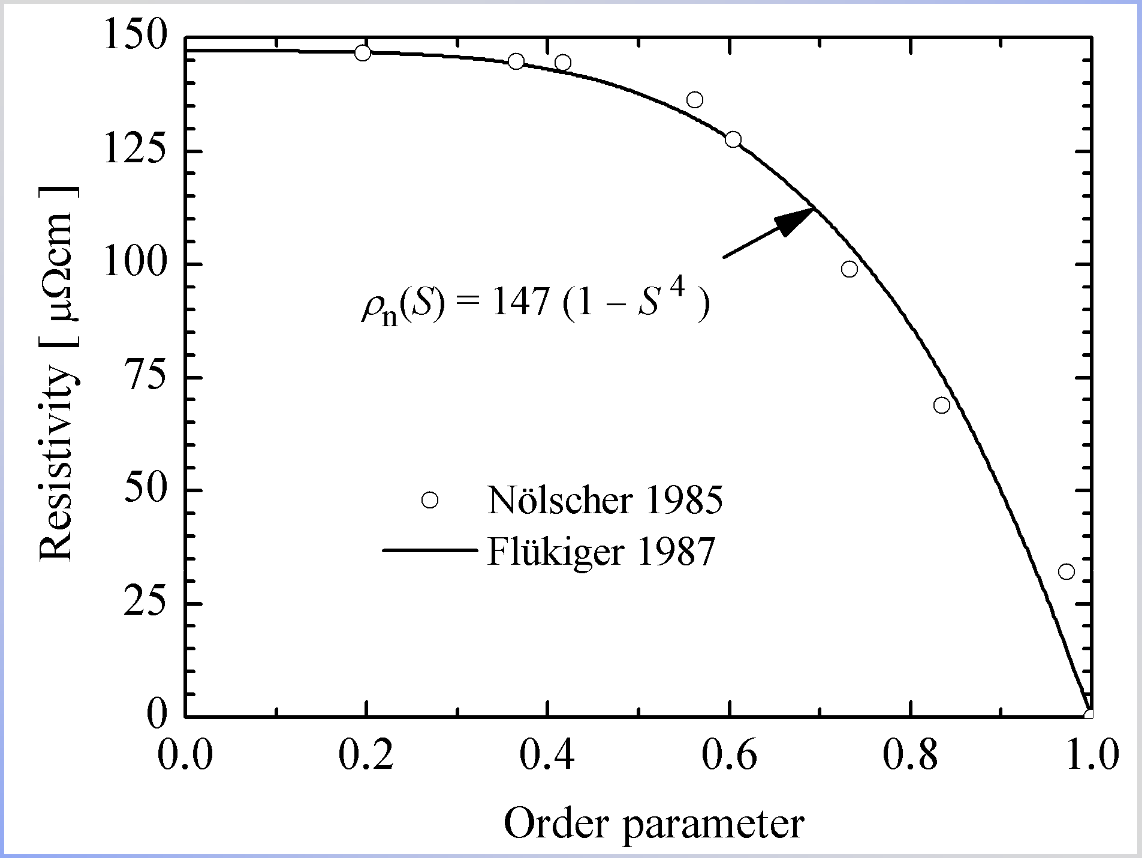

- Effect on ρ_n similar as changing Sn content
- *a*, *S* and ρ_n can all be related to atomic Sn content

Liquid Sn Diffusion?

Bulk Nb substrate dipping in a liquid Tin bath → Sample Annealing

- No nucleation sites on Nb are required
- Fast growth of Nb_3Sn layer
- Deasirable uniform thickness

Technique Choice Reasons

Used System

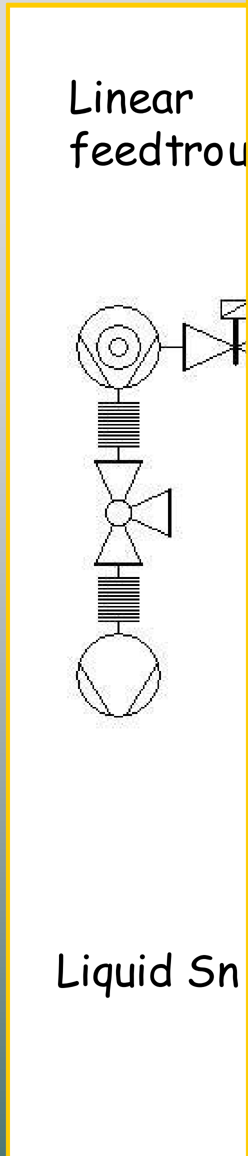

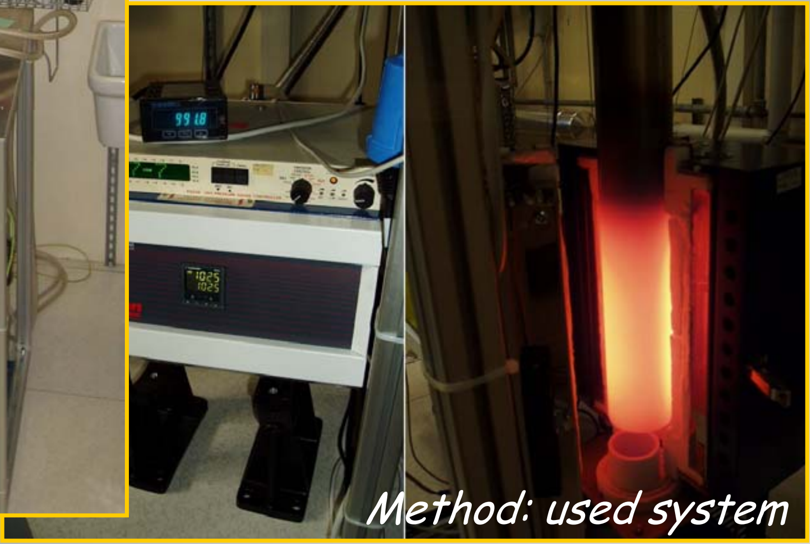

S.Deambrosis et al

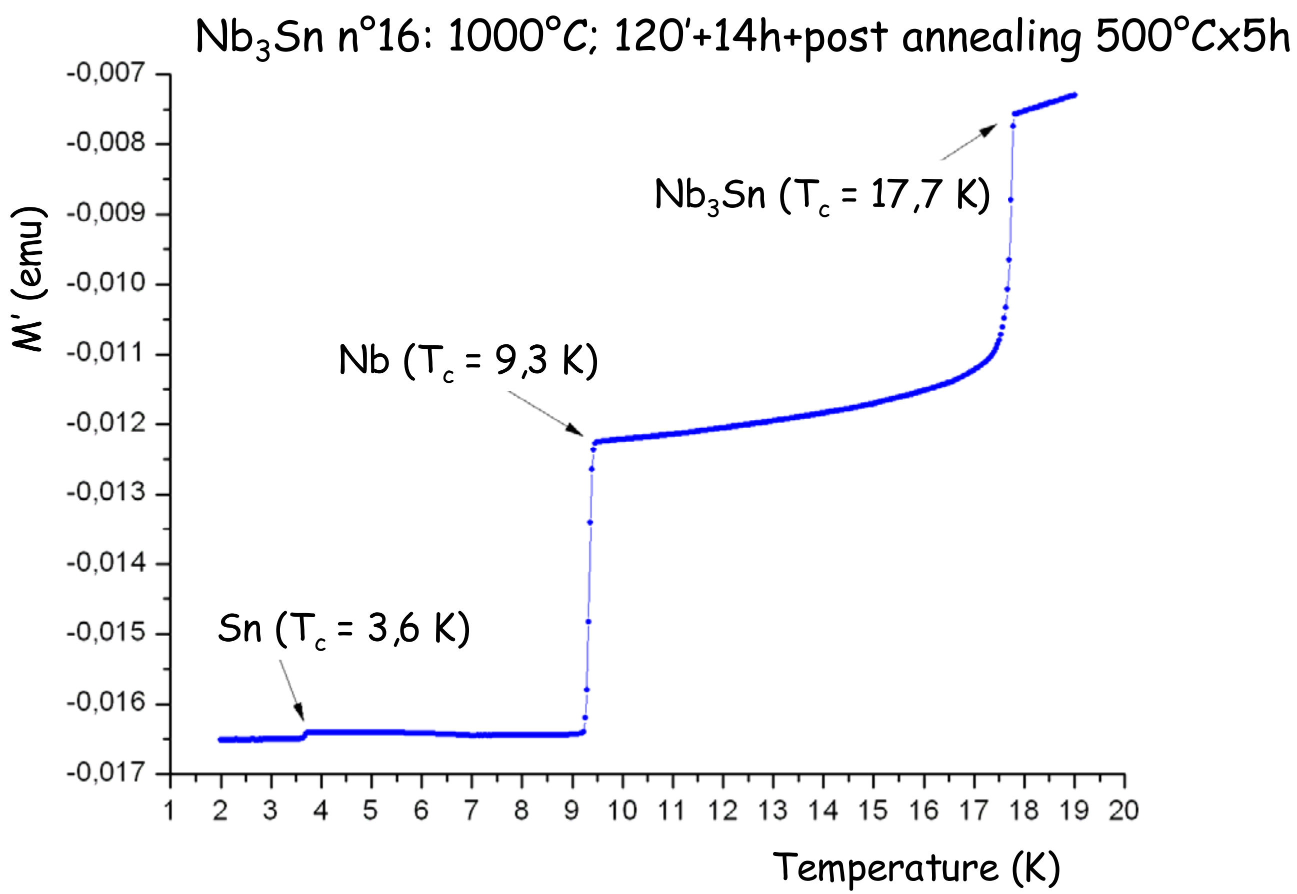

Method: "1 step" process

V3Si

At T = 4.2 K,
f = 500 MHz,
s = 4,
R_{BCS} depends on Δ and ρ_n

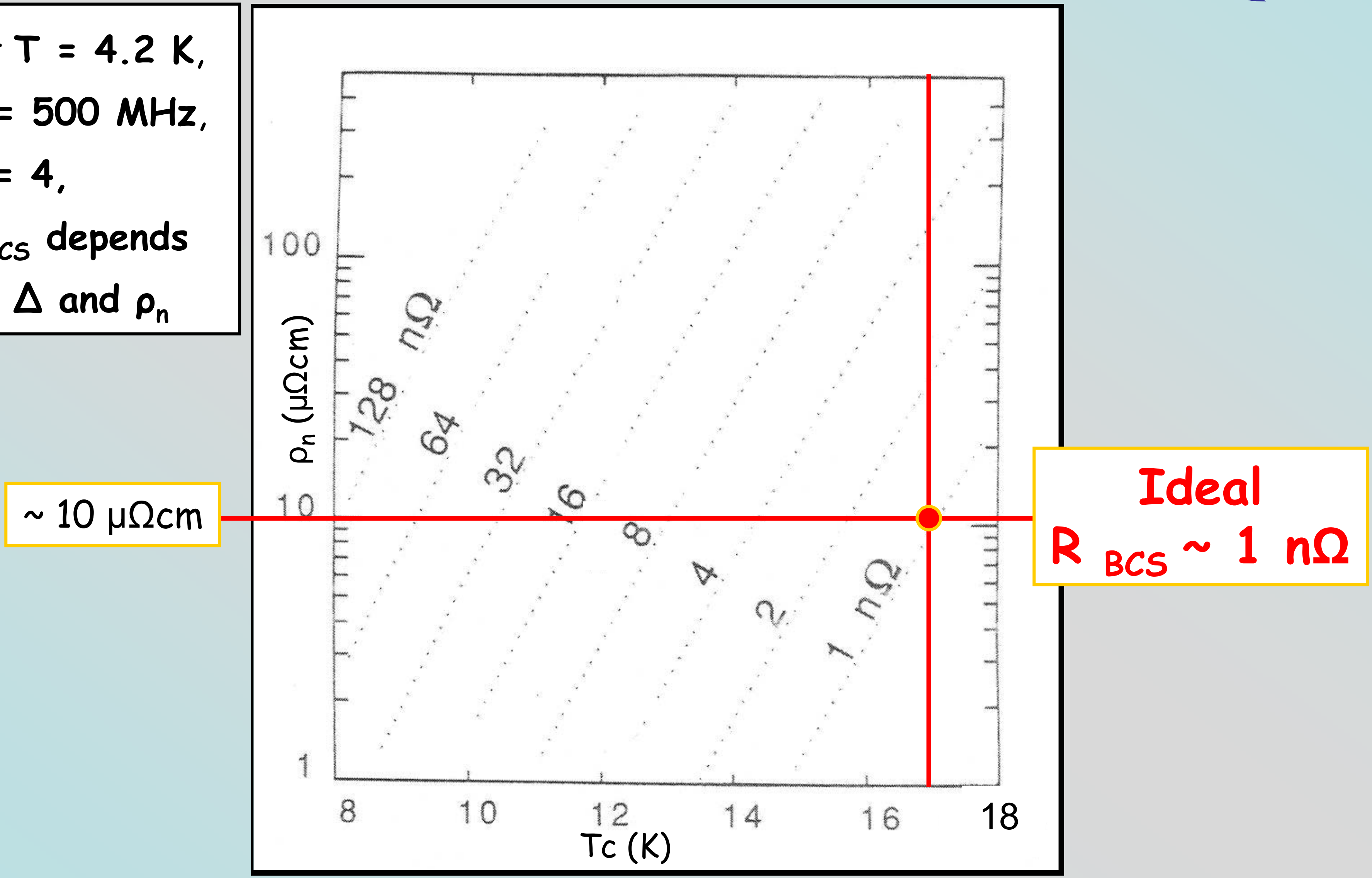

After Benvenuti, Pqlmieri, Vaglio

Reactive sputtered V_3Si films

Y. Zhang, V. Palmieri, W. Venturini, R. Preciso, Legnaro National Laboratory - INFN, Italy

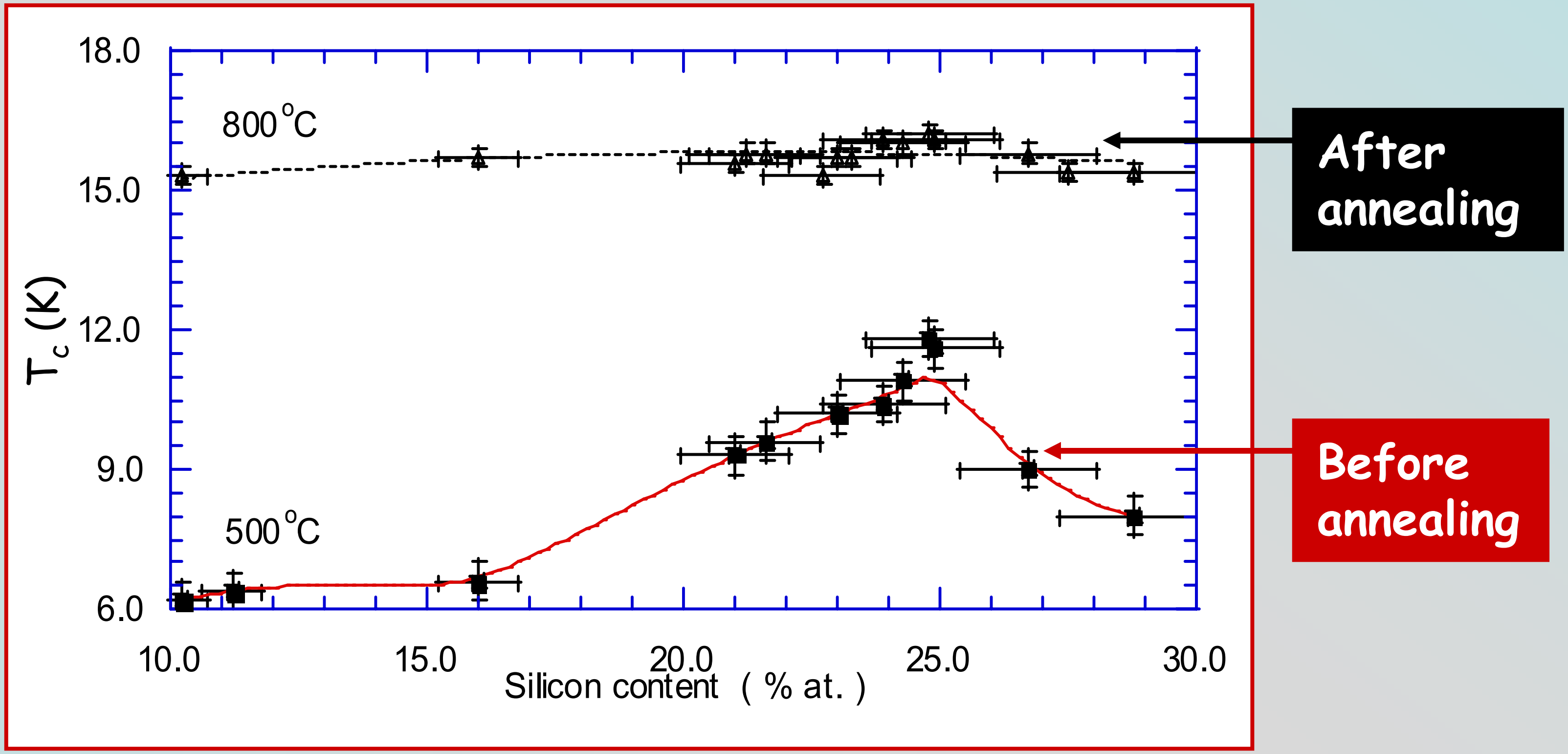

Surface of two annealed samples under SEM: Grain size, (a) 0.2μm, (b) 0.5μm

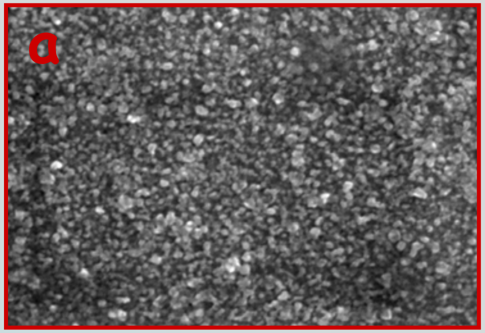

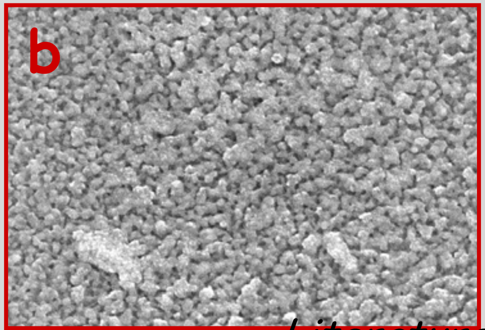

Literature

1- Pentakis(dimethylamide)niobium $Nb(NMe_2)_5$

- Me_2NH gas bubled into 50 mL LiBut 1,6 M (80mmol) for 90 min;

$$Me_2NH + LiBut \rightarrow LiNMe_2 + BuH$$

added 4,3 g $NbCl_5$ (16 mmol)

$$NbCl_5 + 5\,LiNMe_2 \xrightarrow{\text{pentane}} Nb(NMe_2)_5 + 5\,LiCl$$

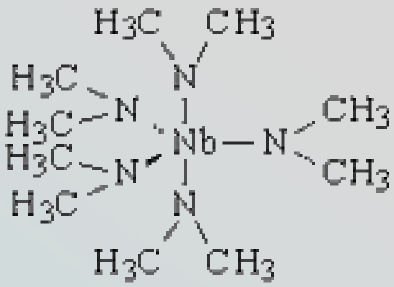

- after filtering LiCl the solution was dried under vacuum obtaining a dark brown solid;
- purification by sublimation at 130°C under vacuum;
- NMR ^{1}H and ^{13}C characterization: good product but with a low volatility.

This compound was not used for the MOCVD deposition.

Thermal diffusion of V_3Si films

Y. Zhang, V. Palmieri, W. Venturini, F. Stivanello, R. Preciso, Legnaro National Laboratory, ITALY

Diffusion Parameters:

Silane pressure	Heat power	Temperature	Diffuse in silane	Anneal in vacuum
$1.2 \cdot 10^{-4}$mbar	300W	900°C	20h	40h

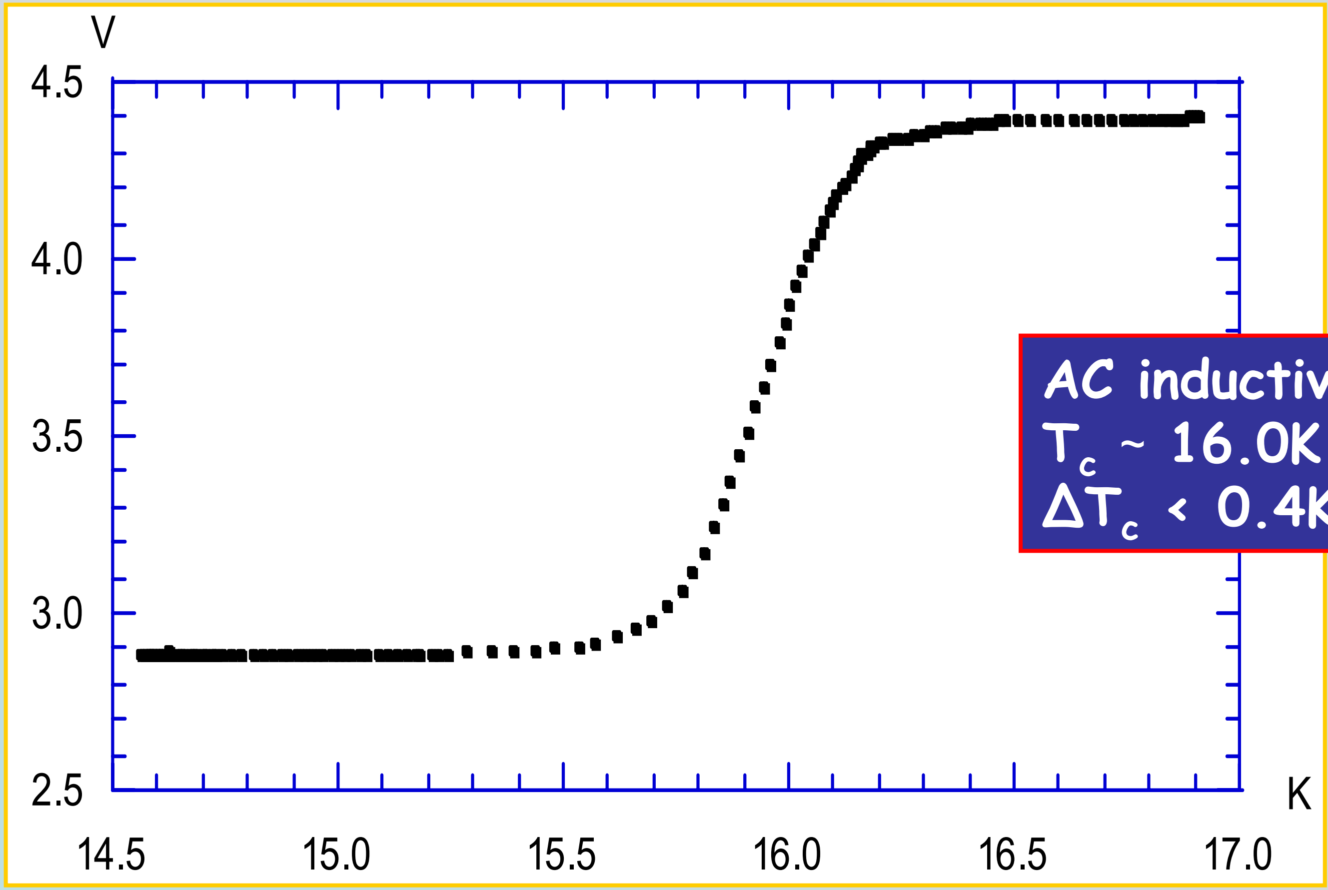

AC inductive measurement:
$T_c \sim 16.0K$
$\Delta T_c < 0.4K$

Literature

How one can get around small H_{c1} in SC cavities with T_c > 9.2K?

AG, Appl. Phys. Lett. 88, 012511 (2006)

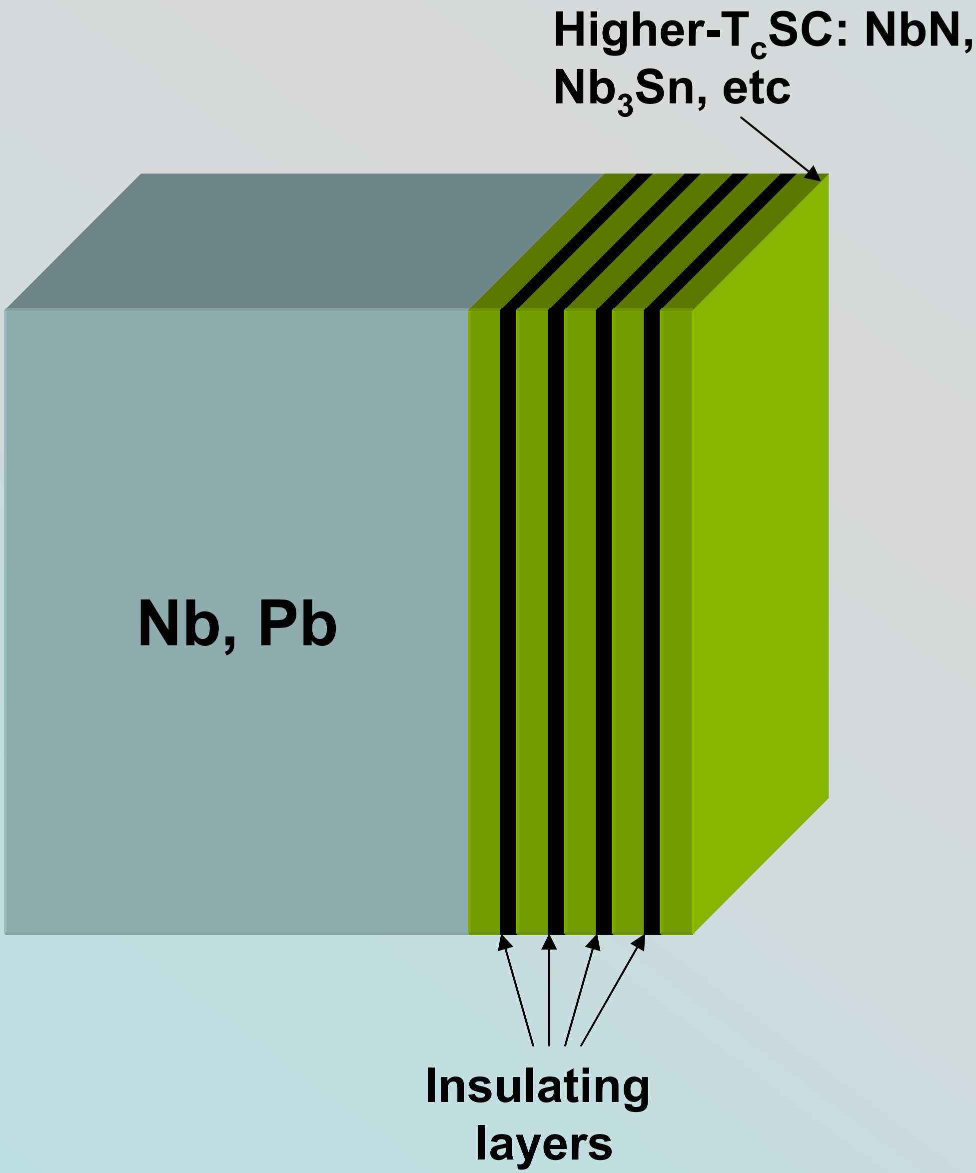

Multilayer coating of SC cavities: alternating SC and insulating layers with $d < \lambda$

Higher T_c thin layers provide magnetic screening of the bulk SC cavity (Nb, Pb) without vortex penetration

For NbN films with d = 20 nm, the rf field can be as high as 4.2 T !

No open ends for the cavity geometry to prevent flux leaks in the insulating layers

A minimalistic solution

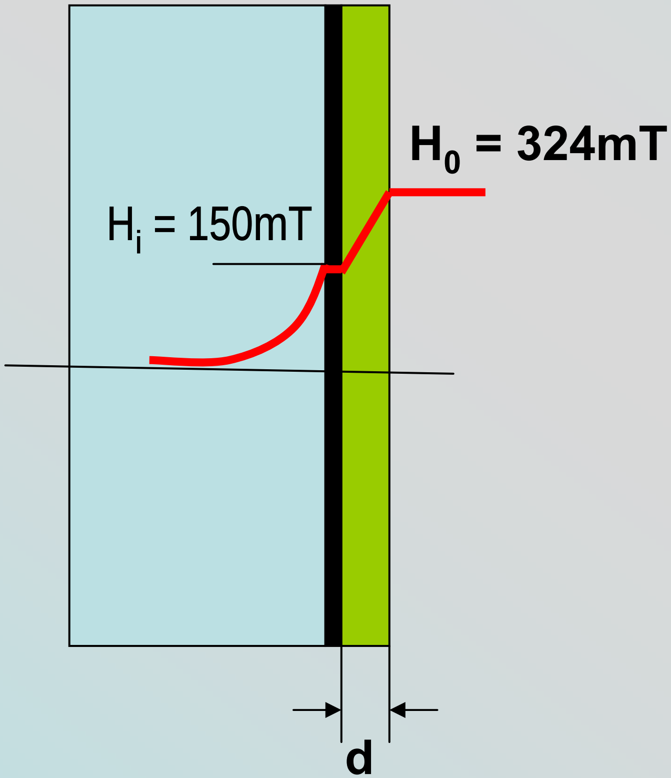

A Nb cavity coated by a single Nb_3Sn layer of thickness d = 50nm and an insulator layer in between

If the Nb cavity can withstand H_i = 150mT, then the external field can be as high as

$$H_0 = H_i \exp(d/\lambda_0) =$$
$$150 \exp(50/65) = 323.7mT$$

Lower critical field for the Nb_3Sn layer with d = 50 nm and ξ = 3nm:
H_{c1} = 1.4T is much higher than H_0

A single layer coating more than doubles the breakdown field with no vortex penetration, enabling $E_{acc}\sim$ 100 MV/m

Gurevitch idea:

- Multilayer S-I-S-I-S coating could make it possible to take advantage of superconductors with much higher H_c, than those for Nb without the penalty of lower H_{c1}
- Strong increase of H_{c1} in films allows using rf fields > H_c of Nb, but lower than those at which flux penetration in grain boundaries may become a problem
- Strong reduction of BCS resistance because of using SC layers with higher Δ (Nb_3Sn, NbN, etc)
- The significant performance gain may justify the extra cost.

Experimental setup: sputtering

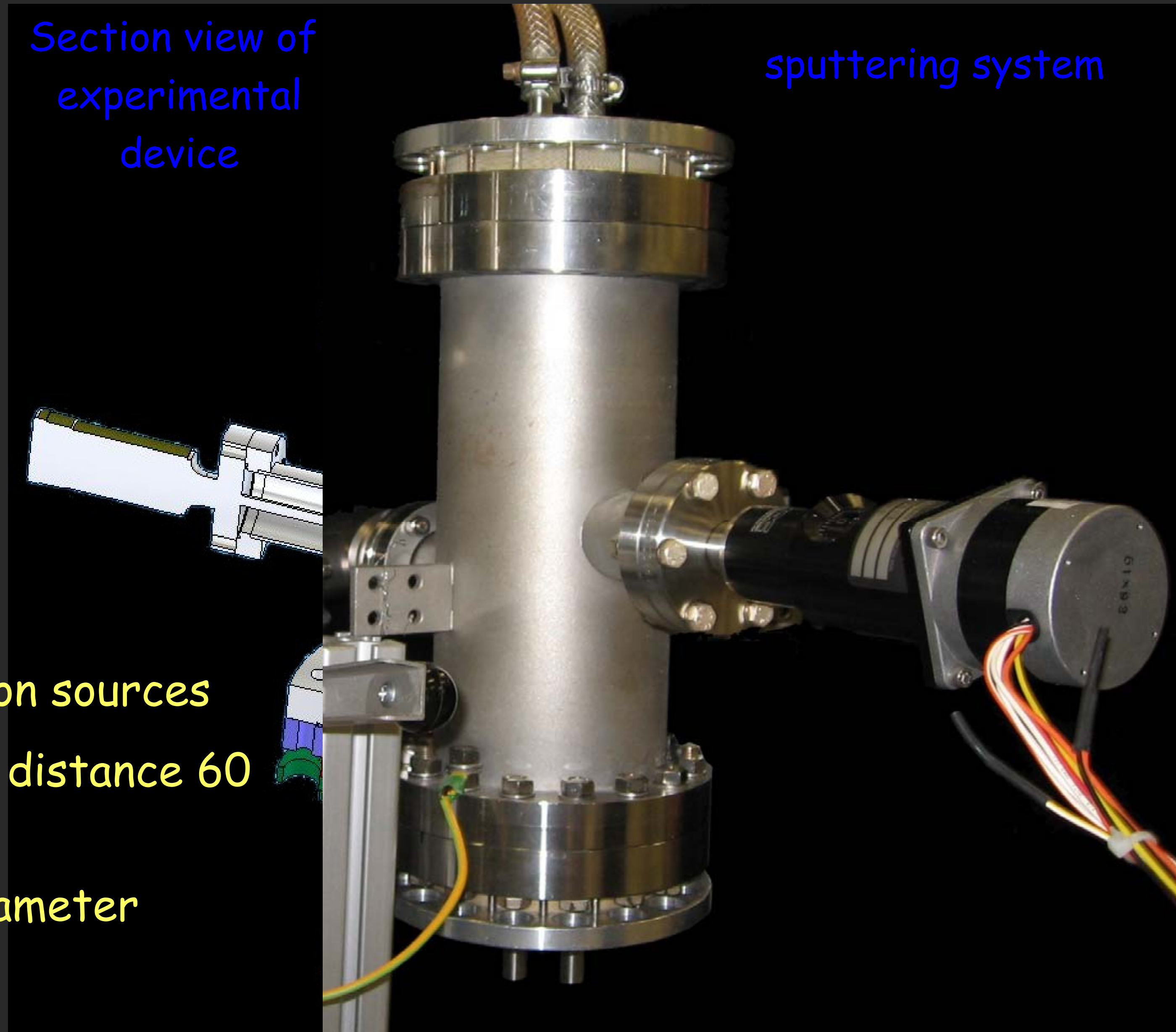

- ✓Balanced Magnetron sources
- ✓Target-Substrate distance 60 mm
- ✓2 inches target diameter

Results: Superconductive characteristic

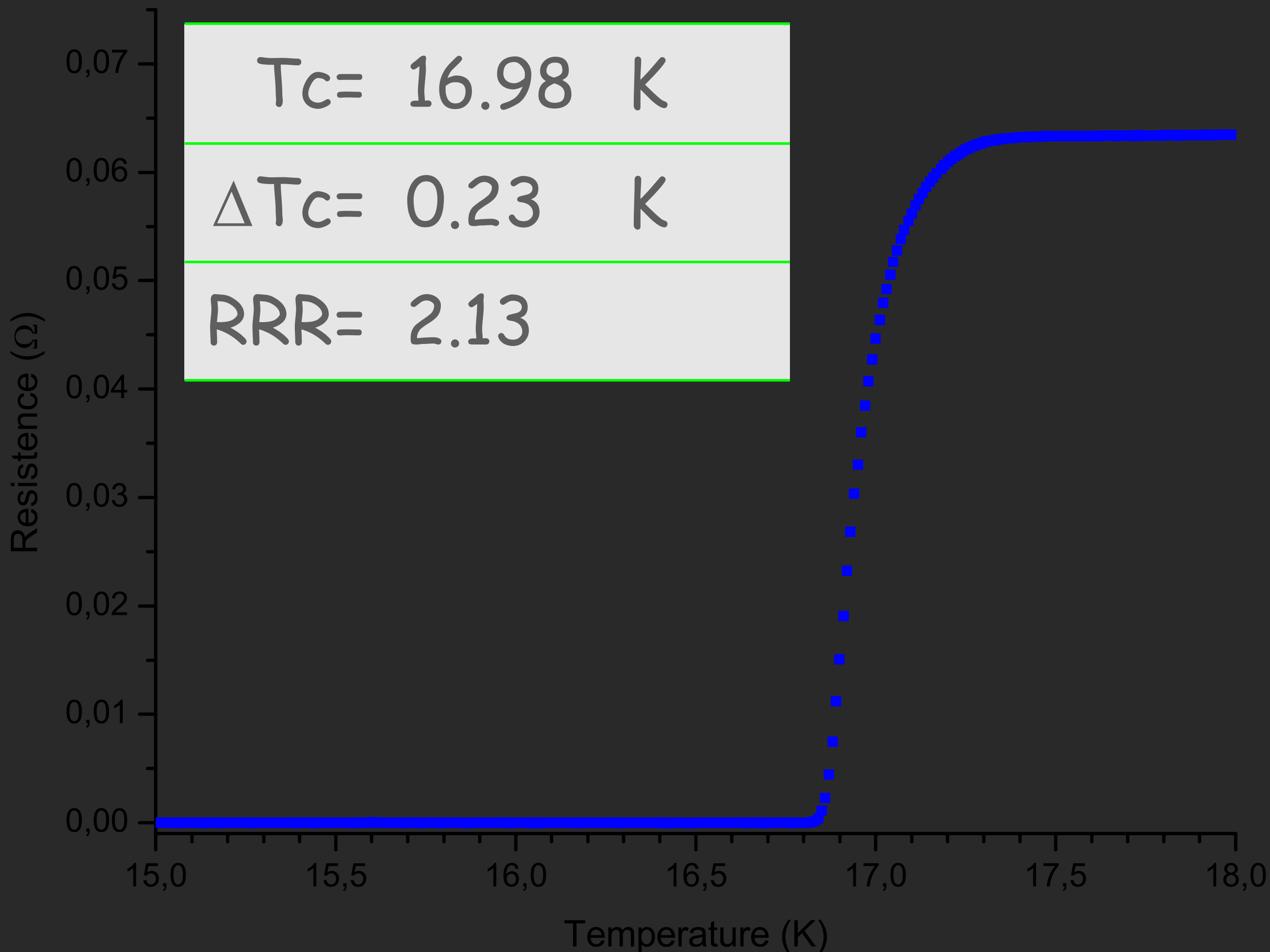

MgB_2 properties-I

Crystalline structure

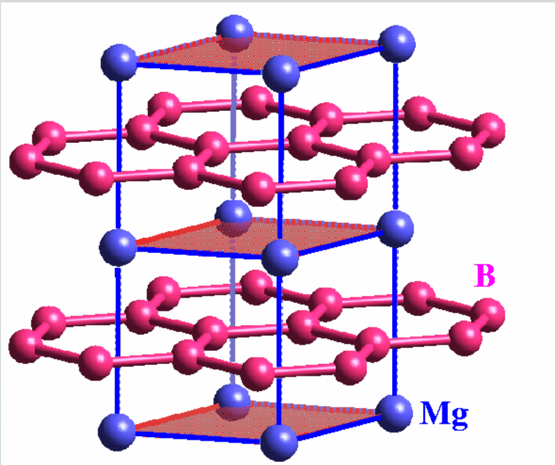

$T_c \approx 40$ K

J.Nagamatsu et al. Nature (2001) 410

Fermi surface

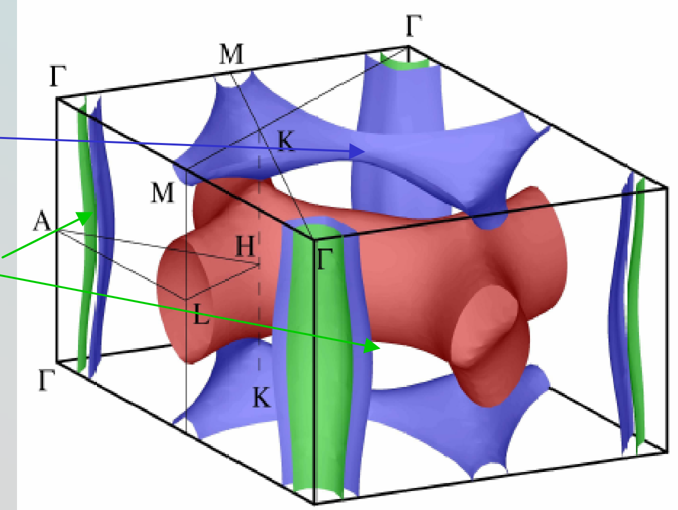

FIG. 3. Fermi surface of MgB_2.

- Simple layered structure
- Covalent bonding between B atoms
- Conventional superconductivity (isotopic effect)
- Coupling with vibrational modes of B atoms (σ bands)

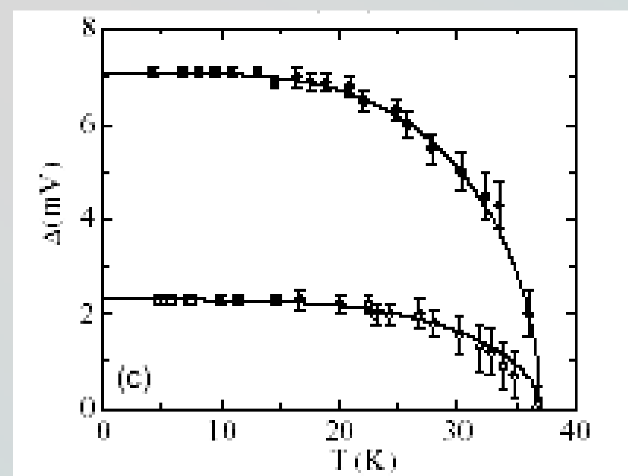

Weak interband scattering
due to different symmetry of the
two bands

⇩

The two bands are two conducting channels in parallel:
crucial role of disorder in coupling them

A comparison with conventional SC for RF applications

	MgB_2	Nb
T_c (K)	39	9.2
ρ_0 ($\mu\Omega$cm)	0.1-10	0.05
RRR	3-30	300
$\Delta_{\pi,\sigma}$ (meV)	2, 7	1.2
$2\,\Delta_{\pi,\sigma}/K_BT_c$ (meV)	1.6, 4	3.9
$\xi_{\pi,\sigma}$ (nm)	50,12	40
λ (nm)	85	80
μ_0H_{c2} (T)	6-50	0.2
R^{BCS}_s @ 4K, 500MHz (nΩ)	2.5/2.3x 10^{-5}	69

from $$R_s^{BCS}(n\Omega)=\left(\frac{1}{T}\right)10^5\nu_{GHz}^2 e^{\left(-\Delta/KT_c\right)}$$

F.Collings et al. SUST 17 (2004)

Pressure-Composition Phase Diagram

Process window: where the thermodynamically stable phases are **Gas+MgB_2**.

If deposition is to take place at **850°C**, Mg partial pressure has to be above **340 mTorr** to keep the MgB_2 phase stable.

Adsorption-controlled growth: automatic composition control if Mg:B ratio is above 1:2.

You can provide as much Mg as you want above stoichiometry without affecting the MgB_2 composition.

***P-x* Phase Diagram at 850°C**

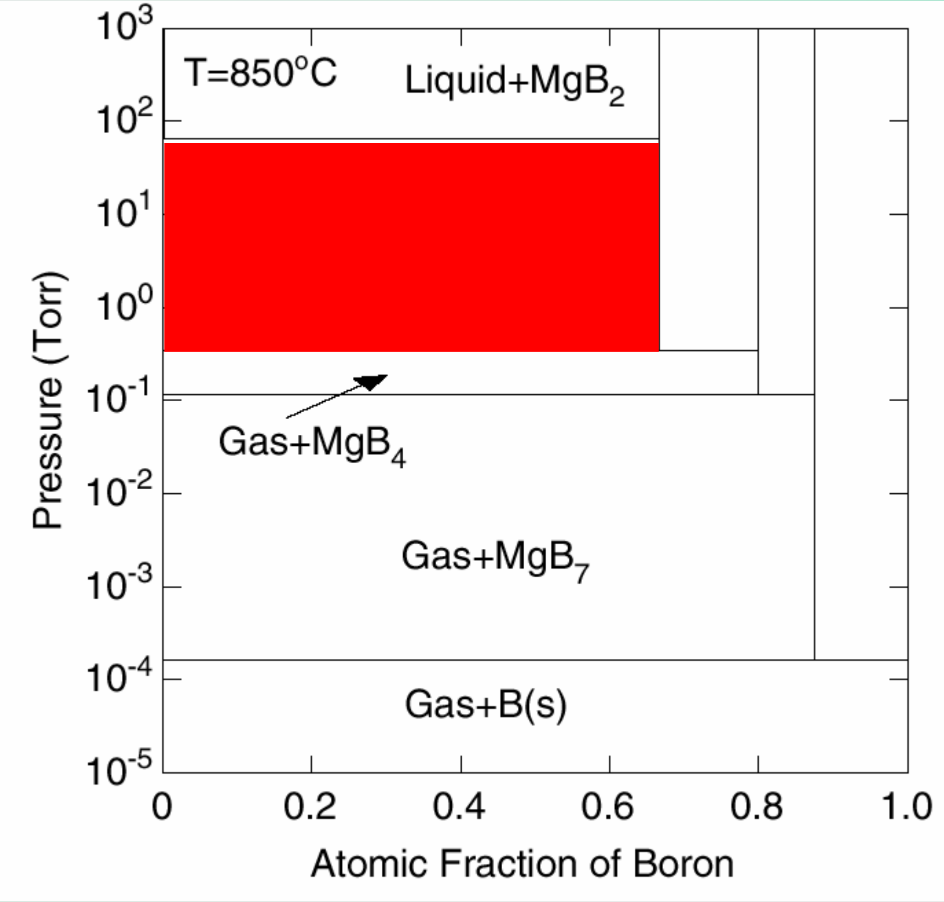

Liu *et al.*, APL 78, 3678 (2001)

Sticking Coefficient of Mg

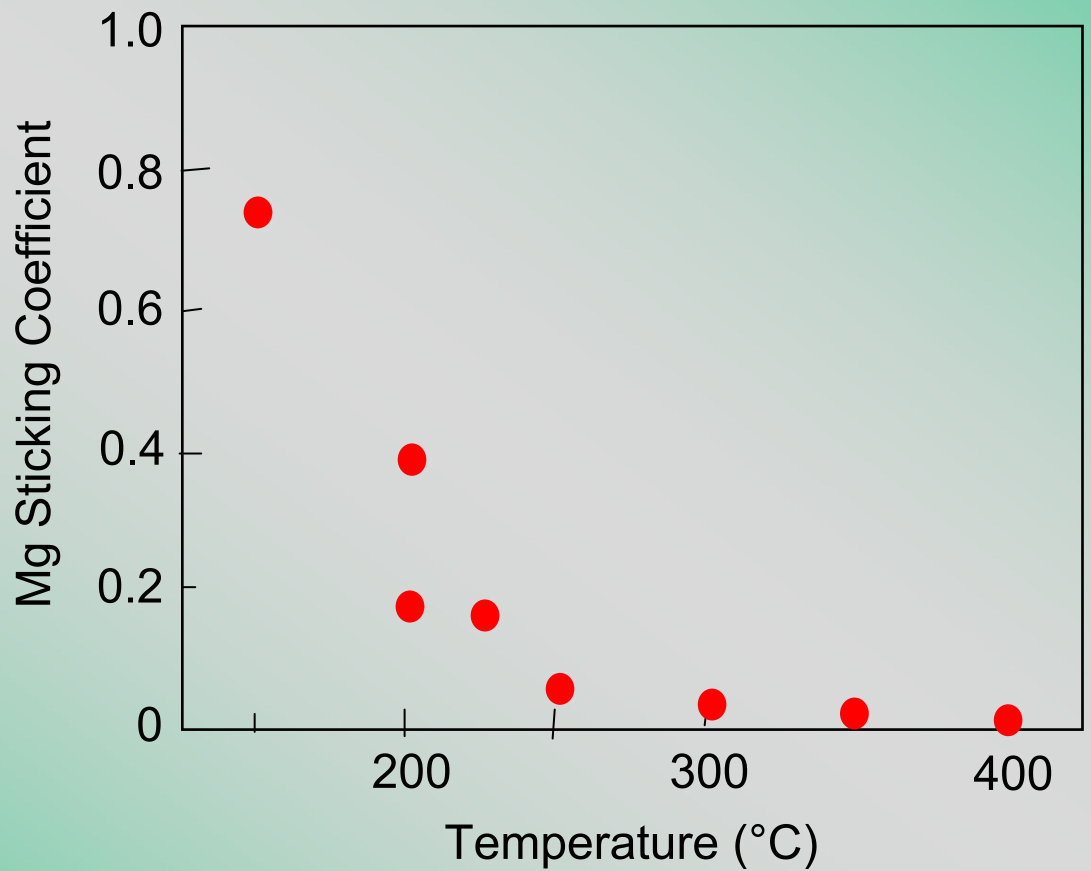

Mg sticking coefficient drops to near zero above 300°C.

Not much Mg available to react with B.

Kim *et al*, IEEE Trans. Appl. Supercond. 13, 3238 (2003)

Hybrid Physical-Chemical Vapor Deposition

Schematic View

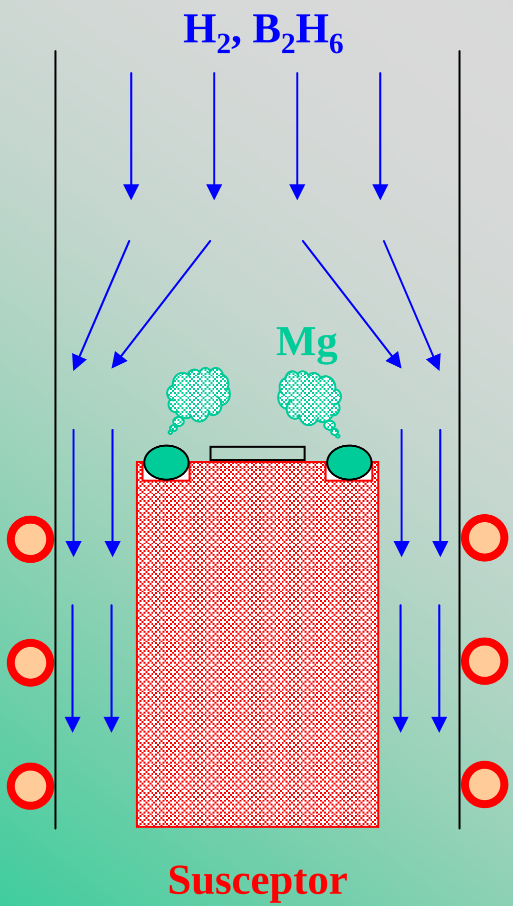

<u>Deposition procedure and parameters:</u>

- Purge with N_2, H_2
- Carrier gas: H_2 — **rid of oxygen prevent oxidation**
- P_{total} = 100 Torr. — **make high Mg pressure possible**
- Inductively heating susceptor, AND Mg, to 550–760 °C. P_{Mg} = ? (44 mTorr is needed at 750 °C according to thermodynamics) — **generate high Mg pressure**; **high enough *T* For epitaxy**
- Start flow of B_2H_6 mixture (1000 ppm in H_2): 25 - 250 sccm. Film starts to grow. — **pure source of B**; **control growth rate**
- Total flow: 400 sccm - 1 slm
- Deposition rate: 3 - 57 Å/sec — **control growth rate**
- Switch off B_2H_6 flow, turn off heater. — **low Mg sticking no Mg deposit**

Very Clean HPCVD MgB_2 Films: *RRR* > 80

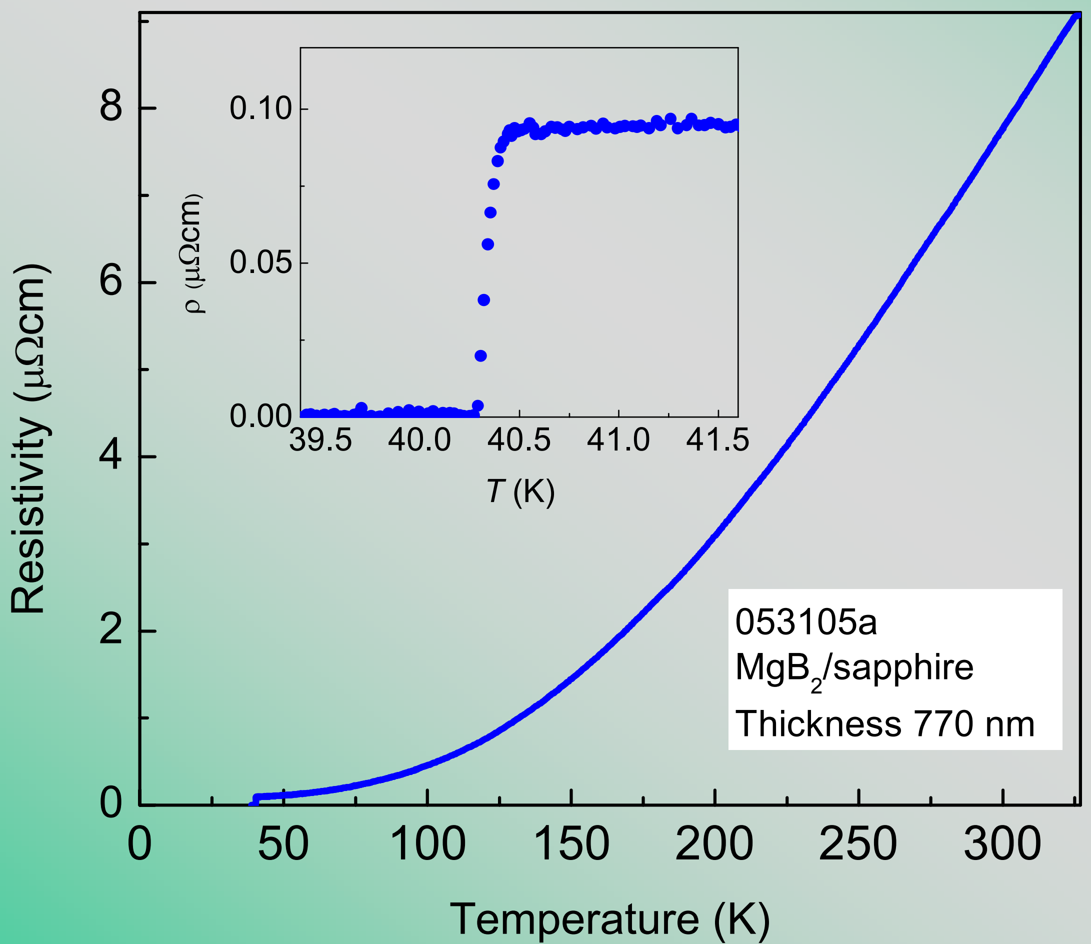

Mean free length is limited by the film thickness.

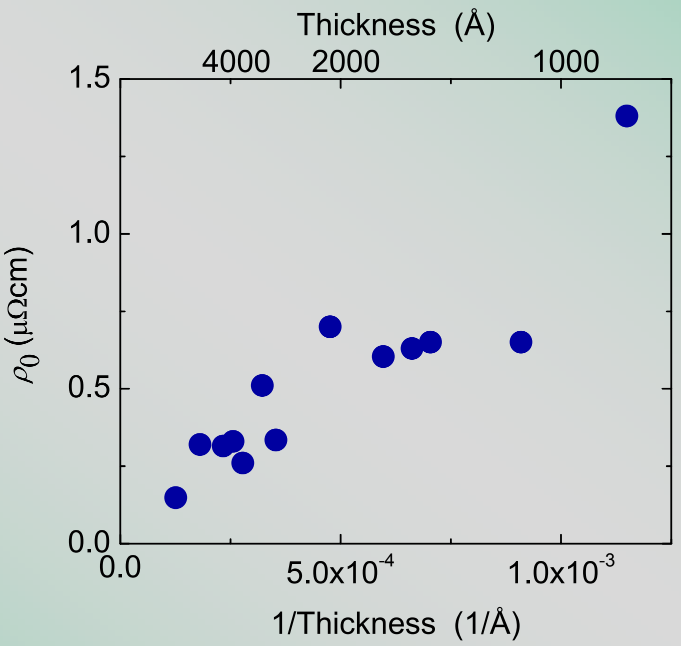

Good Microwave Properties in Clean Films

Microwave measurement: sapphire resonator technique at 18 GHz.

Surface Resistance @ 18 GHz

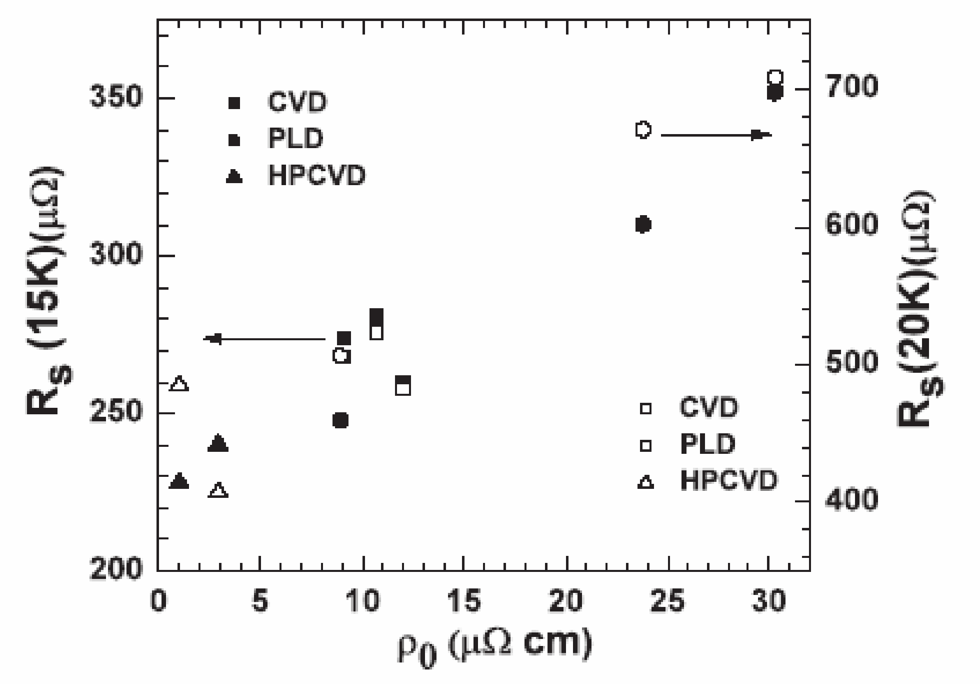

π-Band Gap

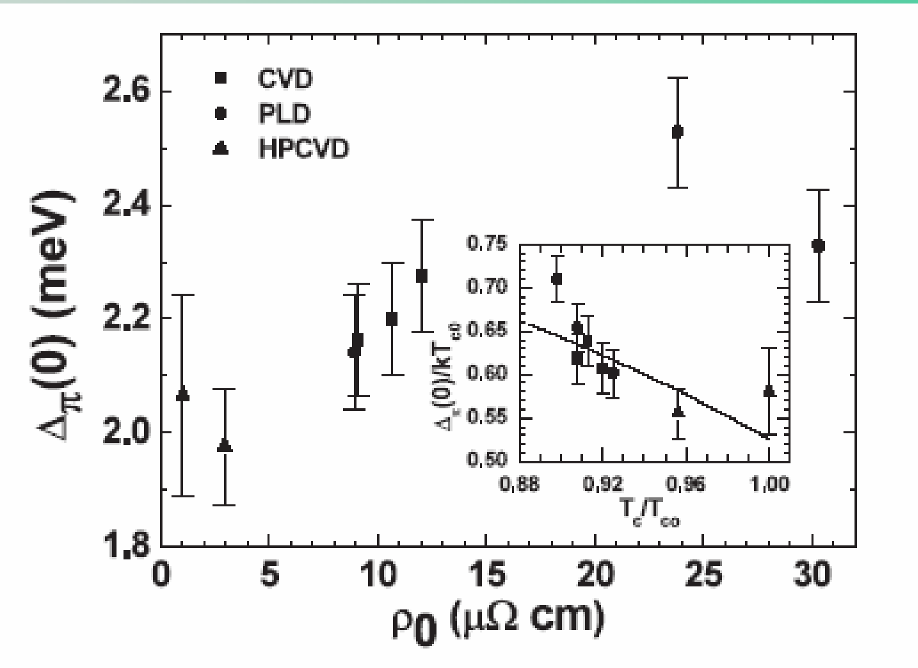

— Surface resistance decreases with residual resistivity. Clean HPCVD films show low surface resistance.

— Interband scattering makes π band gap larger.

Jin *et al*, SC Sci. Tech. 18, L1 (2005)

Short Penetration Depth in Clean Films

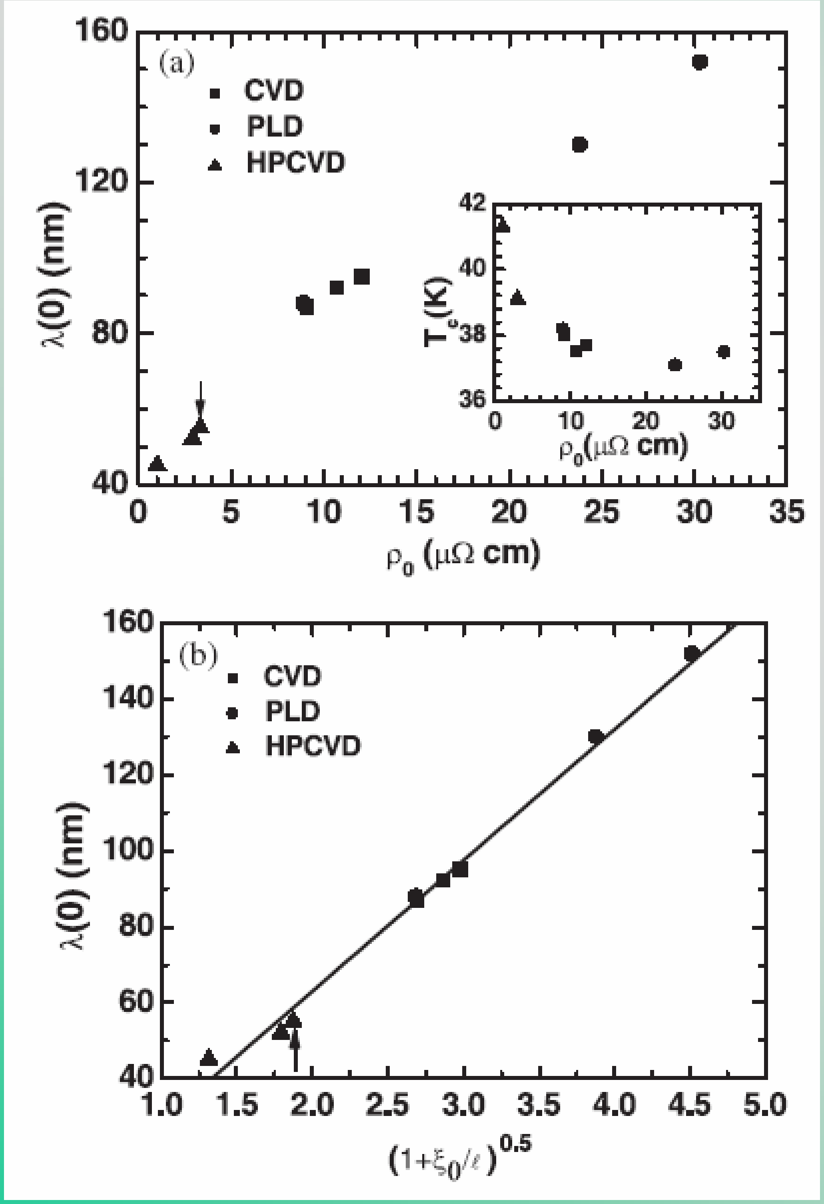

— Penetration depth decrease with residual resistivity.

— London penetration depth λ_L: 34.5 nm

Jin *et al*, SC Sci. Tech. 18, L1 (2005)

HPCVD MgB_2 Films on Metal Substrates

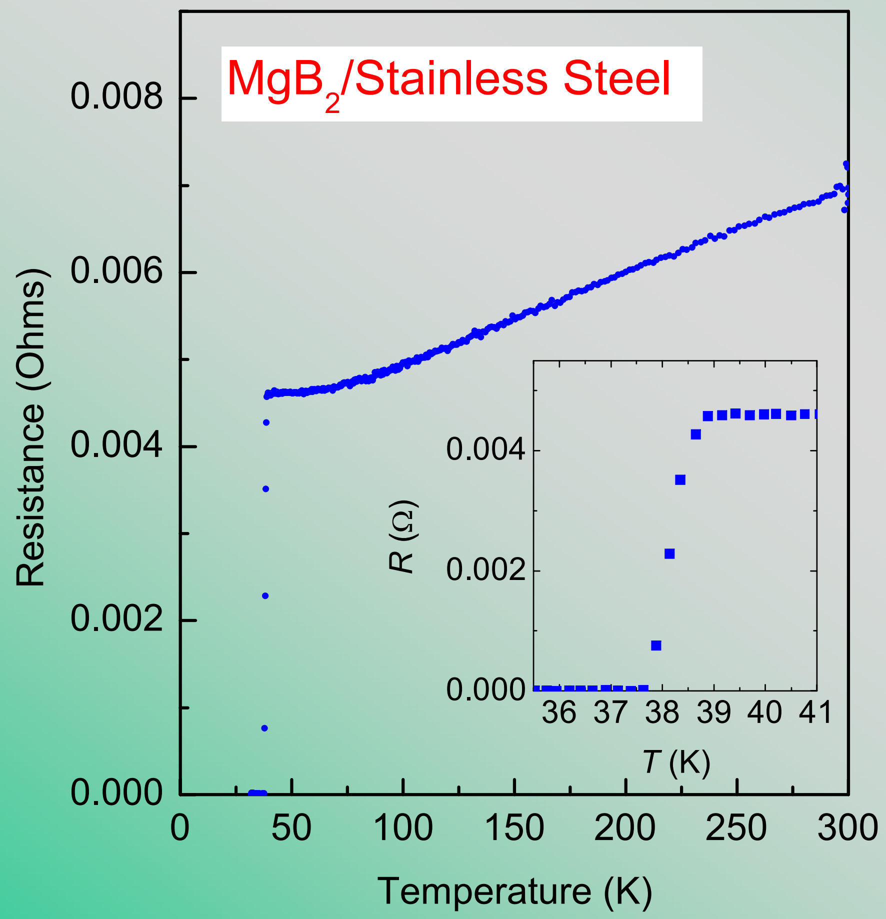

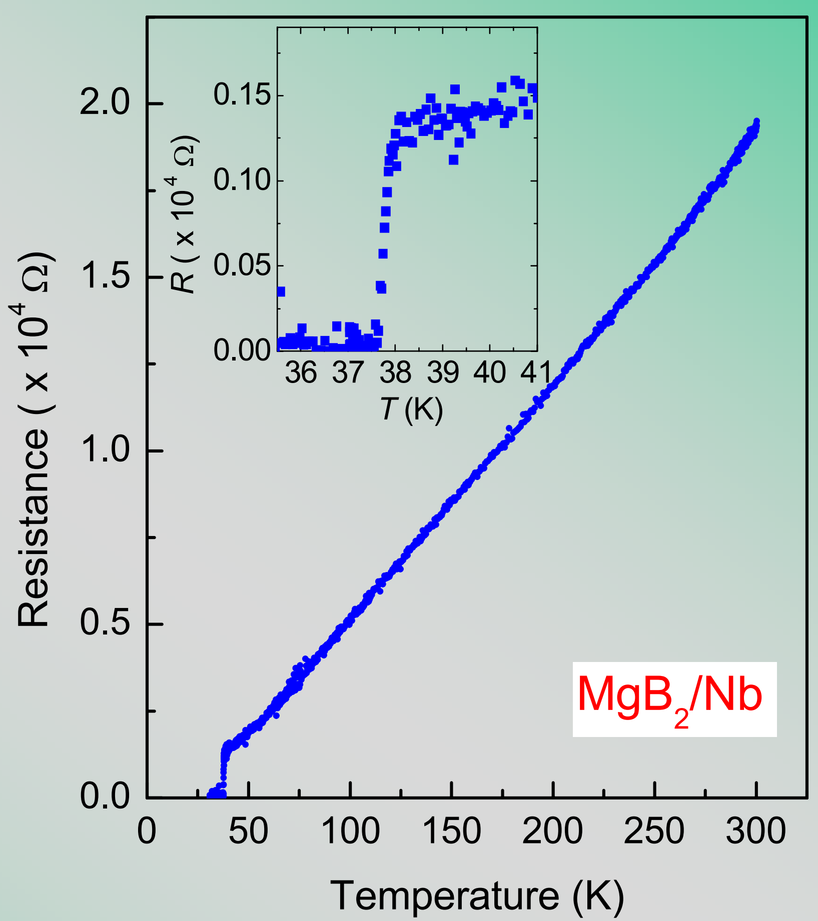

High T_c has been obtained in polycrystalline MgB_2 films on stainless steel, Nb, TiN, and other substrates.

Degradation of HPCVD MgB_2 Films in Water

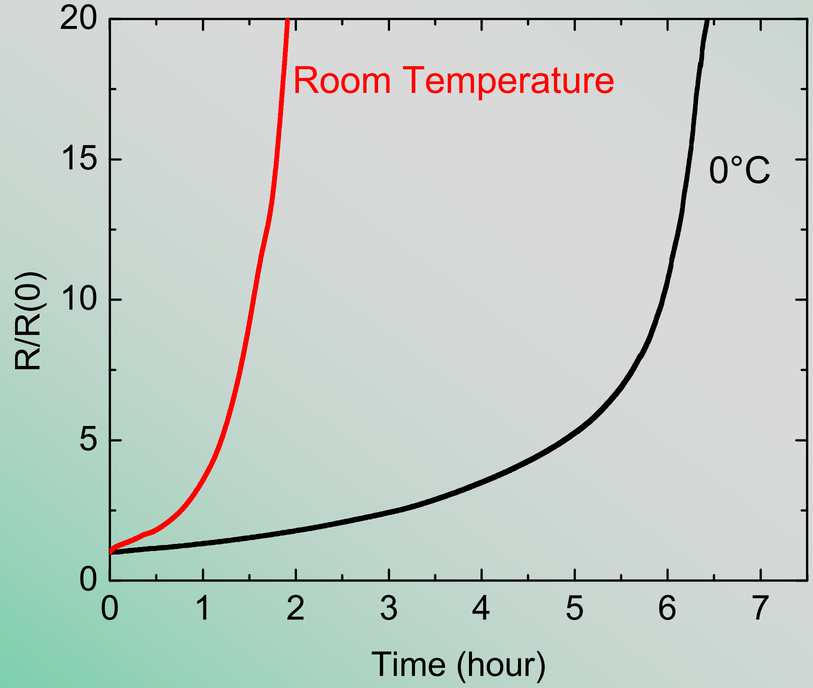

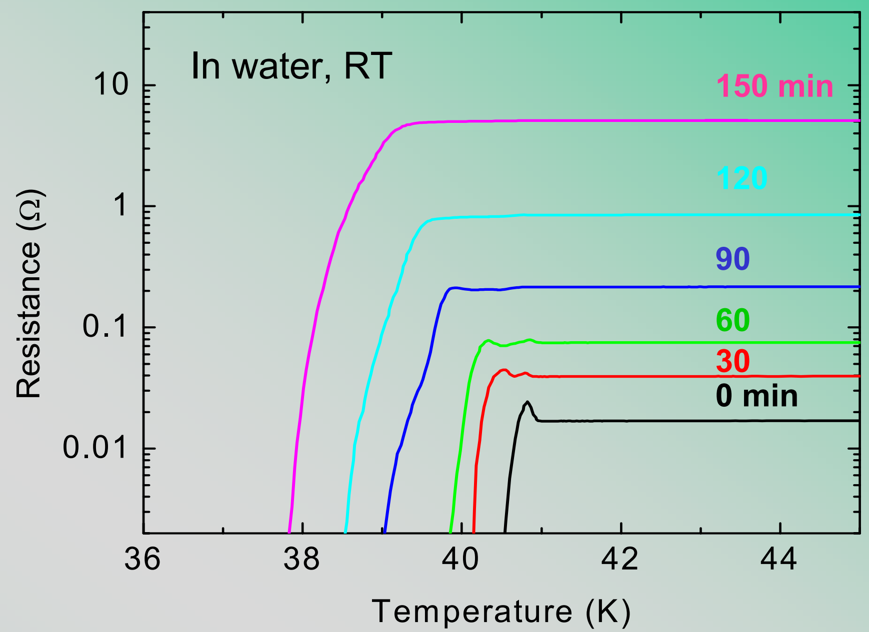

— Film properties degrade with exposure to air/moisture: resistance goes up, T_c goes down

— Experiments show that MgB_2 degrades quickly in water, and is sensitive to temperature.

Mixes containing less than 55% in weight of perchloric acid cannot explode

Unfortunately they are the less interesting for the EP use

The convenient polishing baths are just located in the flammable field

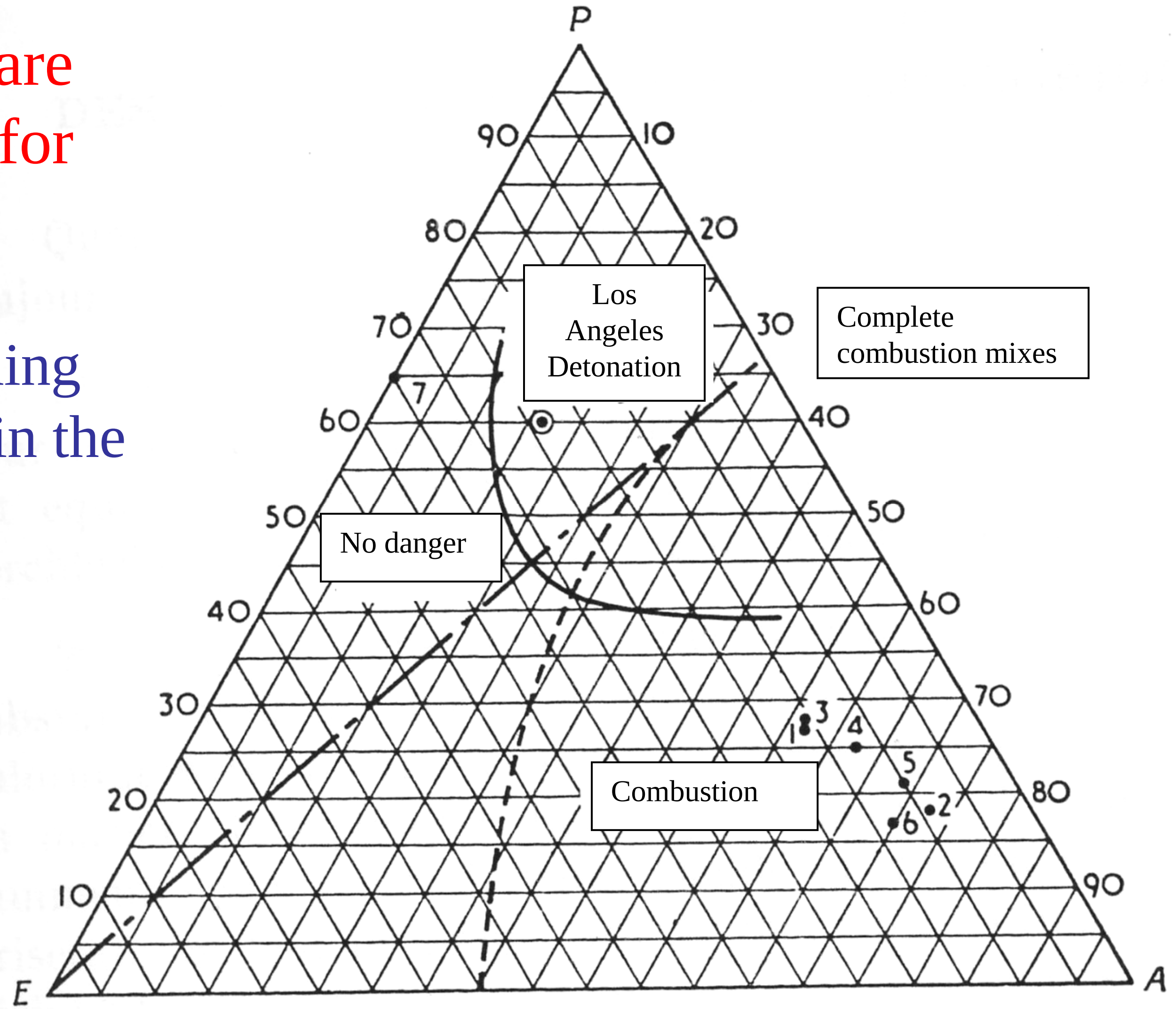

Case 3

A woman etching computer chips developed a pin-hole in her glove during the four hours that she was working in a dip tank with 5% hydrogen fluoride. She went to a doctor's office where **a non-specific burn ointment was applied** (no calcium gluconate was applied). She continued to have pain during the next four days. At that time she had severe pain under the finger nail and the subungual tissues were black. There was mild erythema around the proximal cuticle. Upon removal of the finger nail at a burn treatment center where she was referred, exposed and necrotic bone was identified. The distal phalanx was demineralized and the patient required distal amputation of the finger (Edelman, 1986).

Hydrofluoric acid (HF) differs from other acids because the fluoride ion readily penetrates the skin, causing destruction of deep tissue layers, including bone.

Pain associated with exposure to solutions of HF (1-50%) may be delayed for 1-24 hours. If HF is not rapidly neutralized and the fluoride ion bound, tissue destruction may continue for days and result in limb loss or death.

… Do you really want I continue with case 4?

On the basis of Abbott Patent,

We succeeded in electropolishing Nb!

by a mixture of Choline Cloride, Urea, NH_4F at 80 °C

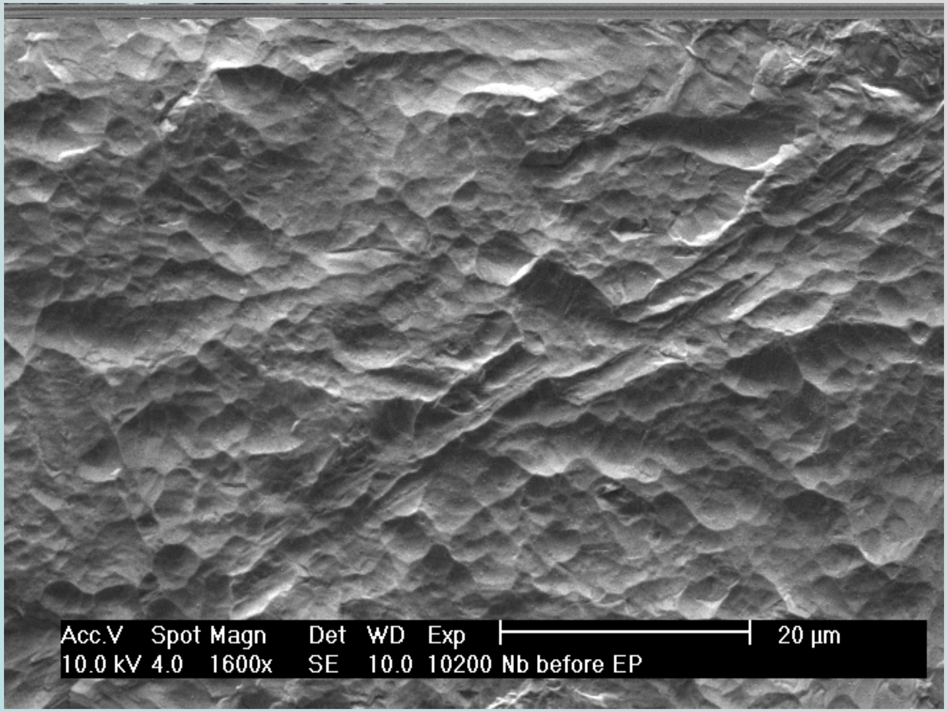

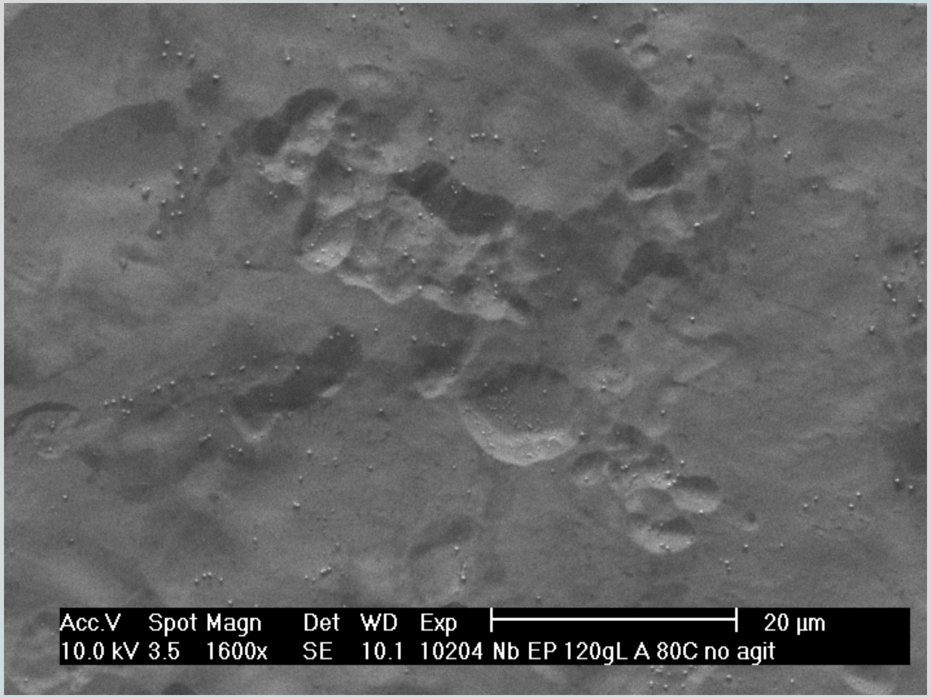

Choline Chloride Drink

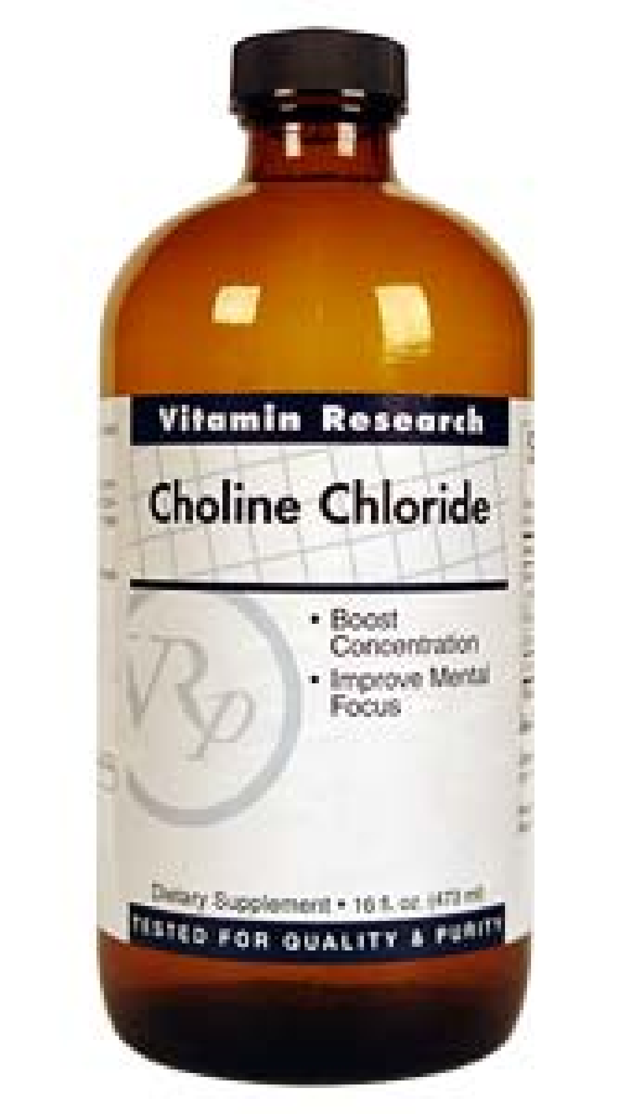

The brain has a voracious appetite for choline. There are two main reasons for the brain's huge need for this nutrient: Choline is required for synthesis of the key neurotransmitter acetylcholine, and it is used for the building and maintenance of brain cell membranes. Acetylcholine is vital for thought, memory and sleep, and is also involved in the control of movements

Dosage and Use

Take 1 to 3 teaspoons daily.

It is best mixed with approximately 2 oz. of juice per teaspoon.

- AP plasma
  - DC → CORONA
  - RF →
    - RF resonance
    - AP Plasma Jet
  - MICROWAVE → MW plasma torch

The early stage of our studies

- Negative Corona inside a 1,5 GHz cavity

- Discharge voltage 30kV

- Strong production of O_3

6 GHz cavity

Cavity

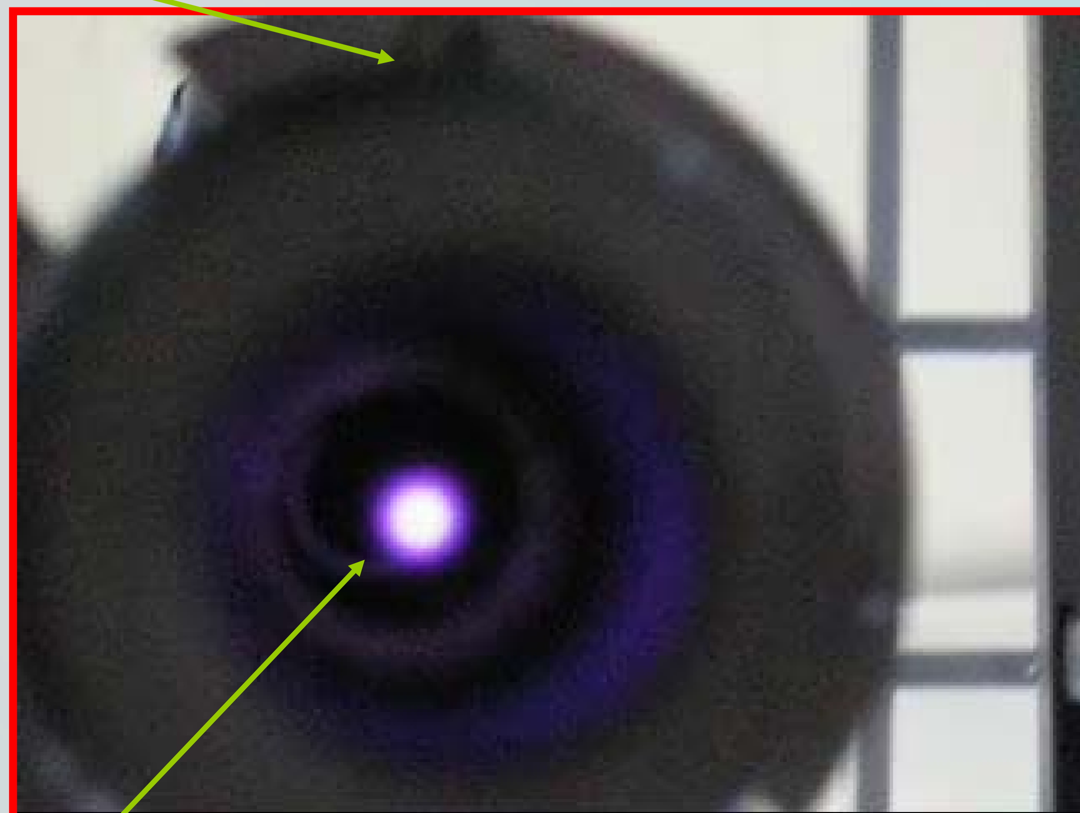

TM010 plasma at a power of 50 W

13,56 MHz / 2,45 GHz APPJ Device

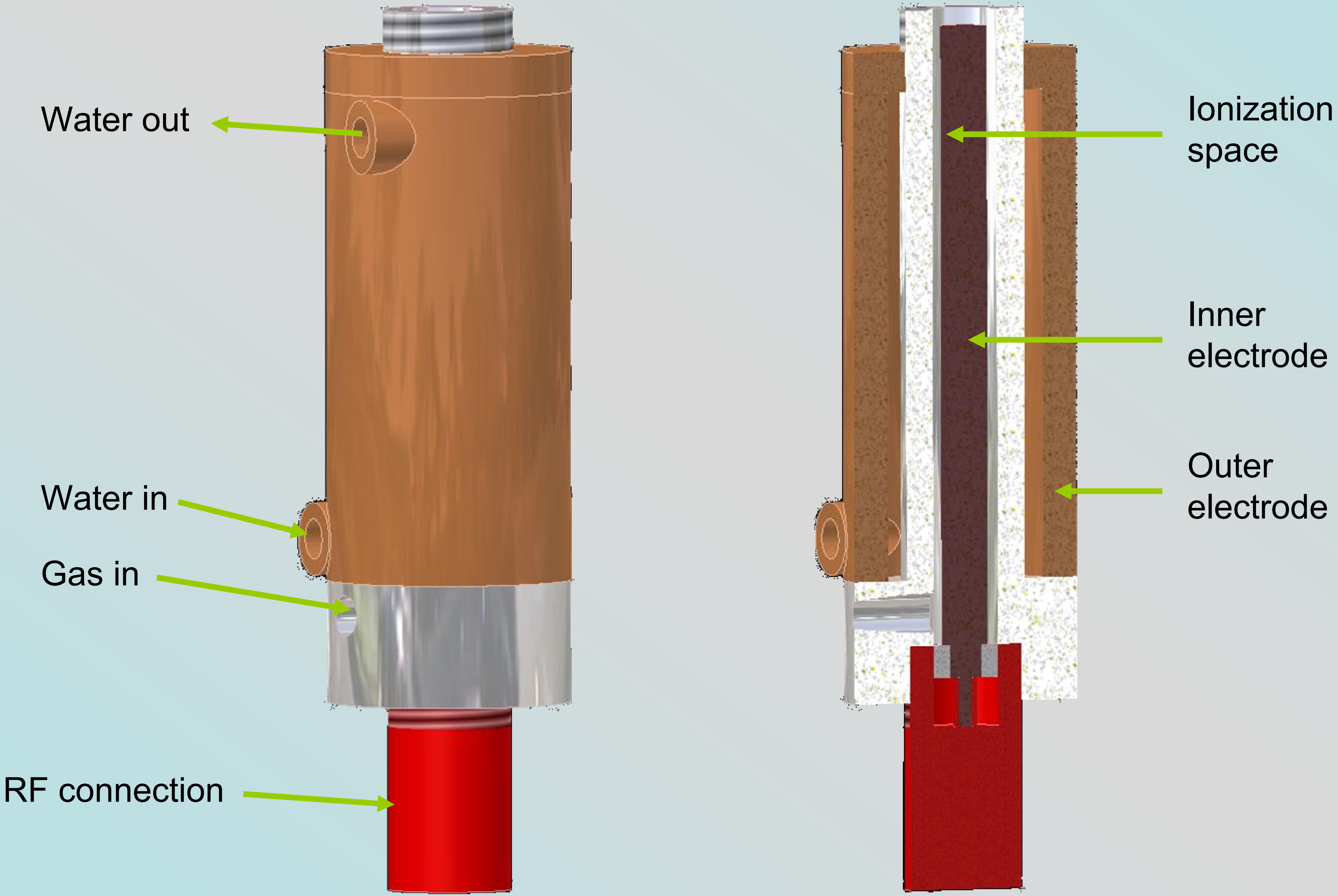

13,56 MHz

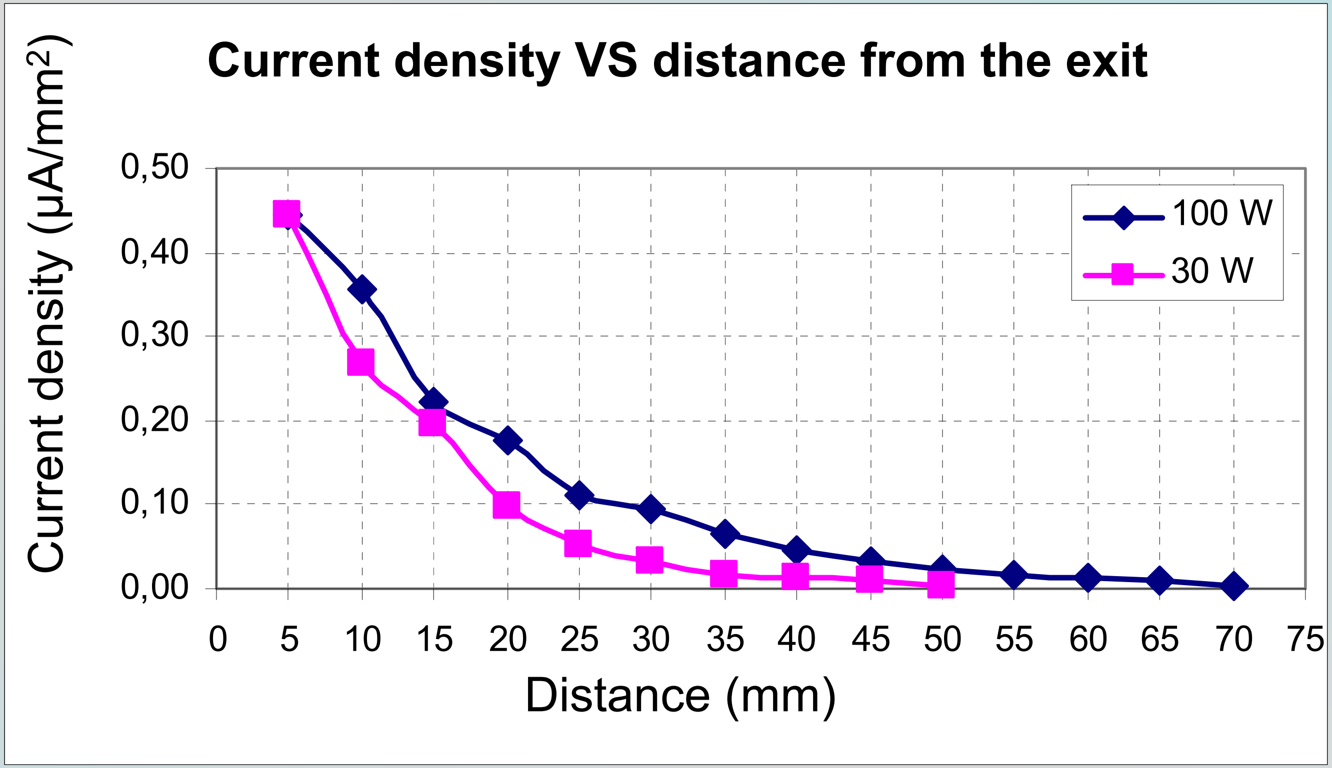
Current density VS distance from the exit
Current density (µA/mm2)
0,50
0,40
0,30
0,20
0,10
0,00
0
5
10
15
20
25
30
35
40
45
50
55
60
65
70
75
Distance (mm)
100 W
30 W

To reduce an amount of micro-droplets one can use a magnetic filter deflecting a plasma-ion stream and separating micro-droplets.

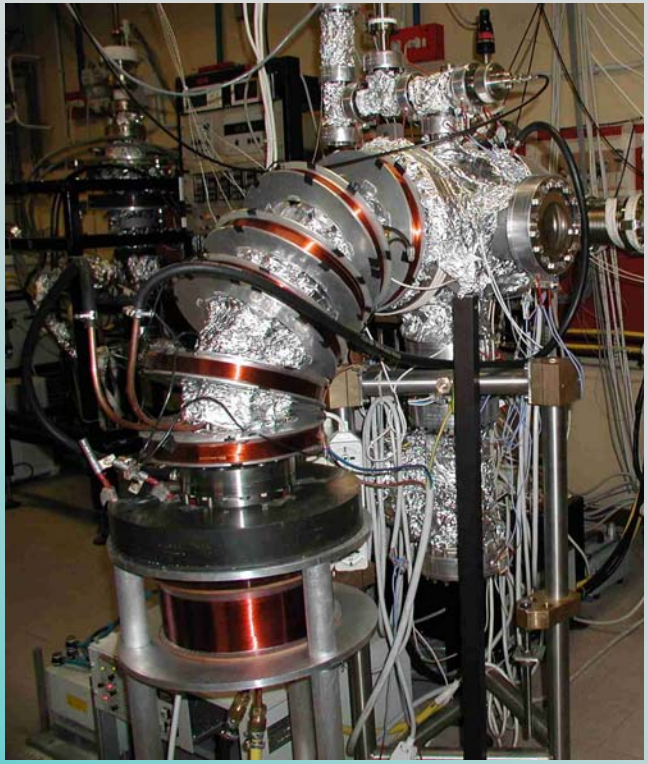

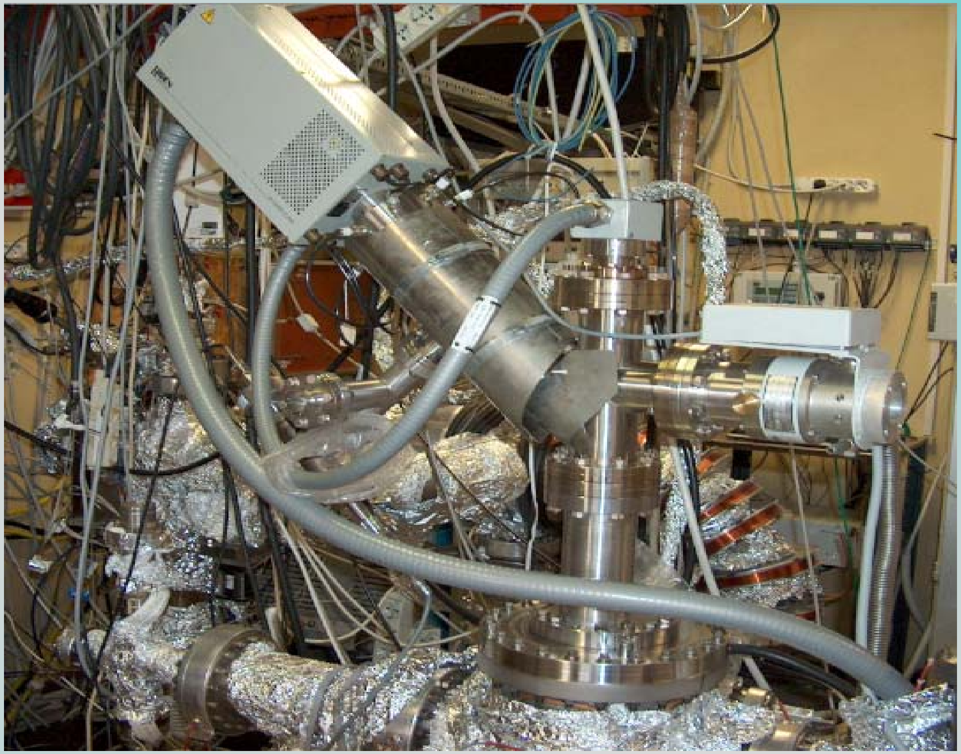

Magnetic filter (on the left) and ion energy analyzer (on the right), as installed upon the second planar-arc facility in Tor Vergata University in 2005.

UHV planar-arc sources constructed at IPJ (Poland)

A new filtered planar-arc system operated at the Dept. of Plasma Physics & Technology.

The detailed description of the UHV arc facilities and their operational characteristics can be found in our previous papers.

J. Langner, M.J. Sadowski, et al., *Czech. J. Phys*. 54 (2004) C914.

R. Russo, L. Catani, et al., *Supercond. Sci. Tech*. 18 (2005) L41.

P. Strzyzewski, J. Langner, et al., *Physica Scripta* T123 (2006) 135.

P. Strzyzewski, L. Catani, et al., *AIP CP* 812 (2006) 485.

UHV arc systems with a linear cathode

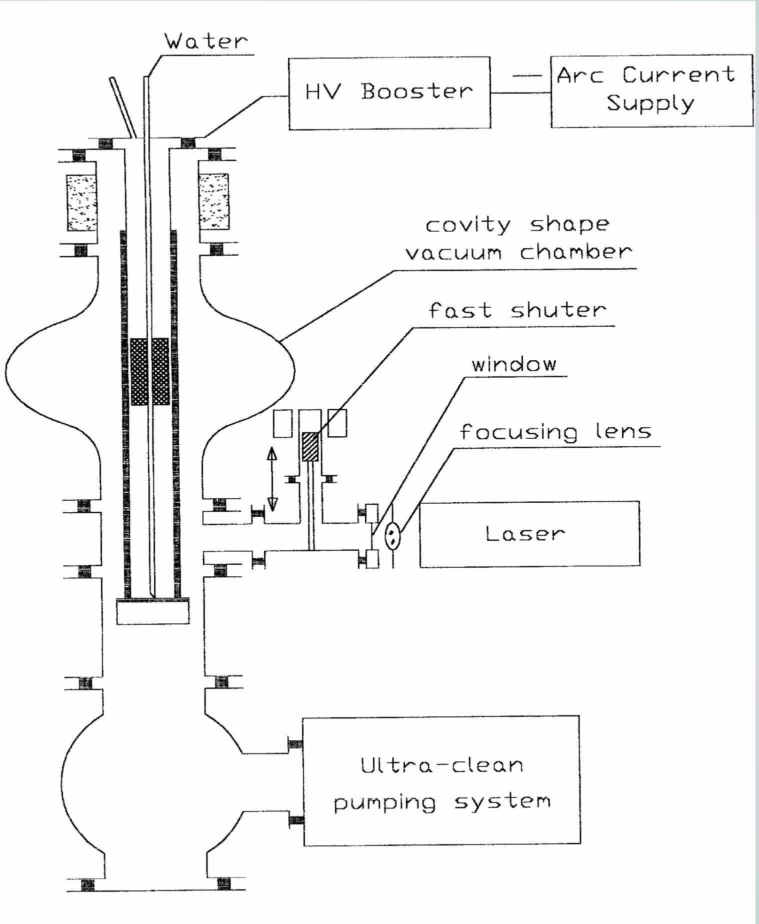

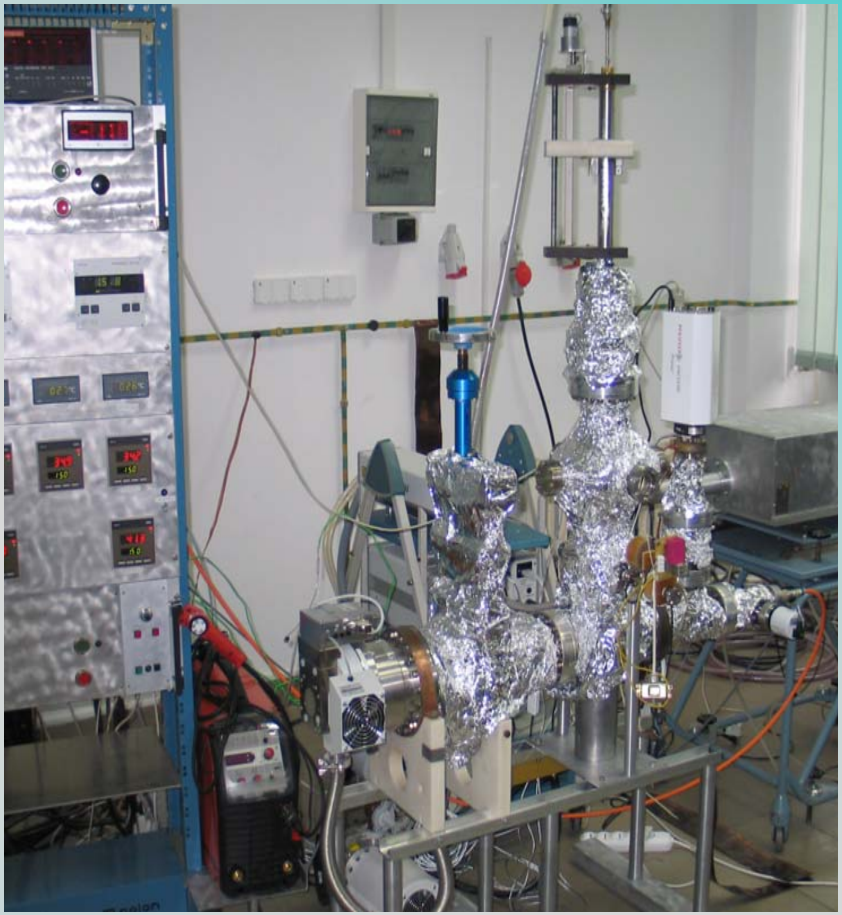

Scheme of the UHV system with a linear (cylindrical) arc and the first linear-arc facility constructed at IPJ in Swierk, Poland, in 2005.

Preliminary test for cavity coating

The first single-cavity taken of the real accelerator unit, after its preparation, has been coated without micro-droplet filtering.

The coated single-cell has been cut along its symmetry axis in order to perform an analysis of the inner surfaces.

Analysis of the coated substrate

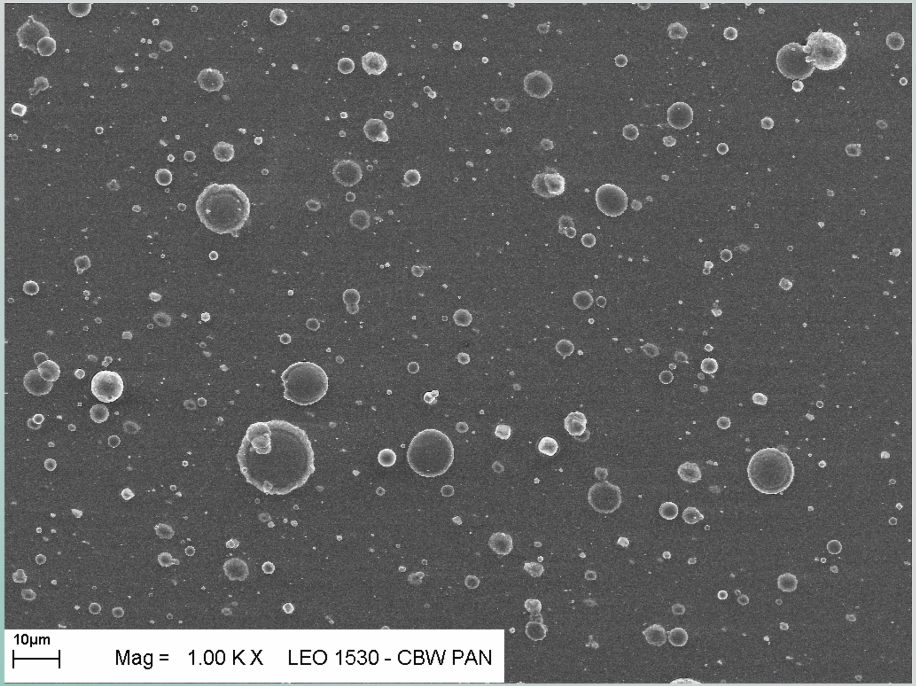

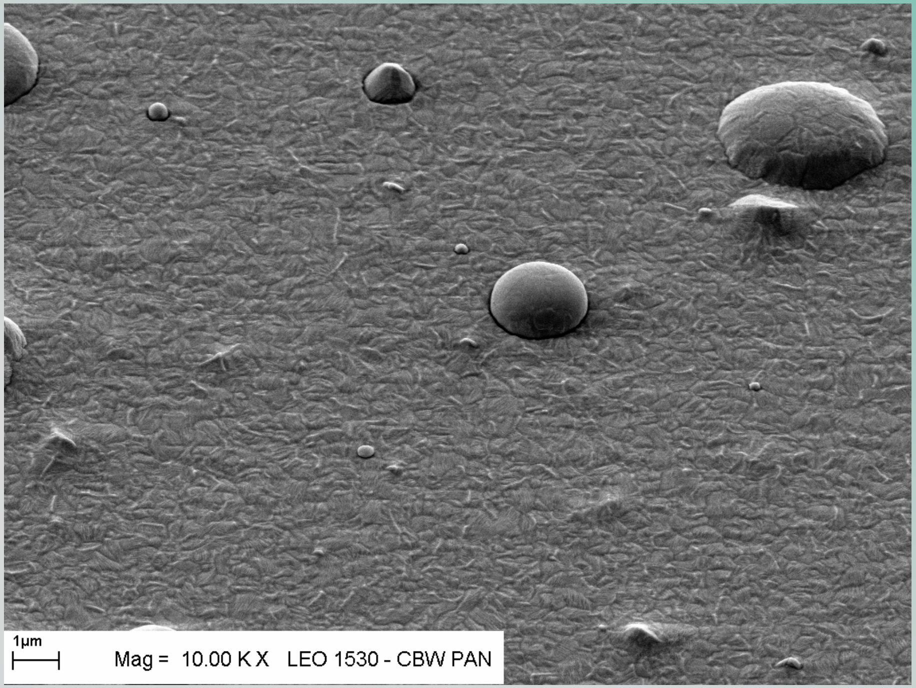

There is a larger number of macrodroplets respect to the planar arc (as aspected)

Most of the particles arrive on the substrate surface still in the liquid phase

To eliminate micro-droplets (macro-particles) or at least to reduce their amount in the UHV linear-arc facility - special cylindrical filters have been considered.

Two different versions of such filters have been designed: a passive Venetian-type filter and an active cylindrical filter (supplied by a magnetizing current and producing an additional magnetic field).

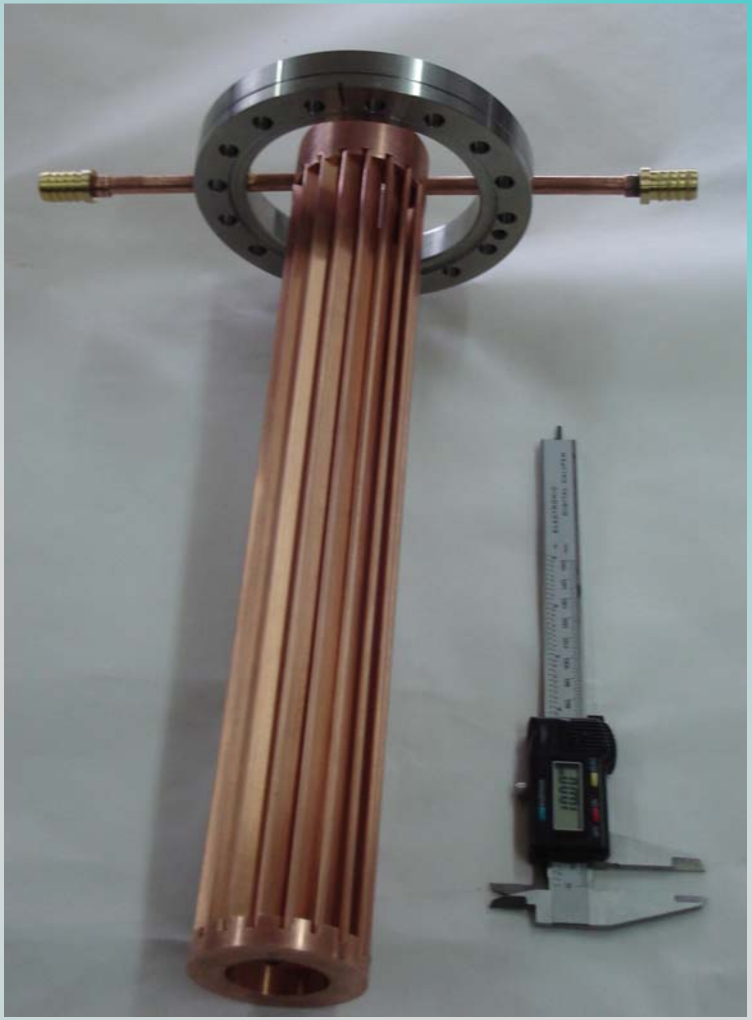

Prototype of a cylindrical Venetian-blind filter.

New cylindrical filters for elimination of micro-droplets

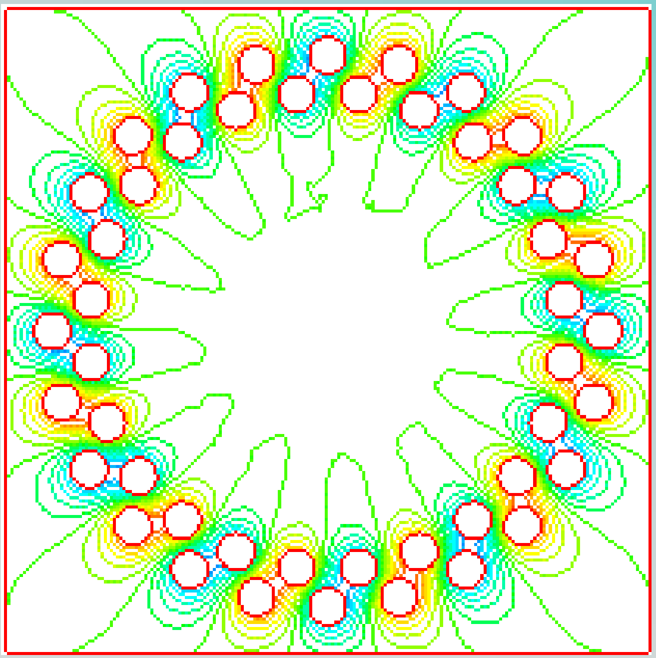

A cylindrical magnetic filter consisting of current-carrying tubes (left) and the distribution of magnetic field lines in its cross-section (right).

Other Arc Modes proposed by Ray Boxman

- Hot Anode Vacuum Arc
  - Crucible anode
- Hot Refractory Anode Vacuum

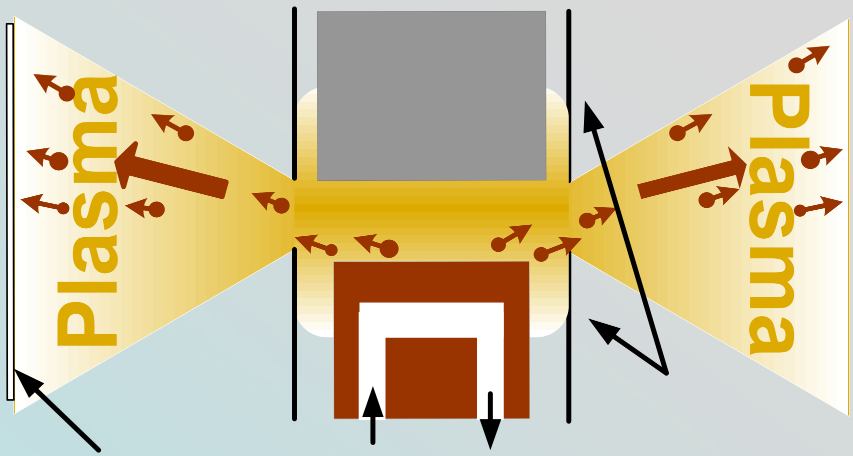

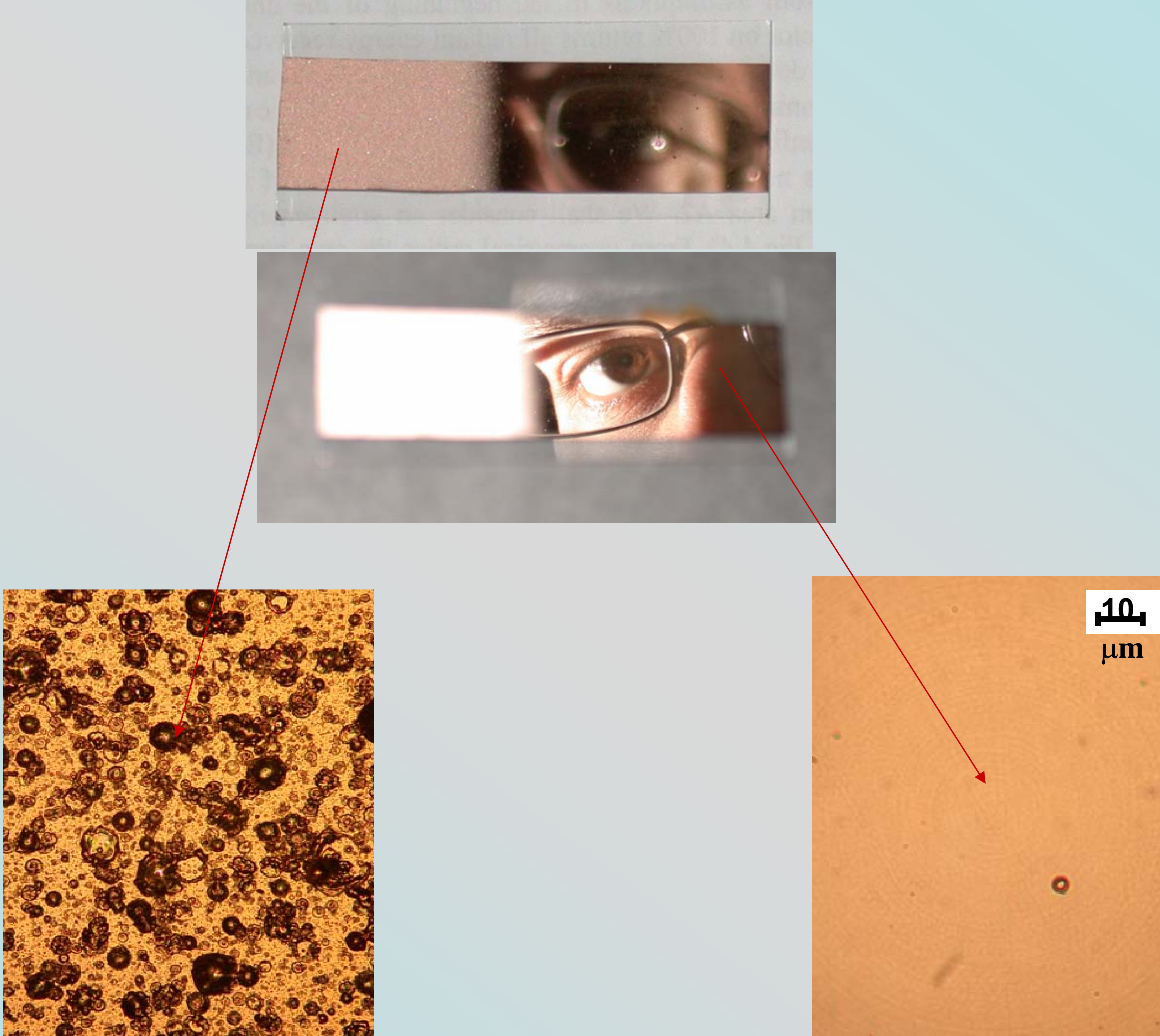
10
μm

Ray Boxman

- Vacuum Arc Deposition
  - (a.k.a. cathode arc deposition, arc evaporation)
  - Most popular method for applying hard coatings in tool industry
  - …but less well known than other PVD (e.g. sputtering, e-beam evaporation) and CVD methods
- Objectives of this lecture:
  - Review:
    - Physics of vacuum arc
    - Engineering issues in vacuum arc deposition
  - Suggest implementations with interior cavity

III. How can we coat the inside of:

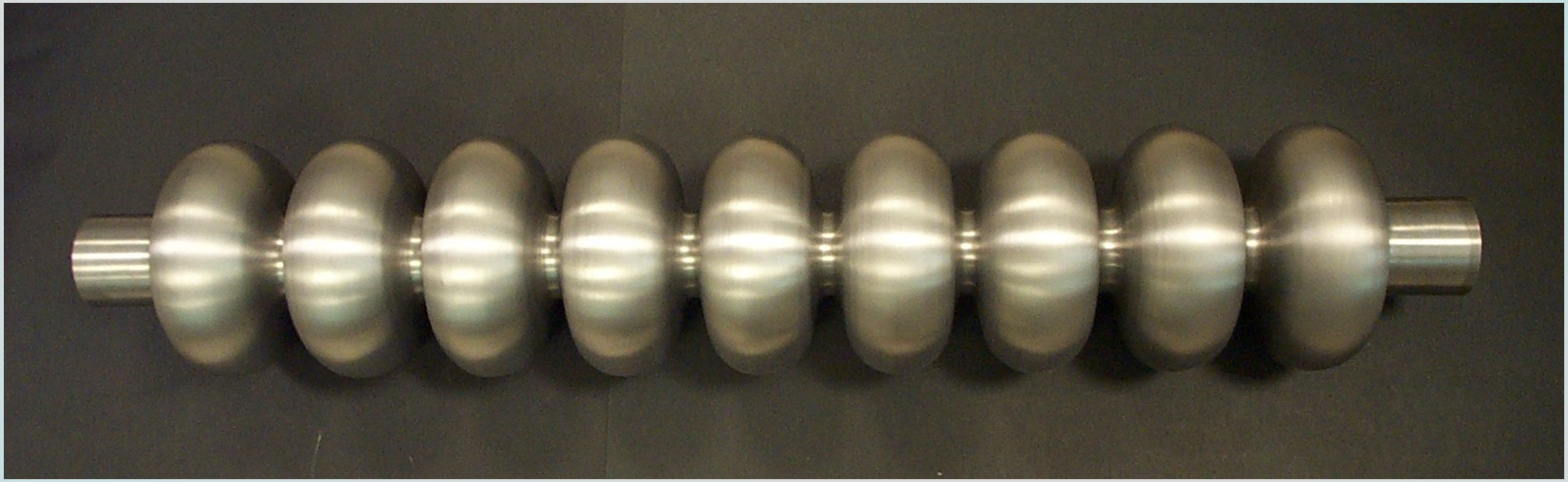

Approach 2: Miniature Filter: Example – Welty Rect. Filter

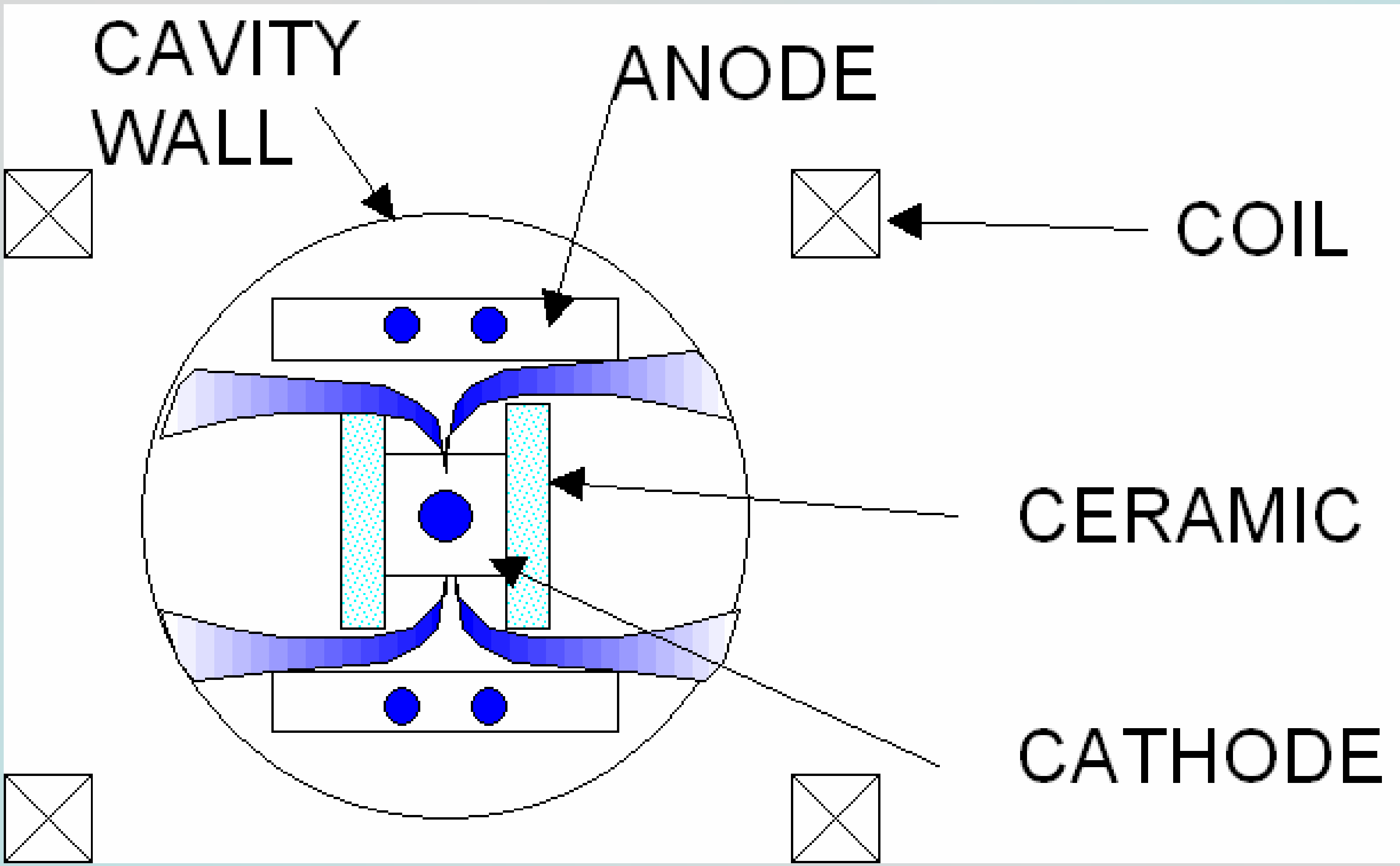

Approach III. Beilis "black-body" HRAVA deposition device

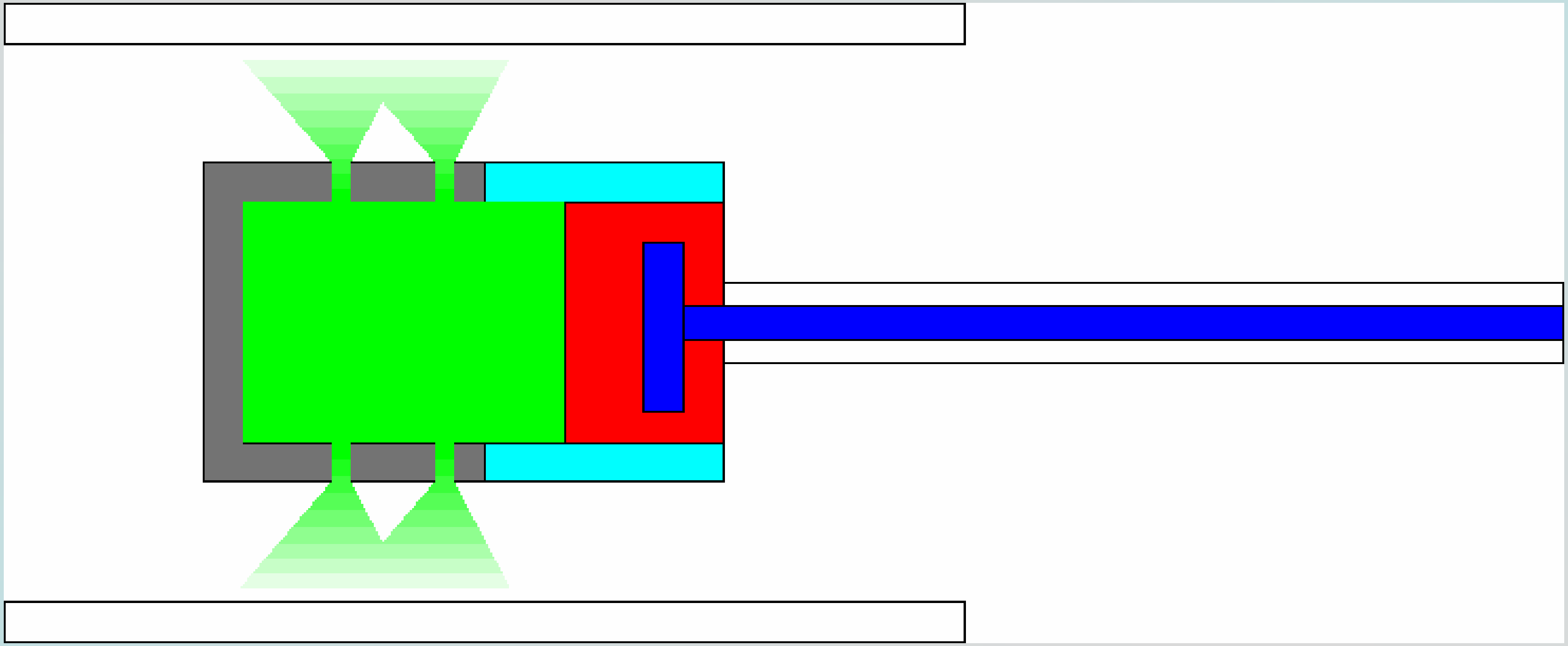

JUST AN EXAMPLE OF HOW TO WORK:

Xiaoxing Xi group (Physics and Materials Sci & Eng); Ke Chen, Derek Wilke, Yi Cui, Chenggang Zhuang (Beijing), Arsen Soukiassian, Valeria Ferrando (Genoa); Pasquale Orgiani (Naples); Alexej Pogrebnyakov, Dmitri Tenne, Xianghui Zeng, Baoting Liu: CVD growth, electrical characterization, junctions

Joan Redwing Group (Materials Sci & Eng): HPCVD growth, modeling

Qi Li Group (Physics): Junctions, transport and magnetic measurements

Darrell Schlom Group (Materials Sci & Eng): structural analysis

Zi-Kui Liu Group (Materials Sci & Eng): Thermodynamics

Xiaoqing Pan Group (U. Michigan): Cross-Section TEM

John Spence Group (ASU): TEM

N. Klein Group (Jülich): Microwave measurement

A. Findikoglu (LANL): Microwave measurement

Qiang Li Group (Brookhaven National Lab): Magneto-optic measurement

Tom Johansen Group (U Oslo): Magneto-optic measurement

Qing-Rong Feng Group (Peking University): SiC fiber

Chang-Beom Eom Group (U Wisconsin): Structural analysis

J. B. Betts and C. H. Mielke (LANL): High field measurement